N73 24925
NASA CR-121102
MCR-72-274

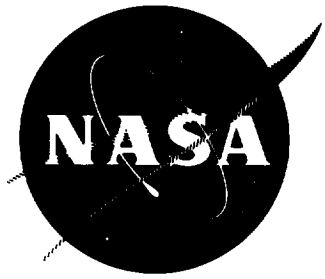

INTERNAL INSULATION SYSTEM DEVELOPMENT

Final Report

by

John P. Gille

May 1973

MARTIN MARIETTA CORPORATION

prepared for

NATIONAL AERONAUTICS AND SPACE ADMINISTRATION

NASA Lewis Research Center
Contract NAS3-14384
J. J. Notardonato, Project Manager

NASA CR-121102
MCR-72-274

FINAL REPORT

INTERNAL INSULATION SYSTEM DEVELOPMENT

by

John P. Gille

MARTIN MARIETTA CORPORATION
P.O. Box 179
Denver, Colorado 80201

prepared for

NATIONAL AERONAUTICS AND SPACE ADMINISTRATION

May 1973

CONTRACT NAS3-14384

NASA Lewis Research Center
Cleveland, Ohio
J. J. Notardonato, Project Manager
Chemical Propulsion Division

FOREWORD

The work described herein was done at the Denver Division of Martin Marietta Corporation, under NASA Contract NAS3-14384 with Mr. J. J. Notardonato, Chemical Propulsion Division, NASA-Lewis Research Center, as Project Manager. Important contributions were also made by Messrs James R. Faddoul, James R. Barber, and Albert J. Pavli, all of the NASA-Lewis Research Center.

ABSTRACT

A program conducted by Martin Marietta Corporation, Denver Division, to develop and test an internal insulation system for cryogenic liquids is described in this report. The insulation system is based on a unique gas-layer concept in which capillary or surface tension effects are used to maintain a stable gas-layer within a cellular core structure between the tank wall and the contained cryogen. In this work, a 1.8 meter (6 ft) diameter tank was insulated and tested with liquid hydrogen. Ability to withstand cycling of the aluminum tank wall to 450°K (350°F) was a design and test condition.

TABLE OF CONTENTS

Figure

Table

SUMMARY

The objective of this program has been to design, fabricate, install and test an internal insulation system that is applicable for use in liquid hydrogen booster propellant tanks for reusable space vehicles. The insulation concept that was developed is based on using surface tension or capillary forces to position a layer of hydrogen vapor in a cellular structure between the liquid hydrogen and the tank wall.

The insulation system is required to sustain no damage when the aluminum alloy tank wall is repeatedly cycled to a temperature of 450°K (350°F). This capability would permit a design wherein the external thermal protection from aerodynamic heating provided for the tanks could be limited to the minimum amount necessary to protect the metal tank. No additional external thermal protection would be required to prevent damage to the cryogenic insulation system.

In a previous NASA Contract, NAS8-25974, *Development of Advanced Material Composites for Use as Internal Insulation for LH_2 Tanks (Gas Layer Concept)*, a materials system and preliminary design and fabrication procedures for the insulation system were developed to meet these requirements. This insulation system used silicone adhesives, Kapton and Teflon films, and fiberglass batting.

Based on the results of the previous program, the present system was designed for insulating the entire interior of an aluminum tank, 1.8-m (6 ft) in diameter with a 1.8-m cylindrical barrel and shallow domes. The insulation system, consisting of a total of 83 panels of 12 different designs, was fabricated and installed in the tank. Methods and tooling for panel prefabrication were extended and improved, and an approach for the installation of the system in a complete tank was satisfactorily developed.

The insulated tank was tested using liquid hydrogen. Boiloff measurements were made before and after cycling the tank wall temperature five times to 450°K (350°F) and pressurizing the tank to 69,000 N/m^2 (10 psig) during each temperature cycle. The temperature and pressure cycles were carried out while the tank was filled with liquid hydrogen. Boiloff measurements during the first test with liquid hydrogen showed that the thermal conductivity was almost identical to that measured in small sample tests under Contract NAS8-25974, or approximately 0.131 J/m-sec-°K (0.076 Btu/ft-hr-°R) over the temperature range of 20 to 250°K (36 to 450°R). After the tank was subjected to temperature and pressure cycling, boiloff data showed a degradation in performance caused by damage to the insulation. Posttest evaluation showed that the damage resulted from an inadequacy of the "dimpling" process wherein the Teflon facesheet was formed to provide relief for stresses caused by thermal contraction.

INTRODUCTION

Current objectives of the National Aeronautics and Space Administration include the development of reusable spacecraft systems for the Space Shuttle Program. One requirement for reusable systems is that they be capable of withstanding high aerodynamic heating rates with a minimum of damage that would necessitate extensive repair, refurbishment, or replacement.

If large cryogenic propellant tanks are to be included as part of the vehicle, the external thermal insulation required for their protection from aerodynamic heating during reentry or ascent may be a major problem because of the large surface areas involved. The objective of the program described in this report was to design, install, and test an internal insulation system based on a unique capillary gas-layer concept that would minimize the need for external thermal protection of boost propellant tanks for liquid hydrogen.

The minimization of thermal protection is accomplished by designing the insulation with a materials system that will permit an aluminum tank to operate at the maximum temperature at which the aluminum alloy retains useful structural properties. In a previous NASA Program Contract NAS8-25974, *Development of Advanced Material Composites for Use as Internal Insulation for LH_2 Tanks (Gas-Layer Concept)*, a materials system and design and fabrication concepts were developed and evaluated, using small specimens.*

The objectives of the program described in this report were to extend the results of the previous program by insulating and testing an aluminum tank, 1.8 m (6 ft) in diameter with a 1.8-m cylindrical barrel section and shallow domes. Practical considerations, such as internal tank hardware, were simulated in the test tank. Objectives of the test program included measurement of thermal performance of the insulation system and determining the ability of the insulation to withstand repeated elevation of the temperature of tank wall to 450°K (350°F).

This development program was accomplished under four major tasks: design, fabrication, testing, and analysis. This report is organized in chapters covering each of these topics, plus a chapter summarizing conclusions reached during the program and recommendations for future effort.

---

*Martin Marietta Corporation Report MCR 72-130, July 1972.

Additional work toward developing the capillary internal insulation concept for other applications has been conducted on Contract NAS8-25974 and on the following programs:

(1) Contract NAS8-21330, *Development of Advanced Materials for Integrated Tank Insulation System for the Long-Term Storage of Cryogens in Space;*

(2) Contract NAS3-12425, *Insulation Systems for Liquid Methane Fuel Tanks for Supersonic Cruise Aircraft;*

(3) Martin Marietta Corporation internal program to develop an insulation system for storing and transporting liquefied natural gas.

INSULATION SYSTEM DESIGN

Capillary Insulation Concept

The internal insulation system developed during this program is based on the capillary gas layer concept. The basic design concept is illustrated in figure 1. In this insulation, a large cell honeycomb-like core structure bonded to the internal tank wall positions a large number of gas columns, or, in effect, a gas layer between the tank wall and the contained cryogen. A facesheet is bonded to the opposite, or interior side of the core, and the facesheet comes in direct contact with the cryogen. A perforation through the facesheet to each cell permits equalization of the pressure of the gas in the cells with the pressure of the liquid. However, because of the small size of the opening, a stable liquid-gas interface forms at the opening when the pressure is equalized, preventing the interchange of liquid and gas across the facesheet boundary. The cells are filled with a suitable material to inhibit convective heat transfer.

The normally equalized pressure across this interface causes the system to be essentially free of pressure-induced structural loading. Consequently, the insulation system can be designed with a lightweight structure and a wide range of materials. By incorporating excess facesheet and core material to accommodate thermal contraction, the design can be made relatively free of thermally-induced stresses. Since the structural demands on the construction materials are minimal, it has been possible to select materials capable of withstanding high temperatures, and small specimens of the insulation have been successfully tested with wall temperatures up to 617°K (650°F).

Capillary and Thermodynamic Considerations. - The stability of the capillary liquid/gas interface is determined by the same physical relationships that apply to the liquid/gas interface formed when a liquid is positioned at the top of an inverted cylinder closed at one end. The stability of the capillary interface is determined by a critical Bond number (Bo) relationship. The Bond number is a dimensionless ratio of gravity forces to surface tension forces, given by

$$Bo = \frac{\rho g d^2}{\sigma g_c}$$

where:

Bo = Bond number, dimensionless

ρ = density of liquid (minus density of gas), kg/m^3 $\left(\text{or } lb_m/ft^3\right)$

$\frac{g}{g_c}$ = ratio of acceleration or local gravitational field to gravitational constant, N/kg $\left(\text{or } lb_f/lb_m\right)$

d = diameter of capillary opening, m (or ft)

σ = surface tension, N/m $\left(\text{or } lb_f/ft\right)$.

When this number does not exceed 3.37 for any consistent system of units, the capillary interface formed in an inverted circular cylinder will remain stable. The mechanics of the interface formed at a circular opening in a thin membrane are essentially the same, and this criterion is valid although the critical number will vary slightly with the orientation of the opening with respect to the gravity vector.

For liquid hydrogen, assuming

σ = 19 N/m $\left(13.05 \times 10^{-5} \text{ } lb_f/ft\right)$

ρ = 70.96 kg/m^3 $\left(4.43 \text{ } lb_m/ft^3\right)$,

the maximum hole size for which the stability criterion holds is 3.02 mm (0.119 in.) at 1 g or 1.75 mm (0.069 in.) at 3 g. Of course, in a zero-gravity environment any opening size would meet the stability criterion. In practice, a much smaller opening can be used with a greater stability margin.

When a liquid cryogen first contacts the insulation, the gas in the cells cools and contracts, tending to lower the cell pressure. As a result, some liquid enters the cells and begins to vaporize because the temperature within the cells is higher than the boiling point for the cryogen. The gas that is produced then tends to pressurize the cell. As the cell pressure exceeds the local pressure in the bulk liquid, gas is discharged from the cell through the opening, forming bubbles in the liquid.

This process of gas entering the cell, vaporizing, and being discharged from the cell will continue until a state of thermal and pressure equilibrium is reached. If the tank or head pressure is increased, this sequence of events will be repeated until a new equilibrium is achieved. Similarly, if the tank pressure is decreased, gas will be discharged from the cell until the pressure is again equalized.

The pressure that exists across the facesheet at any time depends on the rate of change of tank pressure and on the relationship between the facesheet hole size (and the consequent flow-loss characteristic) and the cell volume. A small differential (capillary) pressure that can be supported by the surface tension of the interface can exist without any flow of liquid or gas through the facehseet opening, but this pressure is negligibly small (on the order of 10^{-4} atmosphere).

Thermal "Stress-Free" Design Concept. - The insulation system does not support significant steady-state liquid or pressure loads because it is pressure-equalized. Rather, these loads are transmitted through the columns of gas in the insulation cells directly to the tank walls. Factors such as rapid pressure change and changes in the head pressure of the liquid caused by vehicle acceleration and propellant sloshing can produce loads on the insulation, but they are usually minor. Because the structural load-carrying requirements are small, the insulation system can be made light-weight and flexible, and design features can be incorporated to minimize thermally induced stresses.

The design approach used to minimize thermal stresses is to build in additional material, so that members do not become loaded in tension when thermal contraction occurs. For cellular core, this is accomplished by configuring the ribbon that forms the cell walls in an S-shape. The actual length of the ribbon exceeds the straight-line distance between the node bonds by a factor more than sufficient to compensate for contraction.

In practice, the excess ribbon length for each span is approximately 5.5%. For Kapton, with a total contraction of approximately 0.42% from room temperature to the temperature of liquid hydrogen, this provides more than 10 times the required excess length. As the excess ribbon length is increased above 5.5%, buckling occurs in the ribbon, forming an unsymmetrical S-curve between nodes. Since the segments of the ribbons joined by the node bond are common to two adjacent cells, those segments

are not free to distort to accommodate thermal contraction. Therefore, the node bonds are kept narrow in order to increase the portion of the ribbon that is free to distort into a new path between node points.

To compensate for the contraction of the facesheet, it is dimpled. Attempts to analyze the distortion of a facesheet bonded to a distorted cell ribbon and to determine the minimum dimpling required have been inconclusive. It is obvious that the increase in dimension of the facesheet between the fixed node points on opposite sides and ends of the cell must be at least as great as the contraction that occurs when it is cooled to the cryogenic temperature. Results obtained under Contract NAS8-25974 led to the conclusion, based on small sample testing, that a dimple depth of 0.075 times the cell height or width was adequate for a Teflon facesheet. As will be pointed out in the chapter on *Analysis of Results*, the criterion proved inadequate for the complete insulation system as installed in the 1.8-m model tank, and it is now concluded that the small specimen tests did not properly account for "complete tank" effects.

Cell Size Considerations. - The primary limitation on cell size is set by the nature of the transient pressure changes on the tank and the ability of the facesheet to momentarily withstand a pressure load. There is also a limit, based on capillary stability considerations, to the size of the opening in the facesheet. Therefore, for a given rate of pressure change in the tank, assuming the other parameters are fixed, the rate of pressure equalization, and consequently the maximum differential pressure across the facesheet, can be limited by limiting the cell volume. In addition, the core material must be able to withstand the compressive load induced by a differential pressure across the facesheet, as well as other loads that may be imposed. Probably the most severe compressive loads normally imposed on the core will be those incurred during panel fabrication. Current fabrication methods require the core to be capable of withstanding a compressive load of 7,000 to 14,000 N/m^2 (1 to 2 psi).

Other considerations affecting cell size are system weight and possibly cost. Since the total length of the ribbon and the number of node bonds per unit area decrease as the cell size increases, the weight of adhesive would also decrease as the cells are made larger.

Design Requirements

The objective undertaken in this program was to develop an insulation system to satisfy the requirements of reusable hydrogen boost tanks for the Space Shuttle vehicles, as defined in Phase B Shuttle design studies conducted by McDonnell Douglas and North American-Rockwell. In addition to meeting the special problems inherent in these tanks, a primary design goal was to provide an internal cryogenic insulation system that would permit the aluminum alloy tanks to be operated to the maximum operating temperature of the metal, thus minimizing requirements for external thermal protection. Reusability with minimum repair and refurbishment was another design goal. Therefore, for fabrication of the insulation we selected a materials system with a capability of repeated operation at a temperature of 450°K (350°F).

The Phase B Shuttle design study reports for both the orbiter and booster hydrogen tanks were reviewed to determine what internal tank structures and hardware were included in the Shuttle tank designs, and which of these to simulate in the model tank.

The results of the review are summarized in figures 2 and 3. As illustrated in the figures, the hardware inside the Shuttle tanks could be grouped into four different categories, and examples from the two studies are shown for each group.

Group I - Single point or limited area intrusions

Group II - Continuous rings or landings

Group III - Screens, baffles, and miscellaneous outlet apparatus

Group IV - Intersecting surfaces

In addition to these types of internal hardware or irregularities, most cryogenic tanks would include outlets for fill, drain, and vent, and manway openings with covers. Internal vertical stringers would also be found in many flightweight tanks.

Simulated internal hardware items were designed for the model tank to demonstrate the methods of insulating over the types of irregularities that would result from the tank features mentioned. To meet the basic requirement of the insulation system, thermal protection of the liquid hydrogen during load, ground hold, and boost, an insulation thickness of 25.4 mm (1 in.) was specified. This insulation thickness is not necessarily an optimum value, but is typical of the requirement for a boost hydrogen tank.

Model Tank

An aluminum tank [1.829 m (72 in.) inside diameter] with a 1.829 m cylindrical barrel section and shallow domes was made available for this program. In its original form, shown in figure 4, the tank barrel was made of 4.77 mm (0.188 in.) type 5086 aluminum alloy, and the domes were made of 6.35 mm (0.250 in.) type 5454 aluminum alloy. The tank was equipped with a 0.762 m (30 in.) manway and a 0.1524 m (6 in.) outlet centrally located in the lower dome. Because the upper dome had been formed after the manway opening was cut out, it was significantly deeper than the lower dome.

Before installing insulation in the tank, some welding and the installation of hardware items to simulate the Shuttle design features were required. Inspection and retesting to requalify the tank for the cryogenic test program was delayed until these welds were completed. Upon radiographic inspection of the tank, the dome-to-barrel and barrel seam welds were found to be of inadequate quality.

After a thorough analysis, it was determined that it was more practical to rebuild the tank replacing the barrel section. Because design and fabrication of the insulation system were well underway at this point, the tank was rebuilt as shown in figure 5 to minimize changes to the internal dimensions. The replacement barrel was made from 6.35 mm (0.250 in.) 5086 aluminum, and the vertical stringers and upper ring frame were eliminated. The original dimensions were held within the specified limits; however, the internal diameter at the two dome-to-barrel weld lines experienced shrinkage of up to 6 mm (0.25 in.).

Simulated internal hardware was designed, fabricated, and installed in the tank to provide irregularities representative of the internal design features found in the Shuttle design studies. The category I attach point feature was represented by a fiberglass-epoxy angle, shown in figure 6. Category II was simulated by a ring frame segment, as shown in figure 7. A vertical stringer was simulated by a 51 mm (2 in.) channel, 0.6096 m (24 in.) long, welded vertically in the tank (fig. 8). In these cases, the ends of the ring frame and stringer were considered to present an additional type of insulation problem: termination of the members, in addition to demonstrating the insulation of these types of internal structural reinforcements. The typical outlet device, Category III, was simulated with a semi-cylindrical baffle (fig. 9) concentric with the outlet. This shape was chosen over a full cylinder to avoid a trapped volume of liquid when the tank is drained.

No modification was necessary for demonstrating the insulation of the manway and cover and the tank outlet. The Category IV Shuttle design feature, intersecting conical and cylindrical surfaces, was not practical to simulate in this test article. However, the dome-to-barrel intersection in the model tank presents a rather abrupt transition between the cylindrical and dome surfaces, as opposed to the gradual, smooth transition found in the airborne designs.

Insulation System Design

An insulation materials system capable of operation at a 450°K (350°F) wall temperature was selected on the basis of results obtained under Contract NAS8-25974, *Development of Advanced Material Composites for Use as Internal Insulation for LH_2 Tanks (Gas Layer Concept)*. The insulation system components and the selected materials are presented in table 1. Selected properties of these films and adhesives are given in tables 2 and 3.

TABLE I. - SELECTED INSULATION MATERIALS

Component	Material	Manufacturer
Core Ribbon	500-gage Kapton Film (Type H)	Dupont
Facesheet	200-gage Teflon FEP Film (etched both sides)	Dupont
Core Node Adhesive	RTV-156	General Electric
Core-to-Facesheet Adhesive	RTV-560 with 0.25% DTD*	General Electric
Core-to-Metal Adhesive (and grout compound)	RTV-560 with 0.25% DTD*, 5% RTV-9811, and 1 to 2% Cab-O-Sil	General Electric Cabot
Primer on Core, Facesheet, and Metal	DC-1200	Dow Corning
Filler Material	PF-105-450 Fiberglass Batting	Owens-Corning

*Dimethyl Tin Dilaurate curing agent.

TABLE II. - PROPERTIES OF FACESHEET AND CORE MATERIAL

	Teflon FEP	Kapton (Type H)
MANUFACTURERS' DATA		
Normal Temperature Range, °K (°F)	33 to 473 (-400 to 392)	77 to 473 (-322 to 392)
Reduced Properties Temperature Range, °K (°F)	14 to 533 (-435 to 500)	4.5 to 673 (-452 to 752)
Melting Point, °K (°F)	533 to 553 (500 to 535)	None - Decomposes to a Gas
Ultimate Tensile Strength, N/m^2 (psi) 295°K (70°F)	2.1×10^7 (3000)	1.7×10^8 (25,000)
Ultimate Elongation, % 295°K (70°F)	300	70
Tensile Modulus at 295°K (70°F) N/m^2 (psi)	4.8×10^8 (70,000)	2.96×10^9 (430,000)
Specific Gravity	2.15	1.42
TEST DATA		
Temperature at Which Property Change Noted by DSC.* °K (°F)	521 (478)	No change to 773 (932)
Ultimate Tensile Strength at 295°K (70°F), N/m^2 (psi)	2.15×10^7 (3120)	1.85×10^8 (26,800)
Ultimate Elongation at 295°K (70°F), %	320	18
Tensile Modulus at 295°K (70°F), N/m^2 (psi)	3×10^8 (44,000)	1.39×10^9 (201,000)
Ultimate Tensile Strength at 450°K (350°F), N/m^2 (psi)	3.2×10^6 (464)	
Ultimate Elongation at 450°K (350°F), %	126	
Tensile Modulus at 450°K (350°F) N/m^2 (psi)	1.26×10^7 (1822)	
Ultimate Tensile Strength at 617°K (650°F), N/m^2 (psi)	N/A	6.45×10^7 (9360)
Ultimate Elongation at 617°K (650°F), %	N/A	42.6
Tensile Modulus at 617°K (650°F), N/m^2 (psi)	N/A	5.1×10^8 (74,000)
Ultimate Tensile Strength at 20.5°K (-423°F), N/m^2 (psi)	1.14×10^8 (16,600)	3.1×10^8 (45,000)
Ultimate Elongation at 20.5°K (-423°F), %	2.5 to 2.9	2.3 to 7.0
Tensile Modulus at 20.5°K (-423°F), N/m^2 (psi)	3.65×10^9 (530,000)	4.55×10^9 (660,000)
Ultimate Tensile Strength after H_2 Thermal Cycle, N/m^2 (psi)**	1.5×10^7 (2200)	2.87×10^7 (4160)
Ultimate Elongation after H_2 Thermal Cycle, %**	276	4.1
Tensile Modulus after H_2 Thermal Cycle, N/m^2 (psi)	9×10^7 (13,000)	7.1×10^8 (103,000)
Coefficient of Thermal Expansion to 75.8°K (-323°F) m/m-°K (in./in.-°F)	7.0×10^{-6} (3.9×10^{-6})	1.53×10^{-5} (0.85×10^{-5})

*DSC - Differential Scanning Calorimeter

**Thermal cycle tests to 450°K (350°F) for Teflon and to 617°K (650°F) for Kapton in hydrogen environment, 200 cycles.

TABLE III. - PROPERTIES OF SELECTED SILICONE ADHESIVES

Manufacturers' Data	RTV-156	RTV-560
PUBLISHED DATA		
Recommended Temperature Range, °K (°F)	208 to 589 (-85 to 600)	158 to 533 (-175 to 500)
Specific Gravity	1.11	1.42
Thermal Conductivity at Room Temperature, J/m-sec-°K (Btu/ft-hr-°F)	0.208 (0.12)	0.311 (0.18)
TEST DATA		
Ultimate Shear Stress at Room Temperature, N/m^2 (psi)	6.62×10^5 (96)	1.99×10^6 (288)
Ultimate Shear Stress at 450°K (350°F), N/m^2 (psi)	6.61×10^5 (95.9)	2.58×10^5 (37.4)
Ultimate Shear Stress at 20°K (-423°F) N/M^2 (psi)	5.69×10^6 (825)	7.57×10^6 (1098)
Ultimate Shear Stress at Room Temperature after 200 Cycles to 450°K (350°F) in H_2, N/m^2 (psi)	1.59×10^6 (230)	1.53×10^6 (222)

A design concept for the insulation system was adopted wherein the entire tank interior is insulated with prefabricated panels. These panels are of the required size and shape to fit the tank size and contour without excessive gaps or interferences. Panels are either in the shape of curved rectangles, as mounted on the tank barrel, or contoured ring segments for the tank domes. The original panel layout is shown in figure 10. Because of the difference in shape between the upper and lower domes, common designs could not be used for the dome and dome-to-barrel transition panels. The panels are designed without regard to the internally mounted hardware. On installation, cutouts are made in the standardized panels to accommodate the hardware, and special panels are fabricated to insulate over the hardware and cutout areas.

The panels are designed to nest together on all sides when installed, forming a narrow, serpentine gap between the panels. This gap is then filled using a grouting compound with a relatively low thermal conductivity. A typical grout joint is depicted in figure 11. The grout material may have a thermal conductivity several times higher than that of the insulation panel. However, the total cross-section of the grout will normally be on the order of 1% of the total insulated area. Thus, there is no significant degradation in the performance of the overall system.

The curved grout joint can accommodate thermal contraction by changing shape, and consequently does not develop severe stresses. Using the grout joint method, the insulation panels must be designed to the shape and size of the particular tank to be insulated, but reasonable tolerances can be provided by using a thicker section of grout material. Each core panel is designed with an odd number of ribbons and an even number of core node bond lines. This results in panels whose length and width correspond to an odd number of "half" cells. In this context, a "half" cell refers to the total width of the panel in terms of the width of each cell, and not to incomplete or open cells. In other words, the panel's dimensions are equal to

$$w = (n + \tfrac{1}{2})\, w_{cell}$$

$$h = (n + \tfrac{1}{2})\, h_{cell}$$

where

n = number of cells in width or length of panel,

w = panel width,

w_{cell} = cell width,

h = panel height,

h_{cell} = cell height.

The rectangular panels for the tank barrel are designed with a core structure fabricated by bonding straight ribbons of Kapton at appropriate node points. When expanded and curved to the tank contour, the ribbon curvature between bonds varies from the wall side to the inside facesheet surface. If the ratio of

tank diameter to insulation panel thickness decreases, the difference in curvature of the ribbons from one side to the other increases. Below some value of this ratio, estimated at about 30, the ribbons will buckle on the facesheet side and an irregular cell shape will result. In this case, the core would be fabricated from curved ribbons, as shown in figure 12, which would provide a greater ribbon length at the wall side and would prevent the distortion of the cell shape. In either case, the panels are installed so that the core ribbons follow a path parallel to the tank axis.

For the curved domes, the panels are designed in ring segments that are installed in concentric rings about the axis of the tank. All core ribbons radiate from the center of the dome. The number of ribbons doubles at discrete points as the distance from the centerline increases, thus increasing the number of cells and keeping cell dimensions within a fixed range.

The panels are designed with curved core ribbons to conform to the contour of the tank. Each panel nests with its neighbor on all sides, and the joints are grouted in the manner previously described. The six basic panel designs for locations A through F in figure 10 are shown in figures 13 through 18.

An immediate requirement for the prefabricated panels was that they fit through the manway opening. In addition, it was necessary that the insulation covering the tank perimeter be divided into an even number of panels to permit a reduction of the number of panels by a factor of two near the outlet. In the general case, the number of panels forming the complete circumference should be an integral power of 2, providing for the maximum number of possible reductions in the number of panels per ring on the dome as the rings approach the center of the dome. It is also desirable that the number of complete cells forming the panel width be a power of two to permit the maximum number of reductions by a factor of two of the number of cells per panel.

As a result of these design guides, the panels for the barrel (D) were designed to be 16.5 cells in width and 15.5 cells in height. Cell width is nominally 43.9 mm (1.728 in.) arc length, or 44.5 mm at the wall and 43.3 mm at the facesheet side. Cell height is 51.8 mm or 2.039 in. The unexpanded ribbon length between node bonds is 73 mm (2.875 in.). This results in a ribbon length between node bonds (or expansion factor) of 1.05 times the straight line distance between node bonds. Ring segment panels were designed with decreasing cell size and reduction in number of cells as required to fit the tank contour. An expansion ratio of 1.055 was maintained for these panels.

The panel designs presented above were based on dimensions and contours of the model tank before it was rebuilt. After the tank rework was completed, the tank dimensions remained within the tolerances required for use of the existing panel designs except for the dome-to-barrel transition areas. In the weld areas, circumferential shrinkage occurred to the extent that the diameter was reduced at the lines of the welds by as much as 6 mm (0.25 in.). The resulting distortion of the tank wall was greater than could be accommodated by the C and E transition panels.

The panels were redesigned as illustrated in figures 19 and 20. The original C and E panel designs covered the dome-to-barrel transition as well as a portion of the barrel. In the redesign, two panels were substituted for the original single panel; one panel covered only the barrel, and the D panel design, shortened to only $2\frac{1}{2}$ cells in height, was used. The cylindrical panels and the shorter panels covering the actual transition were joined with the standard grouted joint, which was then positioned approximately at the weld line, the point of maximum distortion. By adding the joint at this point, a hinge effect was achieved, wherein the panels were free to assume slightly different orientations, depending on the degree of distortion of the tank.

In the redesigned short panels covering the transition area, the inner surface was made conical, thereby eliminating the highly contoured facesheet originally required. Although a number of panels of the original design were successfully fabricated, this change greatly simplified the facesheet bonding procedure.

The manway cover was insulated with a panel (G) modified from a standard D panel. A concept for closeout of the insulation when the manway is installed is shown in figure 21. A fiberglass-epoxy angle ring is installed at the inside of the aluminum manway ring. This ring is fastened in place by screws and is sealed around the top and at the screw holes with a silicone sealant. When installed, the angle ring and the aluminum manway ring are aligned to form a common plane. A ring of cast silicone rubber is bonded in place beneath this plane with adhesive applied only to the inner and outer edges of the rubber ring, and the upper dome (F) panels are installed to the dome and the silicone rubber ring. The assembly thus formed provides an expansion joint to permit contraction of the glass-epoxy angle.

A circular channel of fiberglass epoxy is similarly installed on the manway cover. The G panel is bonded to the manway cover inside the channel. When the G panel is trimmed to the circular shape, an excess border of the Teflon facesheet is allowed to remain. After filling the open space remaining in the channel with fiberglass batting, the Teflon is formed to the channel and sealed with silicone adhesive. Before installing the manway cover, the glass-epoxy rings, between which there will be a small gap of 0 to 2 mm (3/32 in.), are primed with silicone primer. Just before installing the cover, a narrow bead of silicone adhesive (RTV-560 thickened to a paste consistency with silica) approximately 3 mm (0.125 in.) high is placed on the angle ring. This adhesive forms a seal between the rings as shown in the figure. The annular volume between the rings is vented, by a small hole, into one of the G panel cells.

This design provides for uninterrupted continuation of the insulation over the manway and cover. Because the silicone adhesive has relatively low strength, it will fail when the cover is later removed. After the failed adhesive is removed and the surfaces reprimed, the cover is ready for reinstallation.

Because the test cryogen to be used with this system is liquid hydrogen, vacuum-jacketed lines are required for the fill and drain plumbing. A vacuum-jacketed fill-line adapter was designed, as shown in figure 22. This adapter provides for the transition from the 152 mm (6 in.) tank outlet to the 31.75 mm (1.25 in.) vacuum-jacketed facility plumbing system.

An insulating plug was designed to continue the internal tank insulation to the fill adapter. This plug, shown in figure 23, is fabricated of fiberglass-epoxy composite. It is contoured on the perimeter to nest with the four A panels. The joint between these panels and the plug will be filled with the same grouting material used between the panels. The upper surface of the plug assembly forms a funnel that extends into the inner tube of the vacuum-jacketed fill adapter. When the line is filled with liquid, vapor will form inside the plug, increasing the gas pressure until it equals that of the liquid. A stable, gravity oriented interface will then form between the bottom of the funnel and the inside of the tube, preventing liquid hydrogen from entering the plug.

A capillary screen covers the upper inlet to the funnel section. When flow through the fill line is stopped, the cryogen in the line will vaporize. The capillary screen will permit the vapor to flow out of the line into the tank. Once all the liquid has vaporized, however, the capillary screen will position a stable liquid-gas interface and prevent liquid from flowing from the tank into the line. If valves are opened to initiate either fill or drain, the resulting pressure change in the line will force a flow of liquid or gas through the screen, permitting the line to refill with liquid. The lower portion of the insulator plug serves only as a retainer for the fiberglass batting which serves to limit convective heat transfer within the assembly. The fill adapter is not fastened to the insulator plug and it need only be installed to the tank flange to complete the system.

Special insulation panels were not designed and fabricated in advance to cover the simulated hardware items, i.e., the attaching bracket, the ring-frame segment, the vertical-stringer segment, and the semi-cylindrical outlet baffle, because the exact orientation of the cutouts in the standard panels for the hardware items would not be known until after these panels were installed.

A design study was conducted, however, to develop an approach for insulating over the internal protruberances, and figures 24 and 25 illustrate the concepts that were formulated. After the standard panels with cutouts have been installed, a template will be made to show the size and shape of the cutout and the location of the item to be insulated within the cutout. From this data, a special capping panel will be fabricated with a general outline corresponding to the cutout, minus a grout allowance. The panel height will exceed the hardware item by at least the nominal insulation thickness. The core ribbons will be cut away to provide a close fitting cavity in the panel for the item to be capped. On installation, adhesive will be applied to the tank wall and to the protruding simulated hardware to provide a seal between cells. A similar approach will be followed for the attaching bracket, except the bracket would extend through a cutout in the facesheet. After installation, silicone adhesive will be applied to form a seal between the facesheet and the bracket.

The insulation system design described above accomplishes the goal of insulating the entire inside surface of the tank including internally protruding hardware. The gas-layer concept has been applied for all parts of the insulation system, and it has not been necessary to rely on any other insulating method or to compromise the basic concepts of the capillary gas-layer system.

FABRICATION AND INSTALLATION OF INSULATION SYSTEM

Tooling concepts and fabrication techniques, used in the fabrication of the insulation system, were developed under Contract NAS8-25974, *Development of Advanced Materials Composites for Use As Internal Insulation for LH_2 Tanks (Gas Layer Concept)*. However, to a large extent, the current program and the referenced earlier program overlapped chronologically. As a consequence, some of the problems that we experienced were worked out simultaneously and cooperatively between the two programs.

In the prefabrication of insulation panels, we followed a procedure that had been developed on the basis of the small specimen experiments performed on the earlier program. This procedure, which was updated on the basis of experiences gained in the current program, is presented in Appendix A in the form used at the completion of panel prefabrication. The steps required in the fabrication of insulation panels are discussed in sequence in the following paragraphs.

Honeycomb Core Fabrication

The honeycomb core assemblies were fabricated by bonding ribbons of Kapton film along the required alternating node lines. This operation was performed with the ribbons in a flat plane. In the case of the D panels used for insulating the tank barrel, the ribbons were straight and the Kapton was purchased preslit to the final ribbon width. For the contoured panels to be installed on the tank domes, straight Kapton ribbons were also used, but were sufficiently wide to permit trimming the assembly after bonding to the proper outline.

The adhesive was applied using a simple stencil made from 0.5 mm (0.020 in.) thick acrylic sheet and a scraper blade. The stencil was installed in a printing fixture (fig. 26) that was equipped with a cover and a nitrogen purge system. The purpose of the purge was to extend the working time of the RTV-156 one part silicone adhesive which is activated by exposure to humid air. To purge the printing fixture, nitrogen gas was fed through a tube attached to the inside of the printing frame. Small holes in the tube served as purge nozzles, minimizing the amount of moist air reaching the adhesive. This enabled us to work the adhesive for at least 30 minutes.

For printing the straight ribbons for the D panels, the base of the printing frame was equipped with a punch to facilitate registration of the bond lines. After the ribbon was positioned in the frame, two 1/8-in. registration holes, spaced at exactly half the pitch of the bond line, were punched in each ribbon. Correct bond line registration was achieved by using a guidepost to align alternate holes when stacking the ribbons.

The stacking frame used to hold the ribbons in proper alignment until the adhesive had cured is shown in figure 27 (for the D panel). The ribbons were stacked against a rigid guide rail and forced into alignment by a flexible pad attached to a movable frame. This provided close alignment of the ribbons on the facesheet side even when the width of the ribbons varied within permissible tolerances. A padded pressure bar was then placed on the completed stack to apply a bonding pressure of approximately 2000 N/m^2 (0.3 psi).

For the contoured panels, essentially the same procedure was followed. In this case, however, the Kapton ribbon blanks were first cut to length. Using a drill guide, index holes were then drilled. Locator pins were installed on the printing and stacking fixtures in a matching pattern for alignment of the ribbons. The dome panels are made up of short and long ribbons (and intermediate length ribbons in the case of the A panels). For the short ribbons, the internal ends were trimmed before assembly because these ends are not accessible after the ribbons have been bonded into place. Kraft paper spacers were placed in the assembly as the ribbons were put on the stacking fixture to compensate for the reduced number of layers of Kapton at the inside end of the assembly because of the short ribbons. After the adhesive has cured, the core assemblies are trimmed. For the panels using straight ribbons preslit to the final width, only the ends require trimming. For the curved ribbon panels, the assembly was installed in a trim fixture and the ribbon outline was trimmed using a metal template. The trim fixture also incorporated locating pins to match the original drill guide. The outline was trimmed with a bandsaw, using a special no-set, fine tooth blade.

In the experiments leading to the selection of the RTV-156 silicone adhesive and in the early fabrication of insulation panels, several difficulties and unexpected characteristics were noted. These are summarized as follows:

(1) Initial cure time was decreased and bond strength was increased by controlling the humidity at which the Kapton had been stored prior to use to 40% RH or higher.

(2) Bond strength increased with increasing adhesive thickness in the range of 0.1 to 0.9 mm (0.005 to 0.035 in.)

(3) Bonds were not always permanent. In some instances, after several weeks aging, the strength of the bond at the Kapton-silicone interface decreased to a negligible value in the presence of moisture or high humidity. This characteristic could be readily demonstrated by applying a small pull force to two ribbons bonded together and then breathing on the bond. If the characteristic was present, the bond would instantly begin to peel apart. This characteristic was found to occur more frequently as the thickness of adhesive decreased; however, it was not apparent on newly bonded specimens, but occurred only after several weeks aging.

Because of these characteristics, the Kapton was pretreated, adhesive thickness was increased to near the maximum amount that would not spread excessively, and a postcure treatment was developed. To assure that the Kapton was conditioned to a high humidity level, it was either stored for a number of days in a high humidity environment or was soaked in demineralized or distilled water for a minimum of 12 hours. The latter method was more convenient, and the Kapton strips were wiped dry no more than 30 minutes before the bonding operation. For bonding with the RTV-156 adhesive, no primer is required on the Kapton. By using a 0.5 mm (0.020 in.) thick stencil, a minimum adhesive thickness of approximately 0.4 mm (0.015 in.) was obtained.

The problem of deterioration of bond strength in the presence of moisture or high humidity (previously described) was eliminated by development of a postcure procedure. After the core assembly was allowed to cure in a 40%, or higher, relative humidity environment for a minimum of 72 hours, it was postcured at 505°K (450°F) for 4 hours. An earlier postcure cycle at 339°K (150°F) served to extend the aging period by several weeks. Increasing the temperature to 394°K (250°F) increased the bond life, but the problem eventually recurred. Unfortunately this was discovered after a number of insulation panels had been fabricated and began debonding during ordinary handling. When it was determined that seemingly permanent results were obtained with a postcure cycle of 450°K (350°F) for 4 hours, the final cycle at 505°K (450°F) for 4 hours was adopted.

Priming of Core and Facesheet

After the honeycomb panel had been assembled and postcured, it was expanded on a rake and inspected. If no quality problems were noted, it was cleaned with trichlorethylene and sprayed with silicone primer (Dow Corning 1200). A 0.05 mm (0.002 in.) thick Teflon facesheet was also cut to size, cleaned, and primed. The primer was applied to the facesheet by spraying or wiping in two directions with a saturated cheesecloth pad. The latter method was preferred. For both the core and facesheet, enough primer was applied to permit visual detection, but an excess that would cause a heavy buildup was avoided. Some difficulty was noted in detecting which side of the transparent facesheet had been primed; it was therefore decided to routinely prime both sides of the facesheet. After cleaning and priming, all materials were handled only with clean white nylon gloves to prevent contamination.

The Dow Corning 1200 primer and many other silicone primers require hydrolyzation after they are applied. When the ambient relative humidity is in the normal range of 30% or more, this action takes place in a few hours at most. In our work area, however, the relative humidity dropped to near zero at times in the winter months when the outdoor temperature was very low. At such times, the silicone primer did not achieve a satisfactory cure, even after several days, and satisfactory bonds could not be made with the silicone adhesives.

To solve this problem, an enclosure was built in the work area and equipped with humidifiers (fig. 28). This humidity room provided a relative humidity of 40 to 60% at all times except weekends, when the humidifiers were not operating. The controlled humidity environment also reduces the cure time of the RTV-560 two-part adhesive used for facesheet assembly, and particularly the one-part RTV-156 adhesive used for core assembly for which water vapor absorbed from the air is the sole curing agent. All primer curing and bonding operations were subsequently performed in the humidity room.

Core-to-Facesheet Assembly

The facesheet-to-core bonding operation was accomplished using an assembly tool that positioned the core to its design size and contour and provided means for applying a differential pressure across the facesheet to hold it firmly against the core. Figure 29 shows the design of the rake-vacuum box assembly tool for one of the panels. Examples of the completed tools for the A, B, D, and E panels are shown in figures 30 through 33.

The primed core assembly was carefully assembled on the assembly tool rake, which provides fingers to control the position of each node bond in the panel. To bond the facesheet to the core, a uniform 1.6 mm (1/16 in.) layer of adhesive was first spread on a rubber or polyethylene transfer sheet and this sheet was assembled to the lid of the vacuum box. Next, the expanded core (installed in the assembly tool) was inverted, and this was also assembled to the lid of the vacuum box. A slight vacuum was then used to draw the coated transfer sheet against the core. After approximately 3 minutes, the vacuum was released and the assembly tool, with core installed, was set aside, still in the inverted position. The excess adhesive was allowed to drip for approximately 10 minutes.

After the tool was removed from the lid, the adhesive transfer sheet was removed and the facesheet was installed in its place. The vacuum box/core assembly was then reassembled to the lid and the facesheet was drawn against the core with vacuum (approximately 3500 N/m^2 or 0.5 psid) for a minimum of 12 hours to cure the adhesive. This method ensures intimate contact between the facesheet and the core ribbons, which is essential to achieve consistently good bonding.

In figure 34, two upper dome F panels are shown after this assembly operation, but before they were dimpled, perforated, and trimmed. An unexpanded core assembly is also shown.

Dimpling

Our original method for dimpling the Teflon facesheet was to install the panel in a vacuum box and to use vacuum to stress the material. A hand held heat gun was then used to apply a blast of controlled-temperature hot air to the material. Although this method produced fairly acceptable results, it had two major limitations: the success was somewhat dependent on the skill of the operator, and the temperature was not constant throughout the cross section of the airstream.

A number of experiments were conducted to develop an improved method for facesheet dimpling. One, using a heater blanket, appeared to be an excellent solution to the problem.

As before, the insulation panel (with the core bonded to the facesheet) was installed in a vacuum box and a vacuum was applied to stress the facesheet. Next, an electric heater blanket was positioned over the facesheet and light pressure was applied to

ensure contact with the facesheet. Finally, the temperature of the heater blanket was raised to 495°K (430°F) and held for 1 to 2 minutes at a vacuum of 8600 N/m^2 (1.25 psid). The dimples achieved by this method were very consistent, and dimple depths in excess of 0.12 times the span of the Teflon were achieved. Furthermore, the procedure was straightforward and was not dependent on operator skill. Figure 35 shows the heater blanket that was fabricated for dimpling the D panel.

The success of this method was short-lived, however. It was discovered that when the panel was subsequently heated to 450°K (350°F), the dimples almost completely disappeared due to shrinkage. (Apparently the Teflon did not reach a sufficiently high temperature to eliminate the "memory" of the film.) We found that we were unable to achieve the higher temperature required for permanent dimples using the heater blanket without creating hot spots that melted the film. Radiant heating was also unsatisfactory because of the high heat transmissivity of the Teflon.

We returned to the heated airstream as a means of achieving a sufficiently high temperature of the Teflon to eliminate the memory effect. In experiments, again using a hand-held heat gun, we found that the required dimpling temperature was very near the temperature at which the Teflon begins to melt. We did not measure the Teflon temperature, but the required airstream temperature was in the vicinity of 589°K (600°F). At the higher temperature, there was a tendency for the Teflon to melt through in spots unless the differential pressure across the facesheet was reduced. By reducing the pressure, however, no dimples formed until the temperature reached the critical value, that is, a sufficiently high temperature to produce facesheet dimples that would not shrink at 450°K (350°F). A differential pressure of 2500 N/m^2 (0.36 psid) was found to be sufficiently small that dimples would meet the shrinkage test.

We fabricated a dimpling heater (modifying and adding to an existing air-heater system) that discharged a narrow stream of hot air approximately 0.91 m (36 in.) long (fig. 36 and 37). In this assembly, the air is heated by two 5-kw electric heaters. One heater was connected to an on-off switch while the other was powered through a variable transformer. The heater was mounted on a swing arm assembly that could be moved across the insulation panel at a constant distance from the facesheet. In practice, several slow passes were made across the panel to achieve the maximum dimple depth possible.

Using this device, some melt-throughs occurred. These were apparently caused by occasional weak spots in the Teflon, because melt-throughs were random and no pattern of hot spots in the airstream could be detected. The occasional melt-throughs were tolerated, because repair of the damaged cells was straightforward and was considered an acceptable inconvenience.

The depth of the dimples we were able to produce was disappointing. After some experimentation we developed a 2-step dimpling procedure that resulted in some increase in the depth of the dimples. In the first step, the air temperature was controlled at 539 to 550°K (510 to 530°F), and the differential pressure was controlled at approximately 7500 N/m^2 (1.1 psid). In the first step, a dimple depth of at least 0.095 times the span of the facesheet was obtained. In the second step, the air temperature was increased to 583 to 600°K (590 to 620°F) and the pressure difference was decreased to 2500 N/m^2 (0.36 psid). Under these conditions, the dimple depth would decrease from that obtained in the first step, but was nevertheless greater than had been obtained with the one-step method. With this procedure, it was possible to maintain a dimple depth 0.075 times span, the minimum requirement, but little, if any, in excess of that value.

With the final method of dimpling, it was discovered that the overall panel width experienced a shrinkage of approximately 1.5%. However, panel height remained essentially unchanged. To compensate for this change in dimension, a full column of panels, 2½ cells in width, was cut from spare panels. Thus, the tank circumference was spanned with 8 full-size (16½-cell-width) panels plus one 2½-cell wide panel.

Facesheet Perforating and Trimming

The facesheet was perforated (one opening per cell) using a soldering iron with a 0.9 mm (0.035-in.)-diameter needle. When the needle is heated sufficiently, the holes are partially melted through thus eliminating tears in the facesheet. By carefully controlling the temperature of the needle, and after some practice, satisfactory holes can be produced with a hand-held soldering iron. However, if the iron is attached to a sliding mechanism, the temperature of the needle can be increased well above the melting point of the facesheet without producing elongated holes.

Figure 38 shows a panel being perforated by this method. This operation would lend itself to mechanization for high production rates. However, no particular problems have been experienced with the manual methods that we have used to date.

Next, the excess facesheet material around the perimeter of the panels was trimmed close to the core, removing approximately half of the outside bond line. This manual operation required considerable care and patience. For high production rates, a mechanized means for trimming the panels will be essential.

A barrel D panel is shown at this stage of fabrication in figure 39. In figure 40, four A panels are shown after assembly, dimpling, perforating and trim, nested together to form a ring.

Installation of Filler Material

Several methods were evaluated for installing the fiberglass filler material in the insulation cells. Grinding the material would greatly facilitate its installation, if a means were devised to hold the fibers in place in the cell. A method wherein the bulk fiberglass is vibrated uniformly into the cells and then the exposed surface is sprayed with a binder showed promise. Some types of silicone primers would probably perform the function of holding the fiberglass in place while also priming the bonding surfaces of the Kapton core ribbons. However, when we tried grinding the fiberglass batting, we found that its density increased by a factor of 2 or more.

Since system weight is an important consideration, we adopted a method of installing the filler material that consisted of die-cutting plugs of 1/2-in.-thick PF 105 fiberglass batting to the design shape (fig. 41 and 42). The filler plugs were cut 1% to 5% larger than the cells in length and width to provide excess material for compaction. Two 1/2-in.-thick plugs were used for each cell (for 1-in.-thick insulation).

In all of the insulation panels there are approximately 57 different sizes and shapes of cells, and in many of these cells the size and shape changes considerably between the wall side and the facesheet side of the panel. A computer program was devised and used to select a minimum number of filler plugs that would fit the 114 different positions for all the panels within the tolerance given above. This requirement was met with 9 different plug designs with high usage plus 6 designs for which 128, or fewer, were required. A total of approximately 30,000 filler plugs were required for all panels.

The computer program provided full-scale outline drawings for the plugs, and prepared a usage table. Die sets were made for the high usage items, and they were punched using a small pneumatic punch press. Using a sharp knife and template, the remaining plugs were cut by hand.

Panels were cleaned with trichlorethylene and the plugs were installed by hand according to the usage table. Care was required to prevent distortion or cocking of the cells, and to be sure that the points on the filler plugs fit properly into the points in the cells. After all the plugs had been installed in a panel, they were carefully compressed to a depth of approximately 1.6 mm (1/16 in.) below the edge of the core ribbon.

Primer was then sprayed on the tank wall side of the core to prime the core for installation and retain the filler material during handling. Although this method of using the primer to hold the filler plugs in place had seemed promising in small sample tests, it did not work well on the whole. This apparently was because of the tendency of the primer to eventually become dry and chalky, after which it did not retain the fiberglass plugs. Two panels are shown in figure 43 after the filler plugs had been installed.

Quality Control

Even in the small test tank insulated in this program, the number of insulation cells is quite large. But that number is small compared to the number of cells that would be involved in a booster hydrogen tank. It is obvious that Quality Control procedures that minimize the need for a cell-by-cell inspection should be developed. Ideally, the quality of the insulation panels and their installation would be assured by process control and only spot inspections would be required.

Because of the developmental nature of this program, the tooling, equipment, and fabrication procedures were often inadequate to ensure consistent quality, and considerable rework and repair was necessary. Initially, our Quality Control procedures and criteria were also inadequate, and a number of defects were not detected until they had been repeated in a number of panels. When this inadequacy was fully realized, an intensive revision of the Quality Control program was undertaken, and new procedures for enforcing quality control were put into effect. More detailed inspection criteria were also developed.

The quality of the insulation panels was controlled primarily by visual inspections at six points in the fabrication sequence. These inspections were performed after

(1) printing, assembling, trimming, and postcuring the unexpanded core panels;

(2) priming the core panel and facesheet;

(3) bonding the facesheet to the core;

(4) dimpling the facesheet;

(5) perforating and trimming the panel;

(6) filler plugs were installed and the panel was primed on the wall side.

For the most part, quality checks were made by visual inspections. When the integrity of bonds could not be verified visually, we used a leak test to verify the seal between adjacent cells. This test was performed using a nitrogen pressure source and a rotometer-type flowmeter (fig. 44).

To accomplish the test, the cells were pressurized from the open (wall) side using a flat, soft rubber seal pad connected to the flowmeter by a hose. The nitrogen pressure was regulated to 14,000 N/m^2 (2 psig) with the flow shut off at the seal pad. The pad was then pressed onto the open side of the cell and the flow rate was noted. Leak rates below 8×10^{-8} std m^3/sec (0.01 scf/hr) can be detected using this method.

The same test was used to check for leaks after the panels had been installed. In this case, a smaller nozzle was pressed to the facesheet so as to cover one-cell at a time, allowing the cell to be internally pressurized. Leaks large enough to be detected with the flowmeter were considered unacceptable. However, in the case of installed panels, it was discovered that one could detect any significant cell leakage without watching the flowmeter. The regulated pressure was increased to 28,000 N/m^2 (4 psig), and leakage could be detected, after gaining experience, by the rate of inflation of the cell and the tightness of the facesheet when inflated. Of course, the flowmeter could be checked in case of doubt in the visual check.

A serial number was assigned for and marked on each panel, and a record folder was made for each panel. A quality control document, kept in the panel record folder, served as an inspection checklist, a record of acceptance, and an authorization to proceed to the next step. This Panel Inspection Record is presented in Appendix A together with the detailed criteria used during panel inspection. When a defect was noted at any of the

inspection points, a reject tag was placed in the folder (or attached to the panel). The reason for the reject was noted on the tag. All rejected panels were reviewed for disposition, and in a majority of cases the disposition was to rework the panel. In this case, the reject tag was cleared by a rework authorization form that specified the rework to be accomplished. Only when all the repair work had been inspected and signed off on the rework authorization form could the inspection record be updated to permit the panel to proceed to the next fabrication step. All reject tags and rework authorization forms, as well as the inspection record and an operator sign-off sheet were maintained in the panel record folder.

Panel Repair

Repair techniques were available, or were developed, for correcting most of the defects encountered in fabrication of the insulation panels. The more important types of repairs are described in the following paragraphs.

The most common problem encountered was skips or very thin spots in the facesheet-to-core bond, which appear to be potential leak points. These were readily repaired by manually applying a thin bead of adhesive over the defect area, generally on both sides of the ribbon. This was accomplished by using a narrow spatula or a hypodermic syringe with a 16-gage needle, filled with RTV-560 adhesive diluted approximately 5 to 10% with General Electric RTV-910 thinner. In either case, care must be taken to prevent excessive adhesive from building up and/or spreading the adhesive over a larger area of the facesheet than is desirable.

In some instances, we found that cells on the perimeter of the panel were distorted because of improper fitting of the core to the assembly rake or because of inaccuracies in the tooling. These cells have been successfully repaired. The facesheet was first debonded from the core over the distorted area by failing the adhesive. A template of the proper size and shape was then inserted into the cell to hold the ribbon to the proper contour, and adhesive was applied on the outside of the cell at the facesheet-core intersection using a spatula or syringe. After this first adhesive cured, the template was removed and the bond was completed on the inside intersection of the core and facesheet. An extraneous line of adhesive will remain on the facesheet after this repair is completed. However, no resulting problem in subsequent dimpling of the facesheet has been experienced. Figures 45 and 46 show a distorted cell before and after being repaired.

In a very few cases, tears occurred in the Kapton core ribbon, beginning from the open or wall side of the prefabricated panel. These tears have been repaired by bonding a small Kapton patch over the tear using RTV-156 adhesive.

In some instances the Teflon melted through in isolated cells during dimpling. In such instances, the facesheet was trimmed out for these cells using a sharp knife. A predimpled Teflon patch was then bonded directly over the remaining bond around the perimeter of the cell using RTV-156 adhesive. Figure 47 shows a specimen with a facesheet patch. These patches were cut from facesheets that had been removed from rejected panels after the dimpling operation was completed. No difficulty was experienced because of the RTV-560 that remained on the Teflon.

Small holes in the facesheet were repaired by bonding in a small Teflon patch over them, using either RTV-156 or RTV-560. This method should be limited to holes no larger than 3 mm (1/8 in.) in diameter. It was found that patches in this size range did not significantly affect the subsequent dimpling operation.

In trimming away the excess facesheet material around the perimeter of the cell, the facesheet and adhesive will occasionally be completely removed up to the outer edge of the Kapton ribbon in small areas. This does not in itself affect the integrity of the cell, since the bond will be complete on the opposite side of the ribbon, but such overtrimmed spots were considered potential leak points and were repaired by applying a thin layer of RTV-560 adhesive so that it overlaps the Kapton-Teflon intersection.

The above repairs apply to insulation panels that have not yet been installed on a tank wall. In general, they also can be used to repair damage that may occur after installation. For damage to large areas, however, our recommended method is to completely remove the damage area, carefully trimming the facesheet to the boundary of the remaining cells. A special panel must then be fabricated. This panel will be slightly undersized, but can be bonded in place and grouted in the standard manner.

Special Panels

In addition to the standard A thru F panels, one-of-a-kind panels were fabricated to insulate over the simulated internal hardware. These panels, covering the semi-cylindrical outlet baffle, the ring frame segment, the vertical stringer segment, and the attaching bracket were not fabricated until after the

basic panels, with appropriate cutouts, had been installed around the protrusions. Patterns were taken of the actual cutouts and the location of the hardware items within the cutouts.

The special panels were fabricated using the same design approach and fabrication methods, although simpler tools were improvised for these one-time requirements. The panel for the semi-cylindrical cylinder was made with a 152 mm (6 in.) insulation thickness, and the others had a thickness dimension of 89 mm (3.5 in.) The panels were designed to have outside dimensions corresponding to the cutout, less a 3 mm (0.125 in.) allowance for the grouted joint. An interior cutout was made in the panels to provide for a close fit to the hardware item. The panels to cover the ring frame and the stringer are shown in figures 48 and 49. The semi-circular panel for the outlet device is shown in figure 50 and the attach bracket panel is illustrated in figure 51.

The insulator plug providing the transition from the internal insulation to the vacuum jacketed fill and drain plumbing was fabricated using conventional techniques for fiberglass-epoxy layup. Wooden forms were machined for fabrication of all the component parts except the cover. A form for this part, with its repeating contours, was assembled from 16 plaster castings. The completed insulation plug assembly is shown before installation in figure 52. A flat baffle, also made of fiberglass-epoxy, was attached to the plug assembly. This baffle was incorporated to divert the flow of hydrogen entering the tank and minimize tank pressure collapse from sudden cooling of the gas.

Installation

The insulation panels were installed by bonding them to the tank wall. The basic procedure requires the following steps:

(1) laying out the tank for proper positioning of the panels;

(2) cleaning and priming the interior of the tank;

(3) applying the adhesive;

(4) installing the panels in the proper locations;

(5) holding the panels firmly against the tank wall until the adhesive is cured;

(6) filling joints between the panels with grout compound.

The means used to accomplish these requirements are described in the following sections.

Installation Tooling. - In a spacecraft application of the internal insulation system, it would be important to minimize weight and to optimize thermal performance. Both of these parameters are enhanced by use of a minimum quantity of adhesive in installing the panels.

One way to minimize the quantity of adhesive used in panel installation is to use a stencil in applying the adhesive to the wall. The stencil would apply a narrow adhesive pattern that would register with the core ribbons when the panel was put into place on the wall. To do this successfully, two requirements must be met: (1) the pattern of the core ribbons must be regular and repeatable; (2) means must be provided to assure accurate positioning of the panels to register with the stencil-applied adhesive.

In development tests conducted under contract NAS3-14384, we were able to successfully install small insulation panels using this method. On this basis, we decided to use the same technique in installing the 16 D panels on the tank barrel section to further evaluate the feasibility of the approach and to fully demonstrate a flightweight insulation system.

To achieve uniformity of the ribbon pattern in the insulation panels, we used an assembly tool (previously described in this chapter) which controlled the location of each node bond. To assure proper registration of the panels with the adhesive, we designed and fabricated an installation tool for positioning a stencil while applying the adhesive. This same tool was used to position the insulation panels as they were brought into contact with the tank wall. The tool was located in the proper position on the tank wall by locator buttons (small steel washers) bonded to the tank wall in accordance with an overall layout drawing. The tool was held in place with 6 suction cups connected to a vacuum pump.

We fabricated an aluminum test panel, rolled to the tank radius and mounted vertically on a stand, to check the installation tooling and procedure. Two spare D panels were installed on the aluminum panel. Unfortunately, we were unable to obtain photographs of this operation in progress. In figure 53 the installation tool is shown in place on the panel after the test was completed. The stencil is in place in the upper panel position. Figure 54 shows the tool with the stencil removed. The same frame that held the stencil also holds the insulation panel as it is brought into the proper position on the tank wall.

Considerably more effort was required than had been planned in fabrication of this tool. Modification of the tool was required to accommodate the distortion that developed in the tank when it was rebuilt; adjustment of the tool was required to achieve precise alignment of the panels. The checkout panel installation was accomplished with only moderate difficulty. When the panels were subsequently leak-checked, however, we found an unacceptable number of intercell connections in several areas.

The checkout results were determined to be unacceptable, and because of budget and schedule considerations it was decided that further development of this installation method could not be accomplished. We then proceeded with the installation of panels in the tank, applying adhesive over the entire surface. However, it did not follow that the stencil method for applying the adhesive was impractical. In fact, considering the complications that were imposed on this experiment by the distortion of the tank welds and the shrinkage of the panels during dimpling, the results obtained were remarkably close to being successful.

Cleaning and Priming. - Paint and other deposits were removed from the inside tank surface by hand cleaning. At this point, the locator buttons for the installation tool were installed, since the checkout of this tool had not yet been accomplished.

The interior was vapor-degreased by installing a vessel for boiling trichlorethylene in the tank. A boiling rate of 0.030 to 0.037 m^3 (8 to 10 gal) per hour was achieved using a power input of 3 to 4 kw, and this rate was maintained for approximately 2.5 hours.

The tank interior was dry-grit-blasted next using 20- to 40-grit silica. This was done after the sandblast equipment was cleaned and a sample panel was blasted and then checked for cleanliness with a water break test. Clean nitrogen was used in the grit-blasting process. Immediately following the grit-blast operation, the tank interior was sprayed with Dow Corning 1200 primer of a sufficient thickness to permit visual detection. The above operations completed the preparation of the tank for installation of the insulation system.

Panel Installation. - After cleaning and priming the tank, it was moved to the installation area, placed upright on a stand, and a scaffold providing access to the tank manway was erected about the tank as shown in figure 55. A vacuum bag to cover the entire tank interior except for the manway and the fill port was fabricated of 0.15 mm (0.006 in.) polyethylene film. This bag was placed in the tank and sealed around the fill port and the

manway opening. Expandable rings of semi-flexible plastic pipe, 19 mm (0.75 in.) in diameter, were installed at the upper and lower dome to the barrel intersections to hold the bag in place. The purpose of the vacuum bag was to force the panels firmly against the tank wall while the adhesive cured. It also served to protect the wall from contamination.

Next, a ladder and work platform, constructed to the drawing shown in figure 56, was installed in the tank. The work platform consisted of one fixed and one removable portion, and could be rotated to any desired orientation.

Panels were installed in the following sequence:

(1) two A and four B panels on bottom dome;

(2) two A and four B panels plus two-cell A and B panels to complete bottom dome;

(3) all C panels (18) consisting of curved and straight sections;

(4) lower tier of D wall panels, consisting of eight full panels plus two-cell panel;

(5) upper tier of D panels;

(6) all E panels, straight and curved section, extending insulation onto upper dome;

(7) F panels on upper dome, consisting of eight full panels plus two-cell panel.

To install panels, the vacuum bag was cut open in the required area, adhesive was applied to the wall, the panels were positioned in place, the vacuum bag was resealed and connected to a vacuum pump, and a vacuum was applied until the adhesive had cured.

A fixture was used to control the outline of the two A and four B panels first installed. In figure 57 these panels are shown in place, with the cutouts as required for clearing the simulated outlet baffle. The outline fixture, the vacuum bag, and the work platform with one half removed can also be seen in this photograph.

The silicone adhesive was spread on the tank wall by hand, using a trowel with 2 mm (0.075 in.) holdup vanes to evenly distribute the adhesive. A vacuum of 750 to 2500 N/m^2 (3 to 10 in.

water column) was achieved, depending on the success achieved in eliminating leaks in the vacuum bag. The vacuum pump requirement was to remove a large volume of air at a relatively low vacuum level. To achieve this, we used two vacuum cleaners in parallel. They were operated with a fairly high bypass opening and a reduced voltage of 60 to 80 volts to prevent them from overheating during the 14- to 20-hour periods of operation.

After all the bottom panels had been installed, they were checked by filling the tank bottom with liquid nitrogen. No damage occurred because of this cryogenic check.

Tooling was fabricated to hold the panels (other than the bottom panels) in place from the time they were initially positioned until the vacuum bag had been installed and vacuum applied to force the panels into contact with the wall. However, it was found that the panels would stay in place on the wall, and the holding tools were not required. The previously installed panels, with which the panels being installed were nested, proved adequate to control the positioning of the insulation.

Figure 58 shows the tank interior after the wall panels were installed. In this photograph, the complete work platform obscures the view of the bottom panels.

The standard panels were trimmed as required to provide cutouts for the hardware items installed on the wall. Figure 59 shows the ring frame and stringer segments and the attach bracket before being insulated. After all of the standard panels had been installed, the special panels were installed over the simulated hardware. Push rods and foam pads, rather than the vacuum bag, were used to hold these panels in place during bonding. The gaps between these panels and the surrounding cell walls, as well as the gaps between all standard panels, were filled with a grouting compound consisting of GE RTV-560 silicone adhesive thickened with from 1.5% to 2% of fumed silica (Cab-O-Sil). The grout was applied using a Semco pneumatic grout gun with a thin modified nozzle.

The final step in the installation process was the bonding of the fill and drain adapter plug. This was necessarily the last step because this plug is mounted in the outlet line and occupies the space required for mounting the work platform. Access for installation, final grouting, inspection, and repair in this area was possible, however, using a small wooden platform supported on soft polyurethane foam. Figure 60 shows the tank interior after all insulation had been installed. Figure 61 is a view of the upper dome and manway as viewed from the bottom of the tank. The insulated manway cover is shown in Figure 62.

Inspection and Repair

All cells, except some of those above the expected maximum liquid level, were leak-checked. Of the approximately 15,000 cells in the complete system, an estimated 800 to 1000 cell interconnections were found. A few of these were due to defects in the prefabricated panels, such as node bond skips, but a vast majority of the interconnections occurred between the core ribbons and the tank wall. These were caused by the following factors:

(1) inadequate wetting action of the adhesive;

(2) entrapped bubbles in the adhesive;

(3) displacement of adhesive due to sliding of the panel after contact with the wall.

The interconnections were repaired by the following procedure. A small opening was made in the facesheet. Thinned silicone adhesive was applied over the wall-core ribbon intersection using a hypodermic needle. The facesheet opening was then closed by bridging with one-part GE RTV-156 silicone adhesive.

During inspection of the insulation after installation, a high incidence of failures of the facesheet-to-core bond was encountered in one of the barrel D panels. These failures was not initially present, but occurred when the individual cells were internally pressurized to 27,000 to 35,000 N/m^2 (4 to 5 psi) during leak-checking. The failures occurred at the interface between the Kapton core ribbon and the silicone adhesive, and were due either to improper application or cure of the silicone primer on the Kapton. This panel was removed entirely and replaced with a spare panel. The removal and replacement procedure proved to be straightforward, and no difficulty was encountered.

In addition, some facesheet-to-core debonds occurred at the panel perimeters caused by stresses incurred during installation. These were repaired by a simple rebonding process using either the RTV-560 or RTV-156 silicone adhesives. On completion of all repairs, the tank was moved to the test area for cryogenic testing.

TEST PROGRAM

The insulated tank was tested to determine its operational characteristics and to evaluate the ability of the insulation system to withstand the simulated environment of a reusable shuttle boost tank. The specific objectives of the test program were to:

(1) measure the thermal insulating capability of the system under conditions similar to the ground-hold mission phase.

(2) determine any degrading effects on the insulation system resulting from fill, pressurization, heating of the tank wall to 450°K (350°F), drain, and warm-up of the tank.

(3) determine the purge characteristics of the insulation system, and formulate a suitable purge procedure. This purge must assure that sufficient air in the insulation cells is removed to prevent the possibility of an explosive hydrogen-oxygen mixture, and reduce the content of condensible gases to a small value that will not affect the proper functioning of the insulation. On returning the system to an inert condition, the hydrogen must be removed from the cells to eliminate the possibility of ignition or explosion.

The insulating capability of the system was evaluated by filling the tank with liquid hydrogen and measuring the rate of boiloff of gaseous hydrogen. The external tank temperature was measured at a number of points, and was controlled by applying heat to maintain stable operating conditions. Insulation system performance was determined by comparing the measured rate of boiloff with that predicted on the basis of thermal conductivity measurements previously obtained in flat-plate calorimeter testing.

The tank wall was cycled to a temperature of 450°K (350°F) while the tank was filled, or partially filled, with liquid hydrogen to simulate the operational environment. The tank was also internally pressurized to 69,000 N/m^2 (10 psi) during each of five temperature cycles. By repeating the boiloff rate test after the series of temperature and pressure cycle tests and comparing the boiloff rates, the effect of the cycle tests on system performance was determined.

To determine the purge characteristics of the insulation system, we equipped five representative cells with gas sampling instrumentation. Purge tests were conducted to replace the initial air or nitrogen in the cells with helium, and to purge the cells with nitrogen when they initially contained hydrogen and/or helium gas. Small gas samples were withdrawn at specific intervals and analyzed to provide a measure of the completeness of the purge operation.

Descriptions of the test equipment and setup, the testing as it was accomplished, and results are presented in this chapter.

Description of Test Setup and Equipment

The cryogenic tests were performed at our Propulsion Research Laboratory, located at our Waterton facility near Denver. The test tank was set up in a test cell, routinely used for liquid hydrogen testing, and all instrumentation read-out and control equipment was located in a remote test control center.

Tank Qualification

Because of the potential hazard encountered when using liquid hydrogen, we performed a cryogenic proof test of the test vessel before installing the insulation system. The test vessel was set up on the aluminum tank stand, which was fabricated for use in the test program, and was filled to overflow with liquid nitrogen. The pressure was increased by closing both the fill and the vent values, and was allowed to reach 131,000 N/m^2 (19 psig). The vent valve was opened to relieve the pressure, and the tank was drained and allowed to warm up.

All major welds in the tank were then radiographically inspected. The X-ray films were compared in detail with those taken before and after the tank was proof tested to 145,000 N/m^2 (21 psig) with water at ambient temperature. No flaw growth could be noted, and none of the flaws that could be detected were judged to be significant. The proof test pressures were selected on the basis of a stress analysis performed after the tank had been rebuilt, and which analysis considered the distortion in the dome-to-barrel weld areas. A normal operating pressure of 69,000 N/m^2 (10 psig) and a maximum operating pressure of 107,000 N/m^2 (15.5 psig) were selected. The pressure capability was found to be limited by potential buckling caused by compressive stresses developed near the dome/barrel junction.

Following the cryogenic proof test, the tank was leak checked using a helium mass spectrometer leak detector system.

Plumbing and Test Setup

After the insulation system had been installed, inspected, and repaired, the tank was again set up in the test cell as shown in figure 63. The tank exterior was painted flat black to increase radiant heat transfer. The overall cell layout and plumbing schematic is shown in figure 64.

The tank was connected (during test) to two 5.68-m^3 (1500-gal) hydrogen supply trailers through a 31.75-mm (1.25-in.) diameter vacuum jacketed facility plumbing system. The transition from the facility plumbing system to the test tank fill and drain port was through the vacuum-jacketed fill adapter shown in figure 65. The trailer connections were located in a service cell area (part of the liquid hydrogen test complex) where either trailer could be replaced by a full one when empty, without interrupting the test in progress. All system liquid valves were remotely operated from the control center.

The vent port of the test tank was connected to the 152-mm (6-in.) diameter, 12-m (40-ft) high vent stack through a 51-mm (2-in.) throttling valve, a 102-mm (4-in.) two-position valve and a 51-mm (2-in.) burst disk with a design burst pressure of 103,000 N/m^2 (15 psid), all connected in parallel. The 51-mm (2-in.) throttling valve was controlled from a loading panel in the control center and the 102-mm valve was remotely operated, but was also connected to a pressure switch set to automatically open the valve at 86,200 N/m^2 (12.5 psig) tank pressure. Tank purge control valves for nitrogen and helium were manually operated from a remote panel located outside the cell.

Instrumentation

Tank instrumentation is shown in figure 66. Fifty-three chromel constantan thermocouples were spot-welded onto the tank wall, and ten were installed on an instrumentation rake inside the tank. An additional six chromel-alumel thermocouples were installed on the tank wall as control sensors. Kistler Redmond nichrome hot wire type liquid level sensors were also installed on the rake at 10% intervals of tank volume from 10% to 90% and at 92%. The thermocouples were read out by means of a digital

printing millivoltmeter, except for control thermocouples and ten selected thermocouples which were patched to potentiometer-type strip chart recorders for trend monitoring. Liquid level was indicated by a Kistler Redmond amplifier-indicator-signal unit.

Tank vent flow rate was measured during heat flux tests by an orifice flowmeter. The orifice was mounted in an orifice holder with flange taps in a 50.8-mm (2-in.) meter run. Differential pressure was read out through an electronic differential pressure transducer and a strip chart recorder. Backup measurement of boiloff flow rate was obtained by logging the times that level sensors were uncovered during heat flux tests

All read-out devices and the pressure and differential pressure transducers that were used were subjected to periodic calibration checks, and their accuracy was verified before the tests. The thermocouples and the orifice meter run were not calibrated; rather, manufacturers' certifications and orifice calculations were taken as a basis for accuracy determinations. Overall system accuracy was calculated to be less than 5% of nominal flow rate for the flowmeter, less than ±3°K (±5°F) for temperature measurements at the expected wall temperatures (but possibly much greater at LH_2 temperature), within ±5 mm (±0.2 in.) for liquid level measurements, but repeatable to ±2.5 mm (±0.1 in.), and within ±3450 N/m^2 (±0.5 psi) for tank pressure.

Tank Heater System

A radiant heating chamber was fabricated to provide a means for heating the tank walls to 450°K (350°F). This heat chamber was fabricated in two halves, and when assembled, enclosed the tank. It is shown as installed during the thermal testing in figure 67. The heater enclosure was fabricated of aluminum specular reflector plate, and the heater assembly uses 576 1000-watt quartz infrared lamps connected to three control zones. These zones, lower, center and upper, provided a means of compensating for the uneven cooling of the tank wall because of variations in the liquid level in the tank. Each zone was connected to a modulating controller with 150-kva control capability. Each controller was equipped with a feedback control circuit and was connected to thermocouples mounted on the tank wall.

The heat chamber enclosed the entire tank barrel section and all of the upper dome except the manway. It was attached to a flange incorporated in the tank stand so as to close the bottom of the annular volume between the tank and the heater. A purge ring was installed at the bottom of the annulus, and a nitrogen purge of this volume was maintained throughout all tests.

Purge Sampling System

The system used to obtain purge gas samples from the instrumented cells is illustrated in figure 68. Sample containers were connected through a valving manifold to the cell interior. The purge sampling setup depends on a calibrated molecular leak to permit the collection of an adequate sample (for mass spectrometer analysis) within a reasonable time period, but not so large as to create a significant disturbance of the gas in the cells. Before withdrawing a sample, the cell isolation valve was closed and the vacuum pump and sample container valves were opened. The system was evacuated using a mechanical vacuum pump to a pressure on the order of 0.001 atmospheres. To obtain a sample, the cell isolation valve was opened for three to five seconds to remove the gas trapped between the valve and the leak. Then, the valve to the vacuum pump was closed and the cell isolation valve opened. After approximately 30 seconds, the cell isolation valve and the sample container valve were closed and the sample container was removed for analysis. Another sample container was then installed for the next test. A purge sample manifold with the sample container is shown in figure 69. The sample container with identification label extends upward and the vacuum pump connection extends downward.

Before use, the sample containers were solvent-cleaned and then baked in a vacuum to remove any contaminants. After the gas samples were taken, the containers were analyzed using a laboratory mass spectrometer to determine the fraction of the purge gas in the cell, either nitrogen or helium, and consequently the maximum contaminant level.

Testing

After all of the plumbing and instrumentation had been connected, the tank was filled with liquid nitrogen as a check of all equipment and to verify the test procedure. Several instrumentation problems were rectified, a valve operator was replaced, and other minor adjustments and repairs were accomplished. After warmup, the tank was purged and then pressurized with gaseous hydrogen. All connections and seals were then checked for leakage using a portable hydrogen detector.

Cryogenic Tests. - The cryogenic test series using liquid hydrogen was then conducted. It consisted of the following steps:

Test 1 - (1) filled tank to 90% and measured boiloff rate;

(2) heated tank wall to 450°K (350°F), pressurized to 69,000 N/m^2 (10 psig), depressurized and drained;

Test 2 - (3) filled tank (after warmup) and performed two temperature and pressure cycle tests (450°K, 69,000 N/m^2);

(4) measured boiloff rate;

(5) performed fourth temperature and pressure cycle test, drained tank;

Test 3 - (6) filled tank (after warmup) and performed fifth temperature and pressure cycle test;

(7) measured boiloff rate, drained tank;

Test 4 - (8) filled tank (after warmup) to 90%, measured boiloff rate, drained tank followed by warmup.

The test sequence was modified slightly from that originally planned because of difficulty in obtaining sufficient liquid hydrogen. Four 5.63-m^3 (1500-gal) LH_2 trailers were used in performing the tests. However, one trailer became unavailable because of a mechanical failure, and several short loads were received for unknown reasons. Because of this, only the first and last boiloff tests were accomplished with the tank initially filled to 90%.

A graphic description of the tests is provided by figures 70 through 73, in which the liquid level is plotted against time. Boiloff rate during the boiloff measurement periods is also plotted, and the figures are annotated to indicate the sequence of events. In figure 74, tank wall temperature and tank pressure are plotted vs time for a typical temperature and pressure cycle sequence. Average tank barrel temperature was controlled to 256° ± 5°K (0°F) except during the temperature cycle tests. The lower dome temperature, which was not controlled, varied from 152° to 188°K (-186° to -121°F) depending on the amount of frost buildup. The colder temperatures noted on the lower dome were also an indication of damage to the insulation. The tank was fully vented, except during the pressure cycle tests, during boiloff measurement and when the cryogen was being transferred back to the supply vessel. During boiloff measurement, the vent gas was routed through the meter run, resulting in a tank pressure of 7,000 to 22,000 N/m² (1 to 3 psig), depending on vent flow rate. Other pertinent test data is summarized in table IV.

TABLE IV SUMMARY OF TEST PARAMETERS

Event	Boiloff Rate Measurement									Temperature/Pressure Cycle				
	Duration		Liquid Level %	Average Tank Temperature				Vent Rate		Maximum Wall Temperature		Maximum Pressure		Liquid Level, %
				Lower Dome		Barrel (to liquid level)								
	k-sec	hr		°K	°F	°K	°F	kg/sec	lb/min	°K	°F	N/m²	psig	
1 Boiloff Rate No. 1	3.6	1	90 60	188 179	-121 -137	254 255	-2 -1	3.14×10^{-3} 2.33×10^{-3}	4.15 3.08					
Temperature/Pressure Cycle No. 1										446	343	73,766	10.7	90
2 Temperature/Pressure Cycle No. 2										465	375	72,387	10.5	87
Temperature/Pressure Cycle No. 3										466	379	69,630	10.1	60
Boiloff Rate No. 2	1.5	0.42	65 50	179 174	-139 -147	252 259	-6 7	3.33×10^{-3} 3.02×10^{-3}	4.4 4.0					
Temperature/Pressure Cycle No. 4										456	361	68,947	10.0	52
3 Temperature/Pressure Cycle No. 5										458	364	69,630	10.1	77
Boiloff Rate No. 3	6.9	1.9	40 10	163 163	-167 -167	257 254	3 -3	2.52×10^{-2} 1.04×10^{-2}	3.33 1.38					
4 Boiloff Rate No. 4	7.5	2.1	90 50 20	152 155 154	-186 -181 -182	261 259 255	10 6 -2	6.4×10^{-2} 3.42×10^{-2} 1.52×10^{-2}	8.43 4.53 2.01					

In the initial boiloff rate test, the insulation performed approximately as predicted. With the tank filled to 90%, the boiloff rate was 3.14×10^{-2} kg/sec (4.15 lb/min), or 32.6%/hr. When the actual tank wall temperatures were considered, an expected boiloff rate of 3.08×10^{-2} kg/sec (4.07 lb/min) was calculated on the basis of previous calorimeter test results.

During the final boiloff rate test, the vent flow rate was 6.4×10^{-2} kg/sec (8.43 lb/min) or 66.2%/hr, or 2.03 times the original boiloff rate. Careful inspection of the test data indicates that no apparent degradation occurred until the first temperature-pressure cycle test. Because of the short fill on the second boiloff test, it could not be determined exactly how much of the degradation had occurred at this intermediate point. From the data that was obtained, however, it was estimated that about 2/3 of the increase in boiloff rate had occurred at that time. When the tank was opened after the cryogenic testing was completed, a large number of tears in the Teflon facesheet were discovered. This accounted for the increased boiloff rate. This damage to the insulation system, other observations after detailed posttest inspection of the insulation, and analysis of test results are discussed in the next chapter.

Purge Tests. - Because of scheduling considerations, the purge tests were not performed before the cryogenic tests as originally planned, but instead they were the final tests of the program. As part of the cryogenic test procedure, we purged the tank and insulation using the pressure purge method. This method consists of 12 cycles to 69,000 N/m^2 (10 psig), each with a 3-minute hold, and then venting to atmosphere. It is essentially the same method we have used successfully in the past for small scale tests.

Before beginning the purge tests, we inspected the individual cells that were instrumented for purge sampling and found them to be intact. The tank was then closed and the purge tests were conducted in the following sequence.

(1) initial tank contents--hydrogen and helium mixture;

(2) sweep purge with nitrogen;

(3) sweep purge with helium;

(4) change tank contents to nitrogen; and

(5) pressure purge with helium.

The sweep purge tests were accomplished by feeding nitrogen into the tank at the bottom and allowing it to flow out of the tank at the top; the reverse direction was used for helium. The flow rate was initially set to approximately one tank volume per five minutes. After ten minutes, the flow was adjusted to a very low rate, estimated at less than one tank volume per hour. Results of the sample analysis indicated that the gas initially in the cell was reduced to 5% (mole fraction) within a maximum period of 3 to 4 hours for both purge conditions.

Removal of nitrogen from the insulation cells by the pressure purge method was accomplished in the following manner. The tank was pressurized by feeding helium into the top of the tank to 10 psig. After a 3-minute hold period, the tank was vented to ambient pressure (approximately 12 psia). The maximum rate of pressure change was limited to 38 N/m^2-sec (1/3 psi/min). This procedure was repeated for a total of 12 cycles with gas samples taken after the fourth, eighth and twelfth cycles. Because of a change in sampling procedure and leakage of one of the sample bottles, the results were somewhat inconsistent and are discussed in the next chapter.

ANALYSIS

An analytical review of the total program was made. The review included evaluation of (1) thermal performance of the insulation system and the effectiveness of purge procedures in comparison with predictions; (2) design, fabrication, installation, inspection and repair methods, and (3) analysis of the damage sustained by the insulation during test. Results of these analyses are presented in this chapter.

Thermal Performance

Boiloff rate predictions were based on test data obtained under Contract NAS8-25974, *Development of Advanced Material Composites for Use as Internal Insulation for LH_2 Tanks (Gas Layer Concept)*. Thermal conductivity was measured in that program for the internal insulation system using the same materials and insulation thickness that we installed in the model tank. A guarded hot plate calorimeter, insulated on two sides and submerged in liquid hydrogen, was used to obtain the effective thermal conductivity of the insulation as a function of the hot-side temperature.

The results of these thermal conductivity tests are shown in figure 75. Test data for horizontal and vertical orientations are given. The figure also shows the integrated or effective thermal conductivity of gaseous para hydrogen. The effective thermal conductivity of hydrogen gas between the temperature of the liquid (20°K) and any other temperature, T_1, is defined by

$$k_{(T_1,\ 20)} = \frac{\int_{20}^{T_1} k(T)\ dt}{T_1 - 20},$$

where

$k_{(T_1,\ 20)}$ = effective thermal conductivity of a layer of hydrogen gas with boundary temperatures of 20°K and T_1 (°K)

k(T) = the thermal conductivity of gaseous para hydrogen at any temperature, T, as given by WADD Technical Report 60-56.*

In the boiloff tests that were conducted, the temperature of the tank barrel was controlled to approximately 256°K (0°F). The lower dome was not heated, but assumed an equilibrium temperature on the basis of heat transfer by convection and radiation to the surrounding environment. The steady-state wall temperatures during the initial heat flux test with the tank filled to 90% are summarized in table V. This table also includes calculations of predicted heat transfer rate, using the measured values of the wall temperature. The temperature zones correspond to the thermocouple locations as shown in figure 66. Expected thermal conductivity was determined from the previous test data, and total expected heat transfer was calculated for each of the 11 zones for which the insulation was in contact with the liquid hydrogen. The calculated 13,945 J/sec (47,618 Btu/hr) would result in a liquid hydrogen boiloff rate of 3.08×10^{-2} kg/sec (4.07 lb/min), or only 2% less than the 3.14×10^{-2} kg/sec that was measured during the test.

However, in the above estimates, no correction was made for increased heat transfer caused by solid silicone grouting compound between panels. In a large tank, the grouting compound should cover no more than 1% of the total tank area, and may be considerably less depending on panel size. We estimated that the grout joints made up approximately 2.1% of the total insulation area in the test tank, caused by the small size panels required for the domes and the dome-to-barrel transition areas. We have not measured the low temperature thermal conductivity of the grouting compound, but estimate an effective value of 0.19

A Compendium of the Properties of Materials at Low Temperature (Phase I). Part I - Properties of Fluids. WADD Technical Report 60-56 [Contract AF33(616)-58-4]. Wright Air Development Division, Air Research and Development Command, Wright-Patterson AFB, Ohio, October 1960.

TABLE V. - HEAT TRANSFER CALCULATIONS

Zone	Area		Average Wall Temperature		Predicted Effective Thermal Conductivity		Predicted Heat Flux		Predicted Zone Heat Transfer	
	m^2	ft^2	°K	°R	J/m-sec-°K	Btu/ft-hr-°R	J/sec-m^2	Btu/hr-ft^2	J/sec	Btu/hr
1	0.66	7.1	178	320	0.0986	0.057	609.1	193.2	402	1,372
2	0.52	5.6	188	339	0.104	0.060	688.5	218.4	358	1,223
3	1.53	16.5	198	356	0.109	0.063	756.6	240	1,160	3,960
4	0.72	7.75	259	467	0.133	0.077	1259.7	399.6	907	3,097
5	1.32	14.22	261	469	0.133	0.077	1263.5	400.8	1,669	5,699
6	1.32	14.22	265	477	0.135	0.078	1312.7	416.4	1,734	5,921
7	1.32	14.22	258	465	0.133	0.077	1252.2	397.2	1,654	5,648
8	1.32	14.22	252	454	0.131	0.076	1203.0	381.6	1,589	5,426
9	1.32	14.22	246	443	0.130	0.075	1150.0	364.8	1,519	5,187
10	1.32	14.22	242	436	0.126	0.073	1108.4	351.6	1,464	5,000
11	1.32	14.22	245	441	0.128	0.074	1127.3	357.6	1,489	5,085
Total	12.67	136.5							13,945	47,618

J/m-sec-°K (0.11 Btu/ft-hr-°R) over the test temperature range based on published room temperature data. In the application of the grout compound, it is desirable to avoid completely filling the space between panels to ensure against overfilling, since excessive grout material tends to flow onto the facesheet. Using the estimated thermal conductivity and assuming the grout thickness to be 90% of the insulation panel thickness, the overall predicted heat transfer would be increased by 1.4%.

No allowance was made for added heat leak, which may occur at the fill and drain port, or may be caused by liquid flowing into the fill line after the fill was completed, and vaporizing. Observations during the tests indicated that there was no degradation of the insulation at the fill port. It was also noted that the vacuum-jacketed fill line boiled dry after the fill valve had been closed, and did not again fill with liquid until the valve was opened, verifying that the capillary screen at the fill port successfully held liquid out of the line.

For the first boiloff test, therefore, the measured and predicted boiloff values, corrected to account for the effect of grouting, were almost identical. After the tank had been subjected to five temperature and pressure cycle tests, the boiloff rate approximately doubled for essentially the same tank wall temperatures. From inspection of the insulation system after the cyrogenic tests, it is estimated that damage had occurred to 15 to 18% of all cells in the barrel panels caused by facesheet failure. Between the initial and the final test, the boiloff rate only increased by 100%, and the variation of measured tank wall temperatures within any zone increased only from 13°K (23.5°F) to 45°K (80°F). We have not evaluated the failure mode heat transfer characteristics in sufficient detail to offer an analytical model, but it is obvious that a few isolated cell failures would not greatly influence overall system performance.

Purging of Insulation

The technique used during purge tests to obtain gas samples from selected insulation cells was based on use of a calibrated restrictor to meter the sample. The sampling procedure was intended to control the sample quantity to approximately 3% of the total gas in the cell. Approximately the same quantity would be initially purged through the sampling system, resulting in a total flow of gas through the cell, equivalent to 6 to 10% of the cell contents.

Results of the purge tests were not consistent because of the inadequacies of this procedure. It is believed that for certain tests, the hand valve was not actuated quickly enough to accurately control the flow periods (a few seconds depending on restrictor calibration) and that excessive gas was drawn through the cells. This resulted in indicated purge rates greater than had been expected. When attempts were made to reduce the valve-open time, results indicated that the initial trapped gas was not removed from the sampling system, resulting in inconsistent, but lower indicated purge rates. Also, in at least two instances it was obvious that sample containers had leaked, although all of the containers and valves had initially been leak checked.

Using the data obtained, and omitting those data points believed most likely to be in error for the reasons given above, we arrived at the following purge test results.

(1) *Sweep Purge with Nitrogen.* - Insulation cells initially filled with 17% helium, 33% hydrogen (mole percent).

After 1 hr - greater than 95% GN_2 in cells
After 2 hr, or more - greater than 99% GN_2 in cells.

(2) *Sweep Purge with Helium.* - Insulation cells initially filled with 99% or greater GN_2.

After 1 hr - 82% helium in cells
After 2 hr - 89% helium in cells
After 4 hr - greater than 97% helium in cells.

(3) *Pressure Purge with Helium.* - Insulation cells initially filled with 99% or greater GN_2.

After 4 cycles - 29% or greater helium in cells.

A conclusion could not be drawn from the data for pressure cycling after 8 and 12 cycles. Extrapolation would indicate that at the end of 12 cycles 35% of the nitrogen would remain. This result is inconsistent with the sweep purge results, and would indicate very poor mixing during the pressure cycles. Additional testing is recommended to substantiate the results; however, it is tentatively concluded that the sweep purge method is at least as acceptable as the pressure purge method for eliminating air or nitrogen from the insulation before fill and for inerting the system after it has been used with liquid hydrogen.

Insulation Design, Fabrication and Installation

In evaluating our design approach, fabrication, and installation methods, we found few problems that were not obvious at the time that they occurred. These problems, along with possible solutions or improvements are discussed in the following paragraphs.

Design. - The nested panel design concept had previously been evaluated in small tanks and with small test specimens. In this first application to a complete tank of moderate size, no fault was found in the design concept, although opportunities for relatively minor improvements were noted. One such improvement was elimination of the highly compound curvature of the facesheet surface when the C and E (dome-to-barrel transition) panels were redesigned. However, the more moderate curvature of the panels for insulation of the tank domes did not present significant problems when using the Teflon facesheet. In a booster size tank, the requirement to insulate over surfaces with curvature as great as that in the current test tank domes is very unlikely.

In the insulation of the tank barrel section, we estimate the total weight of the installed insulation system to be 3.6602 kg/m^2 (0.7497 lb/ft^2) of tank wall area. This estimate is detailed in table VI. It is noted that 75% of the total weight is in the adhesive applied to the tank wall. In our original plan (use of stencil), only 1.186 kg/m^2 (0.243 lb/ft^2) of adhesive would have been applied to the wall, resulting in a system weight of 2.10 kg/m^2 (0.4302 lb/ft^2) with the wall adhesive constituting approximately 56% of the total. The stencil is used to apply the adhesive in a pattern corresponding to the core ribbon locations. From the limited experiments we have conducted in evaluating the stencil method, we feel that it would be practical. Furthermore, increasing the cell size would reduce system weight, particularly if the wall adhesive is applied by stencil. As discussed later, the thickness of adhesive that was used is probably excessive; as little as 50% of the amount used may be adequate.

TABLE VI. - ESTIMATED INSTALLED INSULATION SYSTEM WEIGHT PER UNIT AREA OF TANK WALL

Component	Material	Weight	
		kg/m^2	lb/ft^2
Core Ribbon	0.127 mm (0.005-in.) Kapton	0.2949	0.0604
Node Bond Adhesive	RTV-156	0.0308	0.0063
Facesheet	0.0508 mm (0.002-in.) Teflon FEP	0.1108	0.0227
Facesheet-to-core Adhesvie	RTV-560	0.1655	0.0339
Filler	PF-105-450	0.2651	0.0543
Primer for Pre-fabricated Panels	DC-1200	0.0322	0.0066
Primer for Tank Wall	DC-1200	0.0146	0.0030
Installation Adhesive	RTV-560	2.7463	0.5625
Total Weight		3.6602	0.7497

Panel Fabrication. - Quality Control records show that there were 231 rejections tagged on the 76 standard panels that were fabricated, or an average of 3.04 per panel. A breakdown of these rejections follows:

short core node bonds	15
skips in core node bonds and isolated node debonds	23
core node bond width out of tolerance	4
incorrect ribbon pattern	2
alignment of core ribbons out of tolerance	13
ribbon tears	28
inadequate priming of core or facesheet	11

facesheet-to-core bond width out of tolerance	16
facesheet-to-core bond skips	51
cell distortion	26
facesheet wrinkles	7
holes in facesheet	5
dimple depth below minimum	2
damage to facesheet during trim	25
other	3

This summary does not include a number of panels that were scrapped because of bonding failures in the core assembly.

Most of these defects were repaired, although in some categories, the defects were reviewed and accepted. This would be possible in the case of wrinkling of the facesheet, cell distortion and out of tolerance bond line width. Those defects that would lead to leakage between cells were in all cases repaired. When an excessive number of defects was found in the facesheet-to-core bond, or when the primer action was not adequate, the facesheet was completely removed and the core assembly was recycled through the assembly process. Where dimple depth did not meet the inspection criteria, the panel was recycled back to the dimpling operation.

Many of the operations that were required to fabricate insulation panels could be automated. Improved tooling and procedures would be required for the others in a production operation. Most of the panel defects that we experienced would be eliminated by an improved (second generation) production facility. Although we maintained a minimum relative humidity in our bonding area, it was not closely controlled. While the minimum humidity condition generally eliminated the debonding conditions previously encountered, inconsistencies in the curing rate of the silicone adhesives resulted in wide variations in the bond line widths in the facesheet-to-core assembly, with skips in the bonds occurring for the same reason. A closely controlled environment and further process development would be required to avoid these problems.

A means for achieving greater dimple depth must be found to eliminate the damage to the Teflon facesheet that occurred during cryogenic testing. If the maximum operating temperature of the facesheet is sufficiently less than 450°K (350°F), the heater blanket dimpling method would be adequate. To achieve greater dimple depth, which would not be subject to shrinkage at 450°K (350°F), will require further development. However, the use of a 0.025 mm (0.001 in.) Kapton facesheet is the more obvious solution to this problem. This material has cryogenic properties equal or superior to those of Teflon, and the coefficient of thermal contraction of Kapton is only 22% that of Teflon. For this reason, less dimple would be required. However, we have recently developed a dimpling procedure for Kapton to acheive consistent dimples in the Kapton film with greater depth than can be achieved with the Teflon facesheet, and these dimples, which are formed at a much higher temperature, are not subject to shrinkage at 450°K (350°F).

Quality Control and Repair. - The quality control plan and criteria proved to be adequate for this developmental project. It did little to compensate for the inadequacies that were experienced in our tooling and methods. For future production of insulation for a larger tank, these criteria will be helpful in establishing the adequacy of improved operations. However, future tooling, methods, and process control must be inherently capable of maintaining quality of the insulation panels, with only spot inspections required. Automated inspection equipment would be required for any item requiring 100% surveillance.

While the number of repairs we made to panels was excessive, the methods of repair generally proved satisfactory. And although repairs were often obvious because of excessive use of adhesive, they were not a cause for system degradation or failure in the cryogenic test program.

Installation. - The only significant problem encountered in installation of panels was in achieving a complete seal between the core and the tank wall. On reviewing our methods and inspecting areas where voids did occur, we have concluded that the adhesive was thickened to the point of losing part of its wetting and flow capability. Some increase in viscosity is necessary to prevent running of the adhesive on a vertical wall. Once the adhesive is spread uniformly, however, there is less tendency for it to flow. Also, a lesser thickness of adhesive would reduce the tendency for running. Spraying the adhesive on the wall

would probably be more efficient and would probably reduce the quantity applied and the required viscosity. Applying a small amount of adhesive to the panel, just sufficient to initiate a wetting action, would be helpful.

Inspection of Insulation After Cryogenic Testing

The insulation was inspected in detail after the testing was completed. Facesheet tears had occurred in every panel except the special panels covering the simulated hardware; these panels sustained no damage. The greatest damage occurred to the larger D panels installed on the barrel. Only damage related to the facesheet was found. However, in conjunction with the facesheet tears, there was frequent occurrence of adhesive failures. These included debonding of the core node bonds and debonding of the facesheet-to-core adhesive from the Kapton core ribbons. In a few places where neither of these adhesive failures occurred, the core ribbon was torn at the point of facesheet failure.

It has been concluded that the adhesive and core ribbon failures were secondary; not the causes of the facesheet failure. Microscopic examination of facesheet specimens did not shed light on the origin of the tears. In some instances, tears propagated vertically the full length of the panel. These tears were in the lengthwise direction of the Teflon as it was manufactured, and it was discovered that these full length tears followed areas in the film where its thickness was as much as 25% below nominal.

Much evidence was noted to indicate that the failures occurred with considerable release of energy, and the Teflon appeared to be shattered in places with many secondary failures. Review of the test data indicates that the tank was subjected to several near step changes in pressure of 1.5 to 2 psi. Because the degradation in thermal performance seemed to occur during the temperature and pressure cycle tests, it is suspected that these rapid pressure fluctuations may have contributed to the insulation failures.

The rapid changes in pressure were unintentional, and occurred in switching from the main vent valve to the throttling valve for pressure regulation. This pressure difference should not in itself cause failure of the facesheet, since pressures of up to 15 psig have been applied in tests with liquid nitrogen.

A greater internal cell pressure might have occurred as a result of liquid hydrogen being forced into the cell through the capillary opening and then rapidly vaporizing. However, it is most likely that the facesheet reached a near failure loading because of thermal contraction, and that the loading was increased further when the tank wall was heated to 450°K (350°F) and the pressure suddenly applied. The loading of the facesheet by thermal contraction is, of course, caused by inadequate dimple. Means for providing greater dimple depth were previously discussed.

No damage or failures due to repairs were noted. Leak tests of a large number of cells for which the facesheet was intact failed to indicate any loss of seal between cells. For the cells with facesheet failure, there was no instance where the fiberglass filler plugs had migrated out of the insulation panel. From all the available evidence, it is concluded that the facesheet dimple problem alone was responsible for the insulation system damage.

CONCLUSIONS AND RECOMMENDATIONS

The concept of the internal insulation system using surface tension or capillary forces to position a stable gas layer between the liquid cryogen and tank wall had previously been verified and demonstrated on small specimens. In this program the verification of insulation performance has been extended to a complete tank system of moderate size. In insulating the 1.8-m diameter tank, the concept was demonstrated to be applicable to the insulation of the entire interior of a tank, and typical irregularities in the tank interior were successfully negotiated.

Because of an inadequacy in the design criteria that had been previously established, the tests to demonstrate the capability of the insulation to withstand cycling of the tank wall to elevated temperatures were not successful. An inadequate degree of dimpling of the Teflon facesheet to relieve thermally induced stresses is believed to be responsible for the failure of the facesheet during temperature and pressure cycle tests. Although many other problems were encountered in the fabrication and installation of the insulation system, they were detected and successfully corrected.

The choice of silicone adhesives, particularly in combination with Kapton film and lower-than-average values of relative humidity, presented special bonding problems. The low quantity methods and tooling used in panel fabrication were not totally adequate, and insulation panels were produced only with special attention and considerable rework and repair. Installation procedures were largely untried and on-the-spot modifications and innovations were required. Nevertheless, the system as installed and repaired met all the essential requirements except for the inadequacy of the facesheet dimples.

Recommended future work obviously includes the redefinition of the dimpling requirement and the development of a more adequate dimpling process if Teflon film is to be used as the facesheet. However, a satisfactory process is now available for dimpling a Kapton facesheet. A greater depth of dimple can be achieved for Kapton than was possible for Teflon using the present method. Since Kapton has excellent cryogenic properties, and only a fraction of the thermal contraction rate of Teflon, the change of facesheet materials would be a logical solution for the problem. Unfortunately, at the time the facesheet material was selected for this program, we had not yet successfully solved the dimpling problem for Kapton.

Other recommendations include the development of a next generation of tools and methods which will minimize the dependence of product quality on operator skill and attention. The problems encountered in achieving a seal between the insulation and the tank wall can be solved by using test panels of reasonably large size, and development of tools and procedures should be completed for minimizing the quantity of adhesive required, which would, in turn, minimize system weight.

If system requirements do not include reusability after a large number of exposures to high heating rates, but rather survival after only one exposure, additional materials should be considered. The use of more conventional adhesives, such as epoxy, and lighter film materials, such as polyamide (Nomex) paper, could decrease the weight of the system and eliminate some of the problems encountered which were peculiar to the materials used in this program.

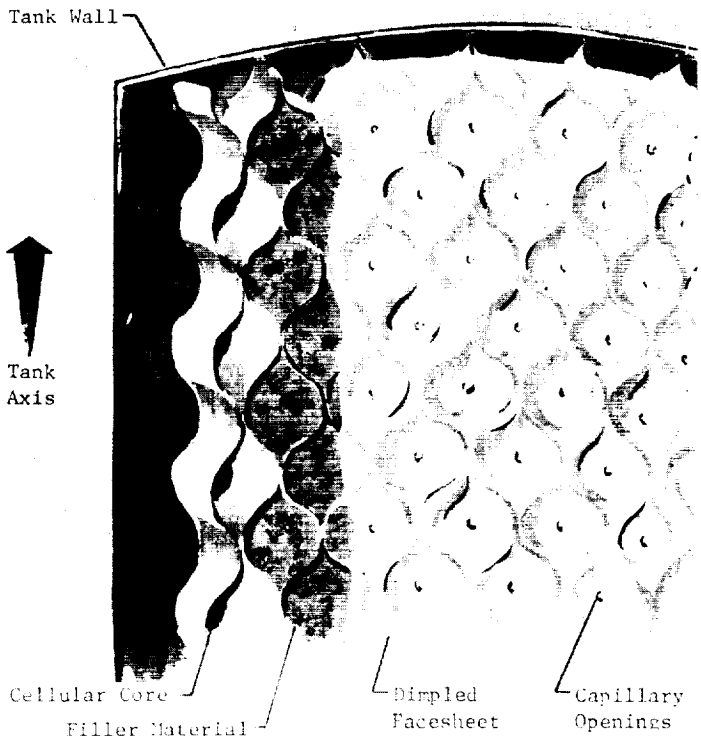

Figure 1. - Capillary Internal Insulation Concept

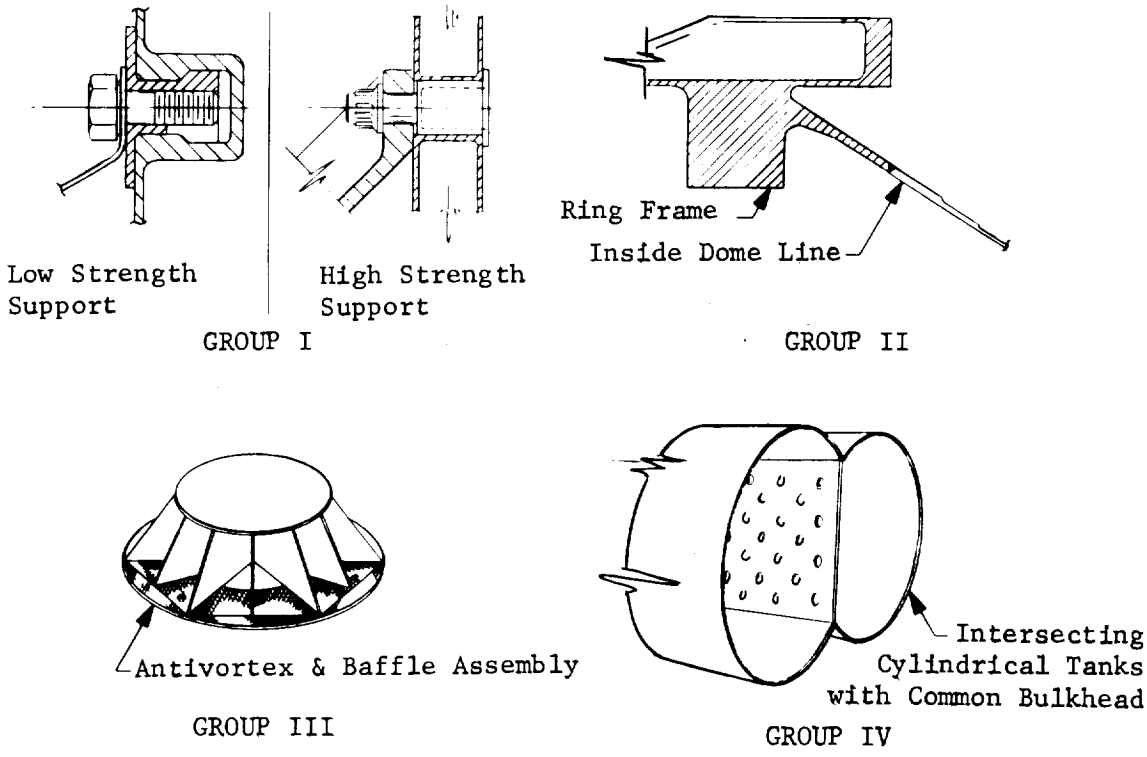

Figure 2. - Phase B Internal Structures and Hardware
(McDonnell Douglas Configuration)

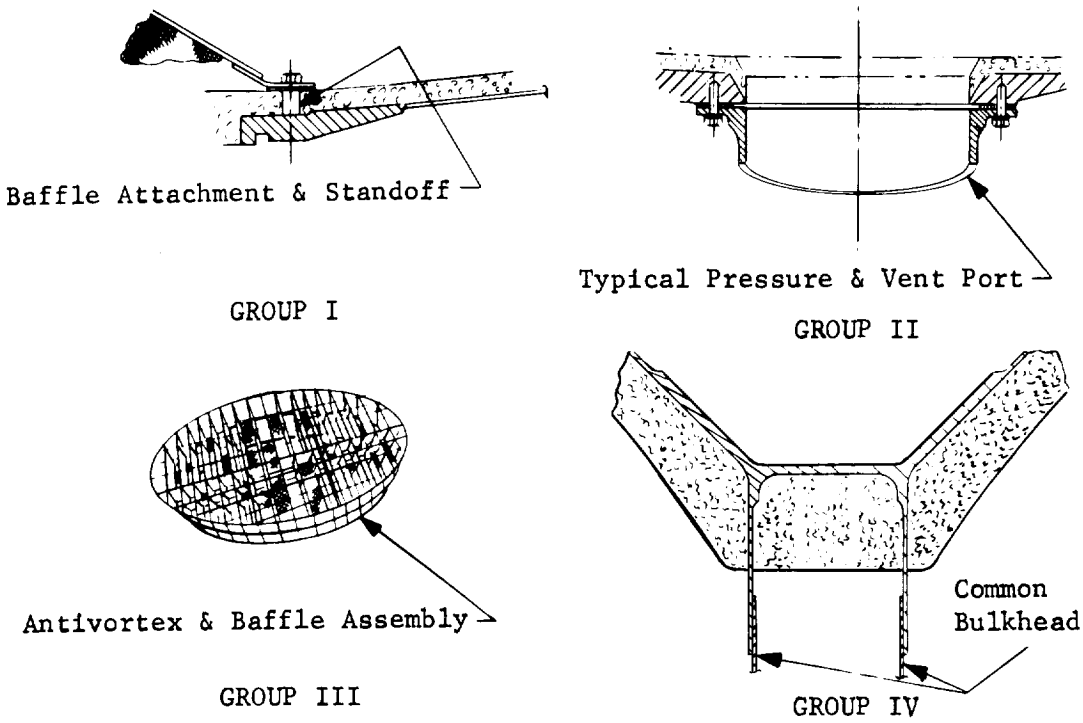

Figure 3. - Phase B Internal Structures and Hardware
(North American - Rockwell Configuration)

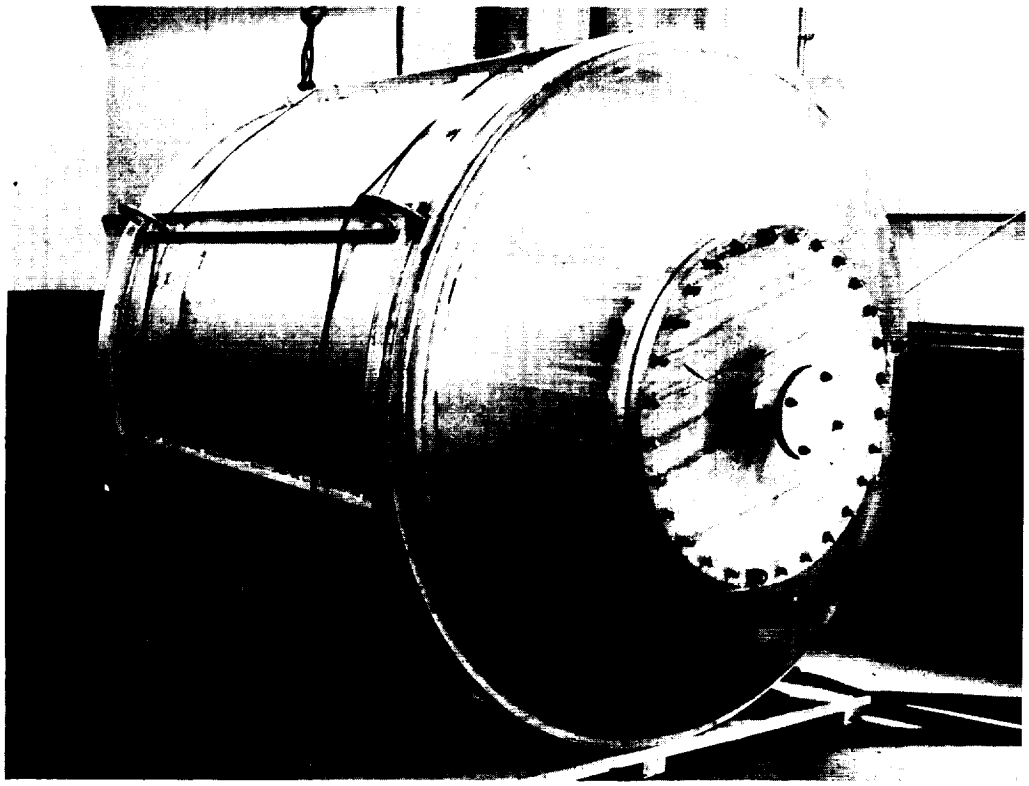

Figure 4. - Model Tank, Original Configuration

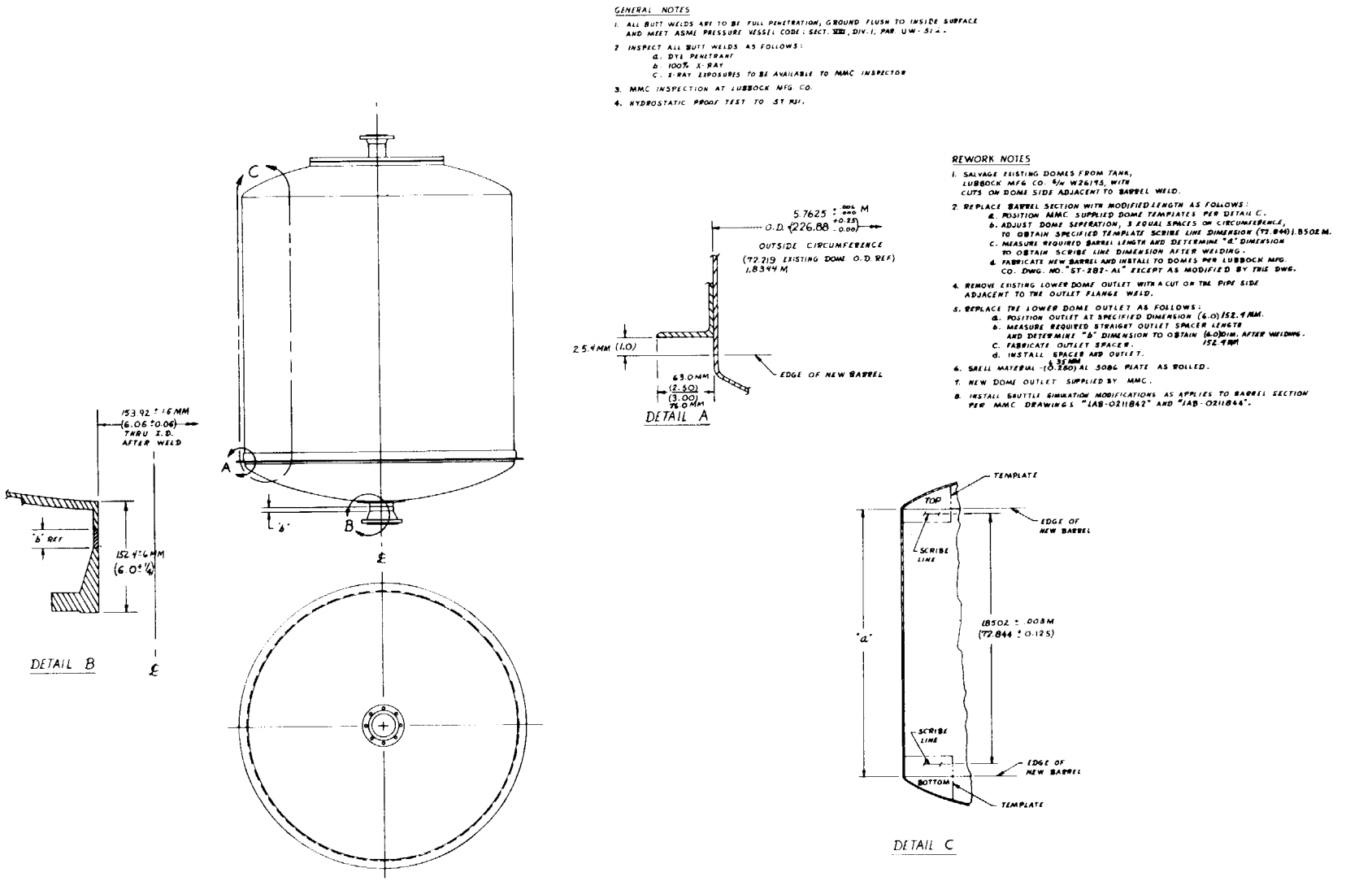

Figure 5. - Tank Modification

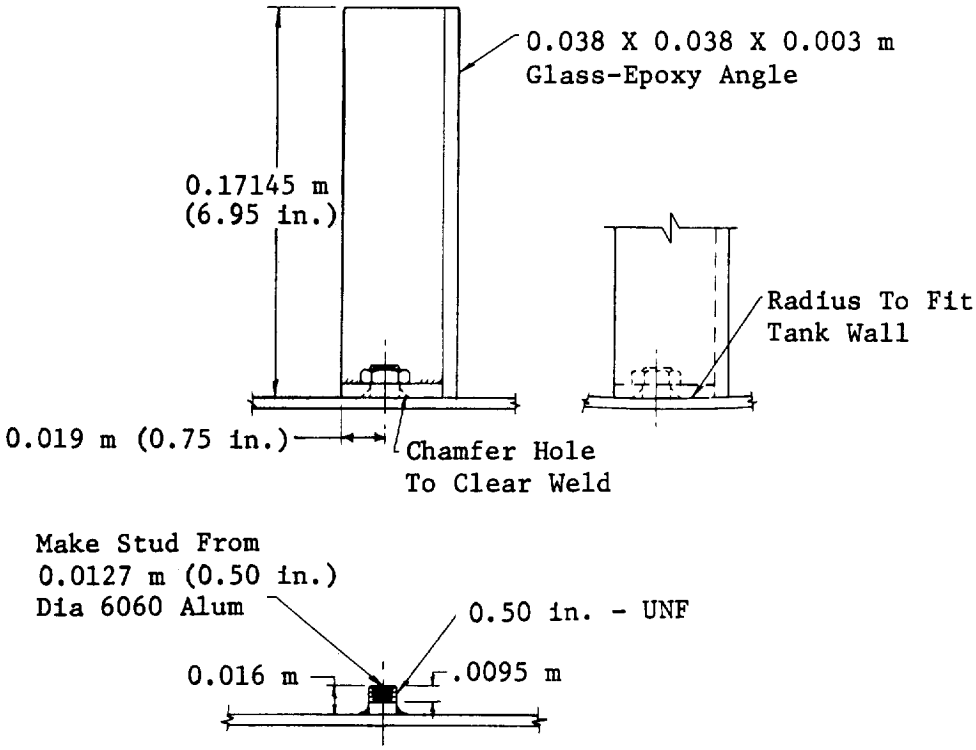

Figure 6. - Simulated Mounting Bracket

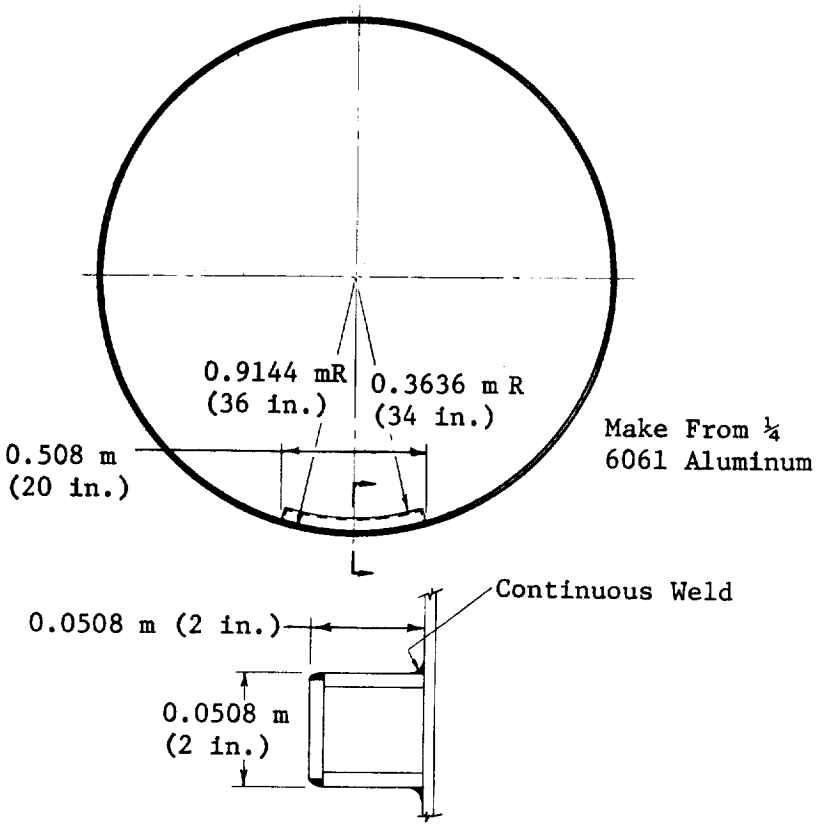

Figure 7. - Simulated Ring Frame

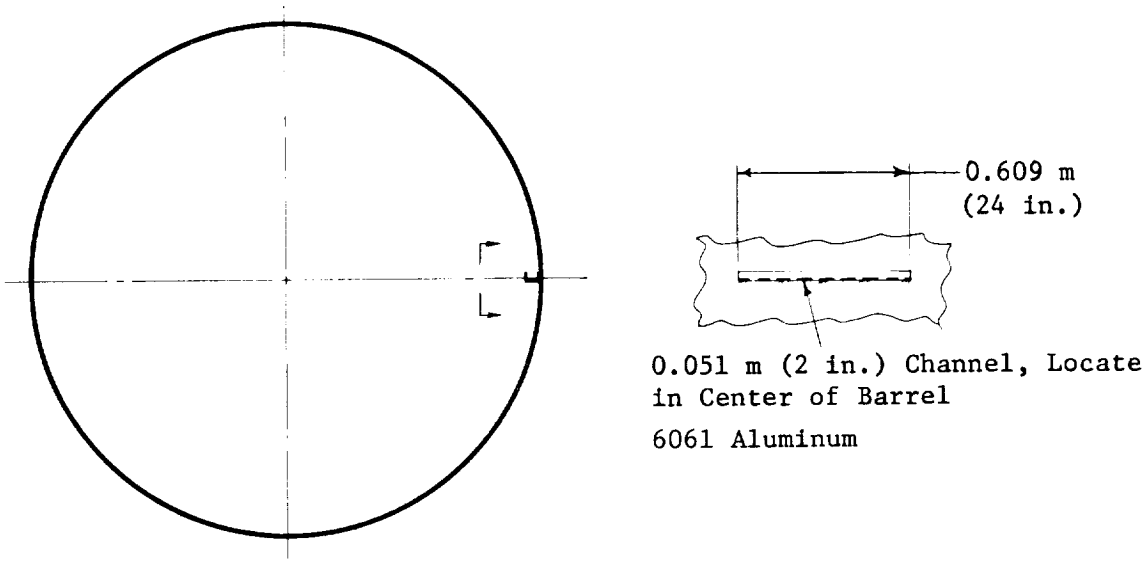

Figure 8. - Simulated Stringer

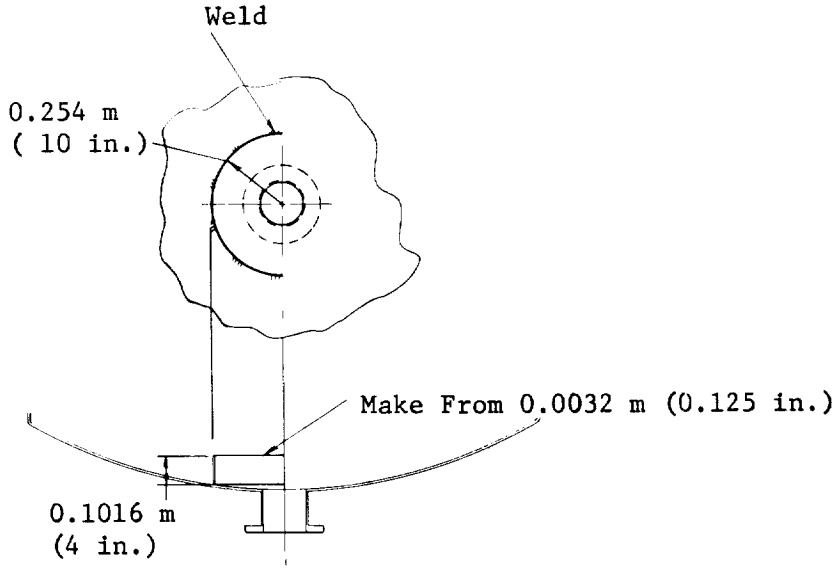

Figure 9. - Simulated Outlet Device

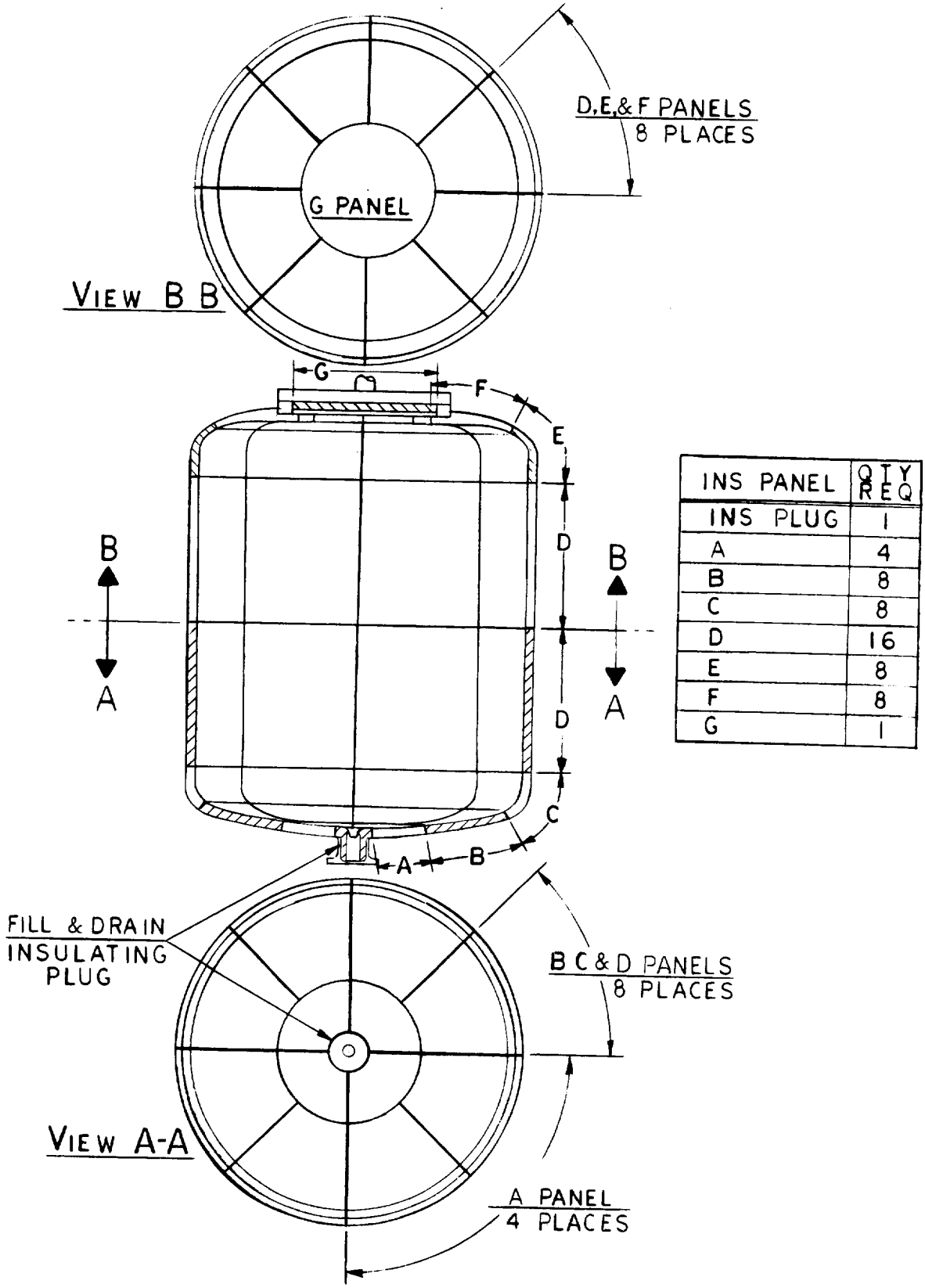

INS PANEL	QTY REQ
INS PLUG	1
A	4
B	8
C	8
D	16
E	8
F	8
G	1

Figure 10. - Insulation Panel Arrangement

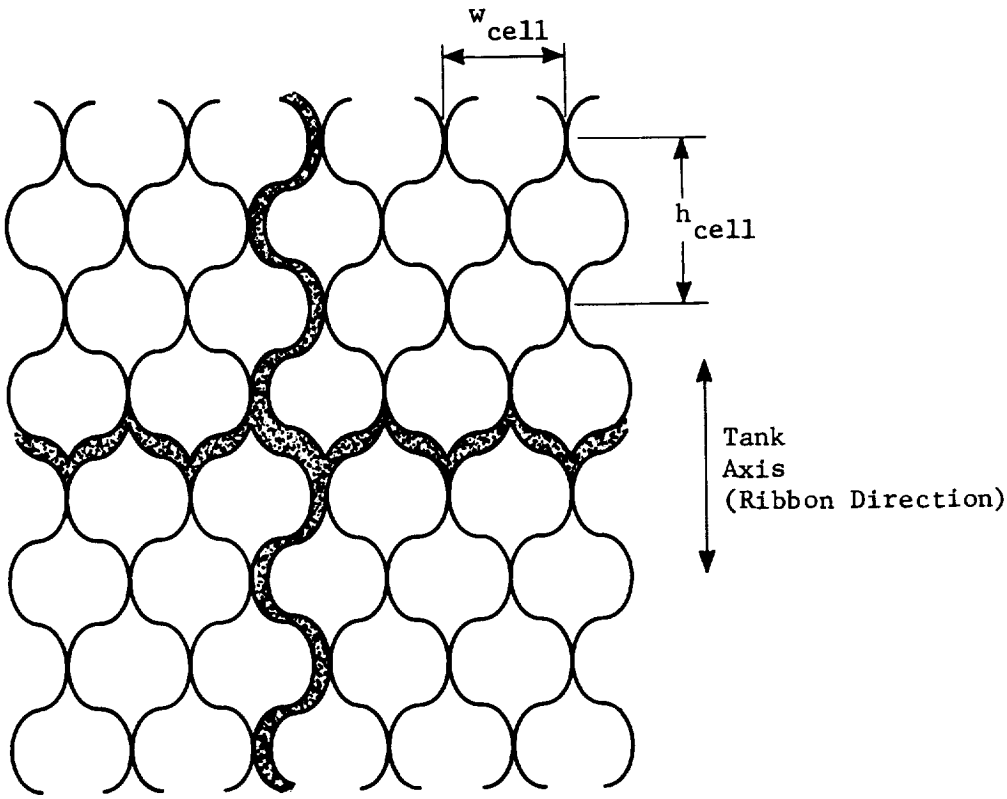

Figure 11. - Nested Grout Joint Concept

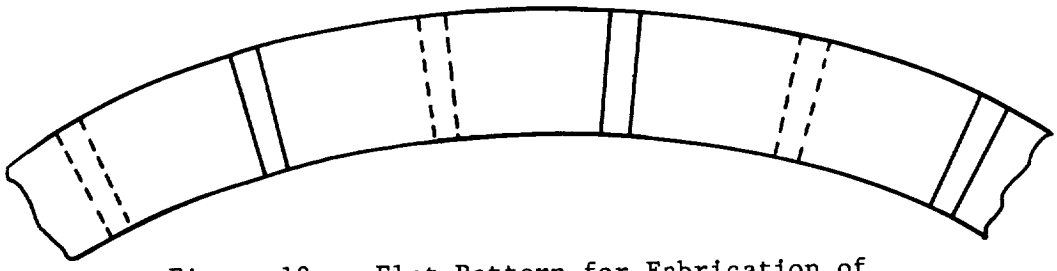

Figure 12. - Flat-Pattern for Fabrication of
Core for a Small Cylindrical Tank

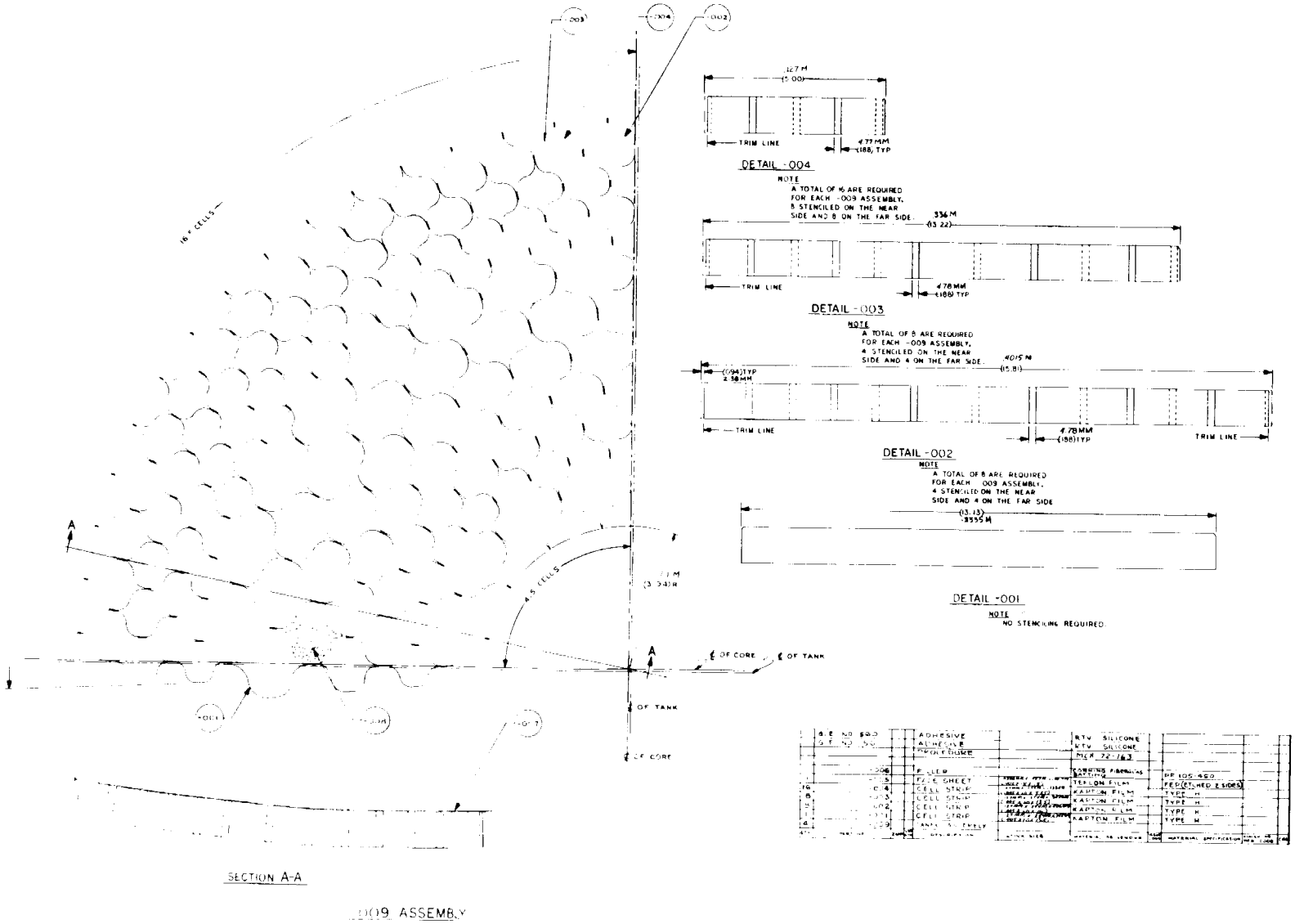

Figure 13. - A Panel, Bottom Dome

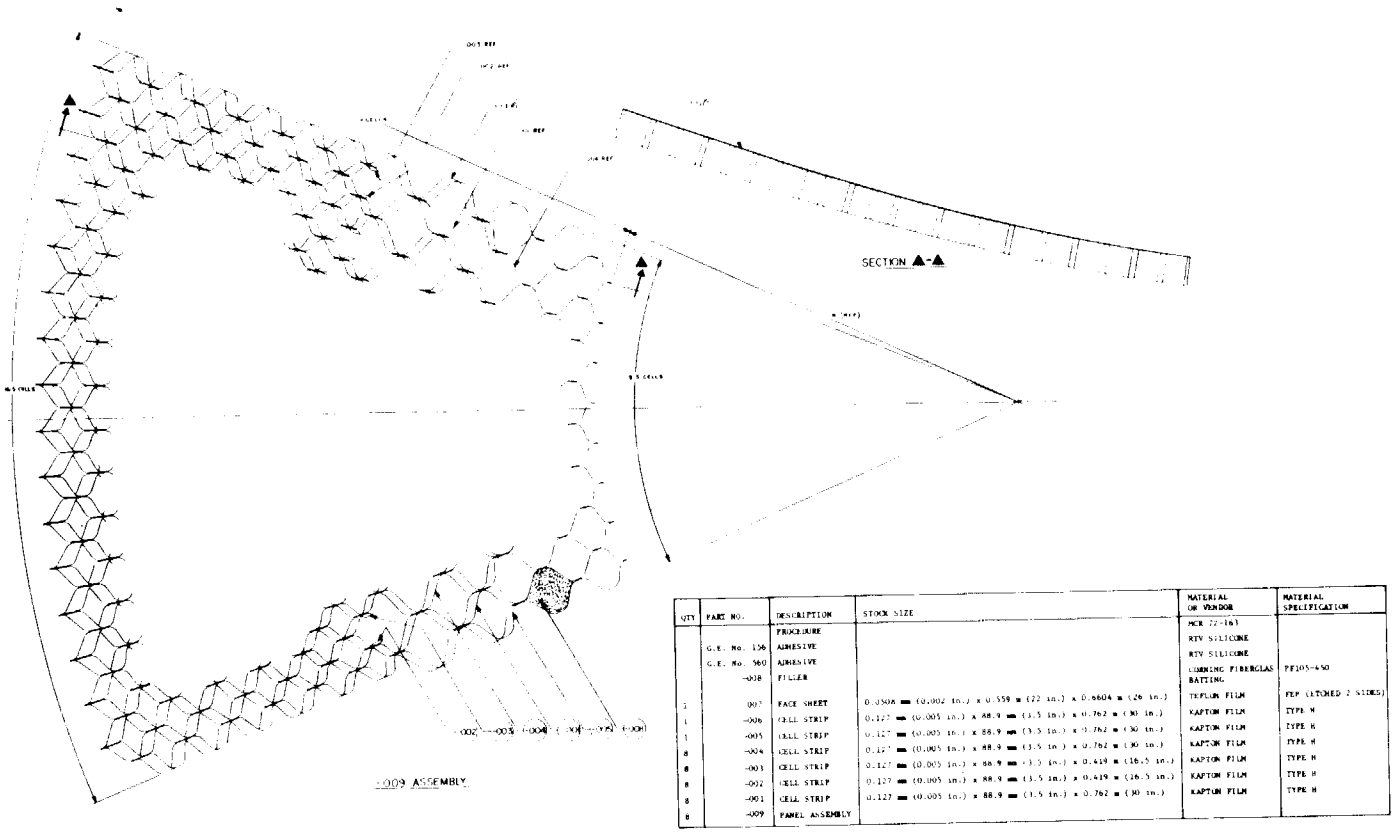

QTY	PART NO.	DESCRIPTION	STOCK SIZE	MATERIAL OR VENDOR	MATERIAL SPECIFICATION
		PROCEDURE		MCR 72-163	
	G.E. No. 136	ADHESIVE		RTV SILICONE	
	G.E. No. 560	ADHESIVE		RTV SILICONE	
	-008	FILLER		LEMMING FIBERGLAS BATTING	PF105-450
1	007	FACE SHEET	0.0508 mm (0.002 in.) x 0.559 m (22 in.) x 0.6604 m (26 in.)	TEFLON FILM	FEP (ETCHED 2 SIDES)
1	-006	CELL STRIP	0.127 mm (0.005 in.) x 88.9 mm (3.5 in.) x 0.762 m (30 in.)	KAPTON FILM	TYPE H
1	-005	CELL STRIP	0.127 mm (0.005 in.) x 88.9 mm (3.5 in.) x 0.762 m (30 in.)	KAPTON FILM	TYPE H
8	-004	CELL STRIP	0.127 mm (0.005 in.) x 88.9 mm (3.5 in.) x 0.762 m (30 in.)	KAPTON FILM	TYPE H
8	-003	CELL STRIP	0.127 mm (0.005 in.) x 88.9 mm (3.5 in.) x 0.419 m (16.5 in.)	KAPTON FILM	TYPE H
8	-002	CELL STRIP	0.127 mm (0.005 in.) x 88.9 mm (3.5 in.) x 0.419 m (16.5 in.)	KAPTON FILM	TYPE H
8	-001	CELL STRIP	0.127 mm (0.005 in.) x 88.9 mm (3.5 in.) x 0.762 m (30 in.)	KAPTON FILM	TYPE H
8	-009	PANEL ASSEMBLY			

Figure 14. - B Panel, Bottom Dome

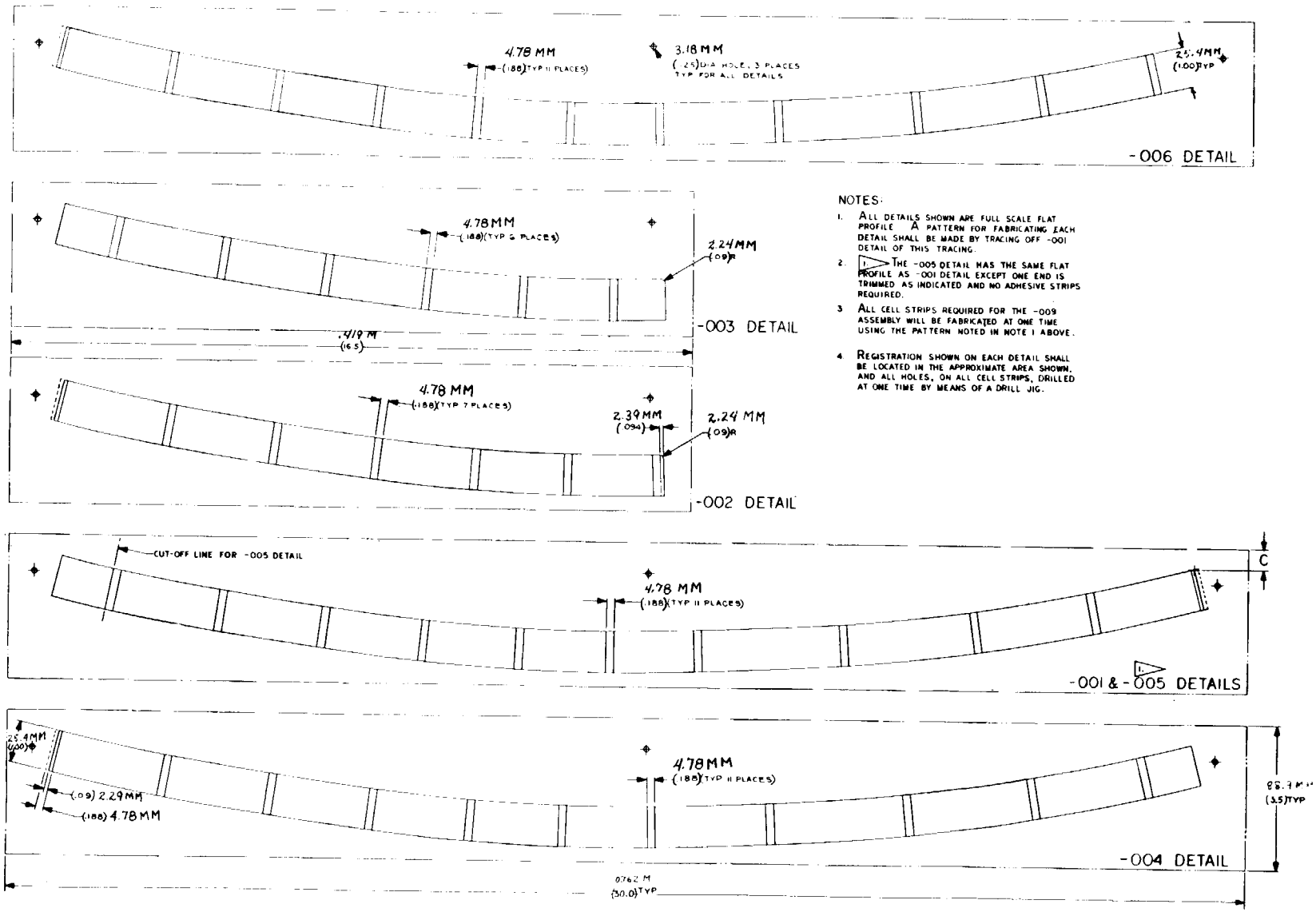

Figure 14. - (concl)

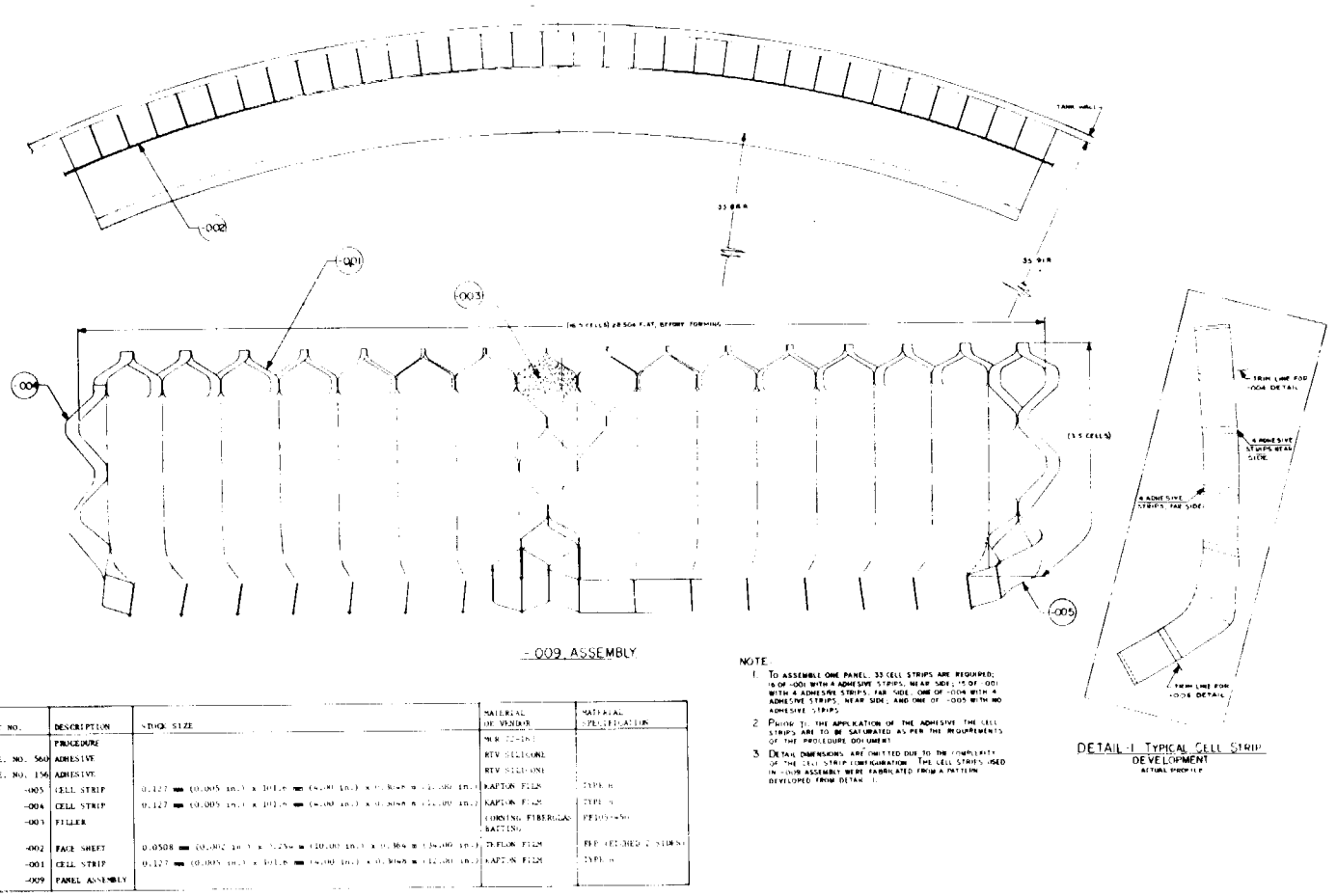

QTY	PART NO.	DESCRIPTION	STOCK SIZE	MATERIAL OR VENDOR	MATERIAL SPECIFICATION
		PROCEDURE			
	G. E. NO. 560	ADHESIVE		RTV SILICONE	
	G. E. NO. 156	ADHESIVE		RTV SILICONE	
1	-005	CELL STRIP	0.127 = (0.005 in.) x 101.6 = (4.00 in.) x [illegible]	KAPTON FILM	TYPE H
1	-004	CELL STRIP	0.127 = (0.005 in.) x 101.6 = (4.00 in.) x [illegible]	KAPTON FILM	TYPE H
	-003	FILLER		CORNING FIBERGLAS BATTING	PF1007-550
1	-002	FACE SHEET	0.0508 = (0.002 in.) x [illegible]	TEFLON FILM	PER (REQUIRED 2 SIDES)
31	-001	CELL STRIP	0.127 = (0.005 in.) x 101.6 = (4.00 in.) x [illegible]	KAPTON FILM	TYPE H
	-009	PANEL ASSEMBLY			

Figure 15. - C Panel, Bottom Dome to Barrel Transition

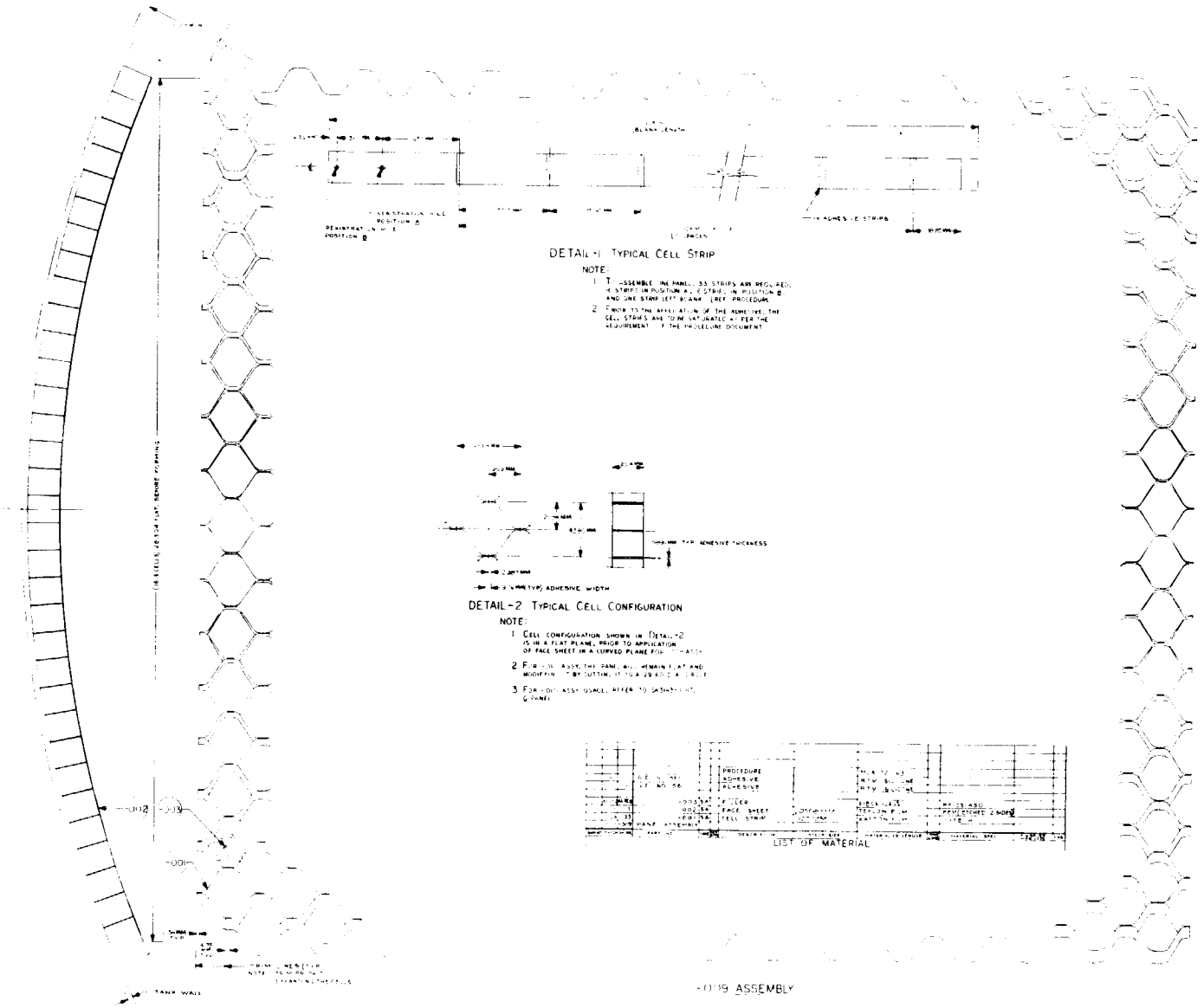

Figure 16. - D Panel, Barrel Section

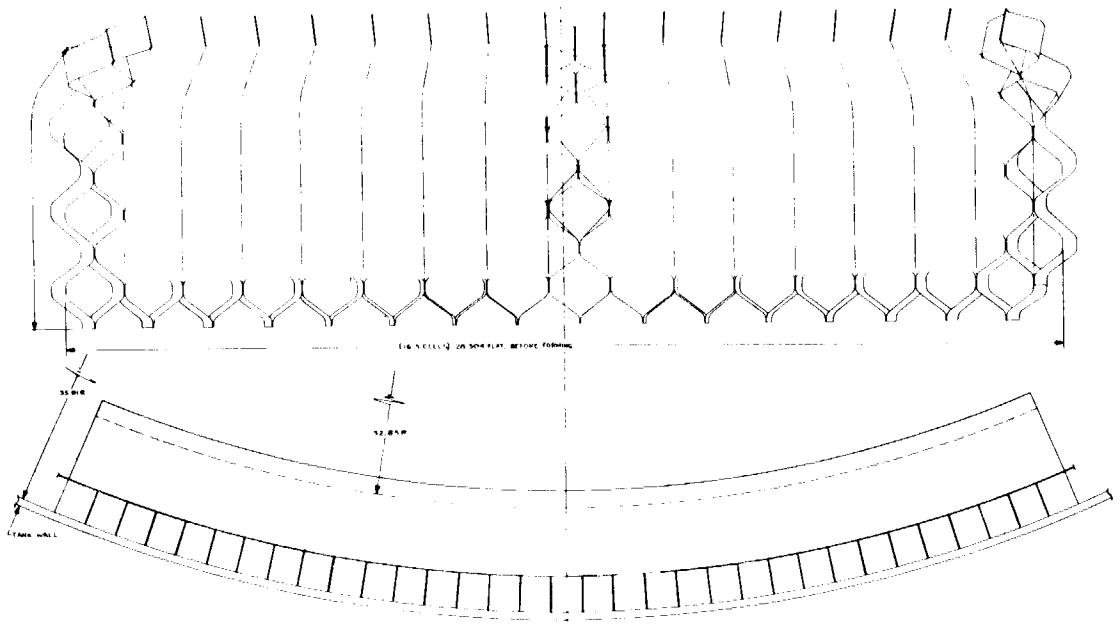

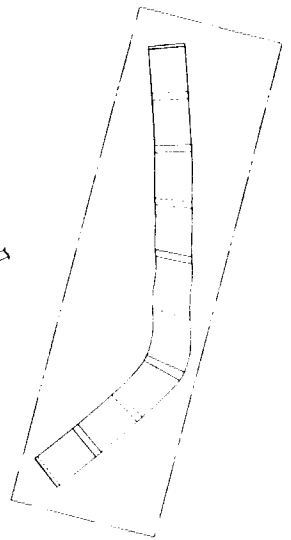

DETAIL 1 TYPICAL CELL STRIP DEVELOPMENT

002 ASSEMBLY

QTY	PART NO.	DESCRIPTION	STOCK SIZE	MATERIAL OR VENDOR	MATERIAL SPECIFICATION
		PROCEDURE		MCR 72-163	
	G.E. NO. 560	ADHESIVE		RTV SILICONE	
	G.E. NO. 156	ADHESIVE		RTV SILICONE	
1	-005	CELL STRIP	0.127 mm (0.005 in.) x 101.6 mm (4.00 in.) x 0.3556 m (14.00 in.)	KAPTON FILM	TYPE H
1	-004	CELL STRIP	0.127 mm (0.005 in.) x 101.6 mm (4.00 in.) x 0.3556 m (14.00 in.)	KAPTON FILM	TYPE H
	-003	FILLER		CORNING FIBERGLAS BATTING (PULVERIZED)	PF105-450
1	-002	FACE SHEET	0.0508 mm (0.002 in.) x 0.254 m (10.00 in.) x 0.8636 m (34.00 in.)	TEFLON FILM	FEP (ETCHED 2 SIDES)
31	-001	CELL STRIP	0.127 mm (0.005 in.) x 101.6 mm (4.00 in.) x 0.3556 m (14.00 in.)	KAPTON FILM	TYPE H

NOTE

1. TO ASSEMBLE ONE PANEL, 33 CELL STRIPS ARE REQUIRED. 16 OF -001 WITH 5 ADHESIVE STRIPS, REAR SIDE; 15 OF -004 WITH 5 ADHESIVE STRIPS, FAR SIDE, ONE OF -004 WITH 5 ADHESIVE STRIPS, REAR SIDE, AND ONE OF -005 WITH NO ADHESIVE STRIPS.
2. PRIOR TO THE APPLICATION OF THE ADHESIVE, THE CELL STRIPS ARE TO BE SATURATED AS PER THE REQUIREMENTS OF THE PROCEDURE DOCUMENT.
3. DETAIL DIMENSIONS ARE OMITTED DUE TO THE COMPLEXITY OF THE CELL STRIP CONFIGURATION. THE CELL STRIPS USED IN -002 ASSEMBLY WERE FABRICATED FROM A PATTERN DEVELOPED FROM DETAIL 1.

Figure 17. - E Panel, Top Dome to Barrel Transition

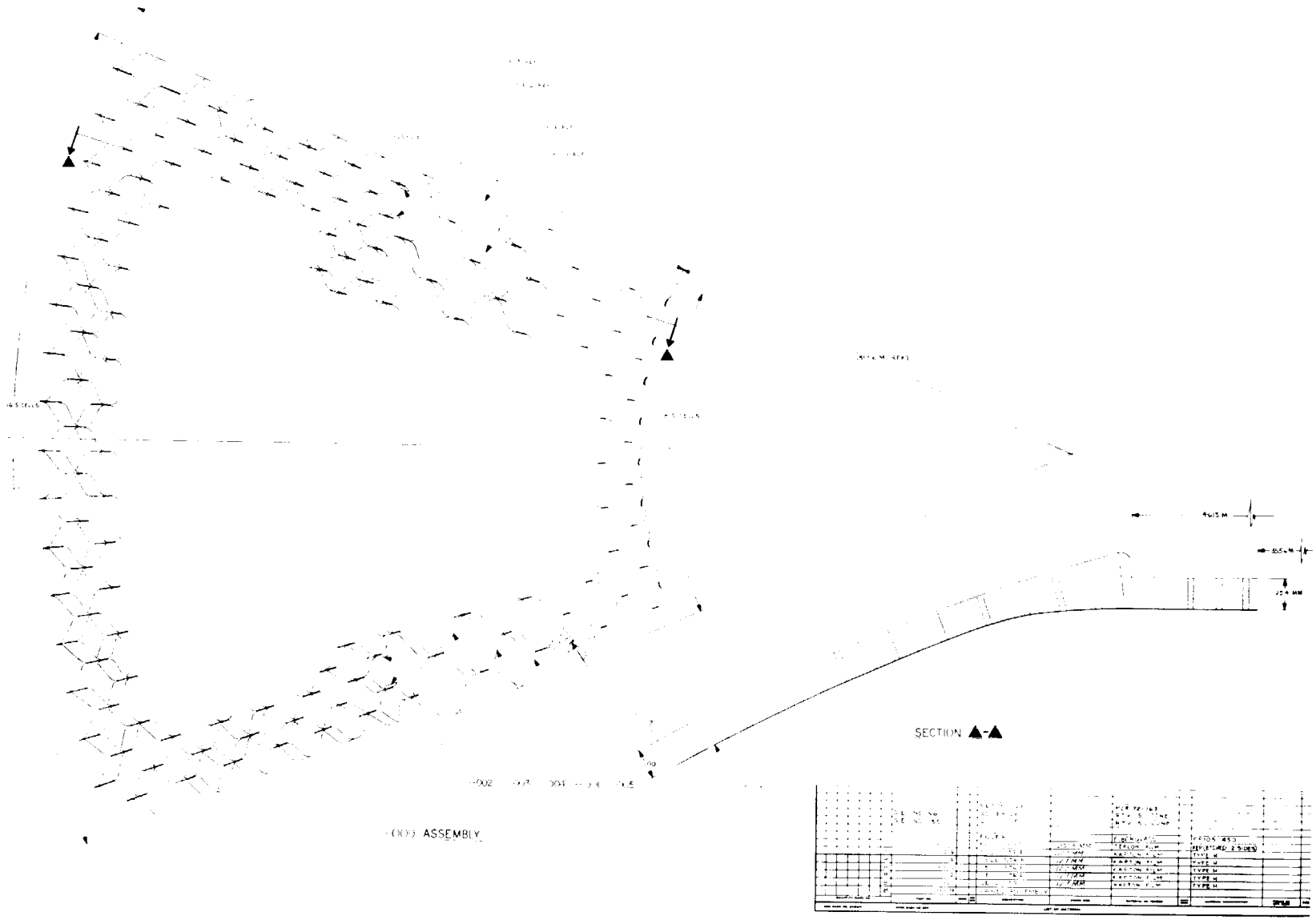

Figure 18. - F Panel, Top Dome

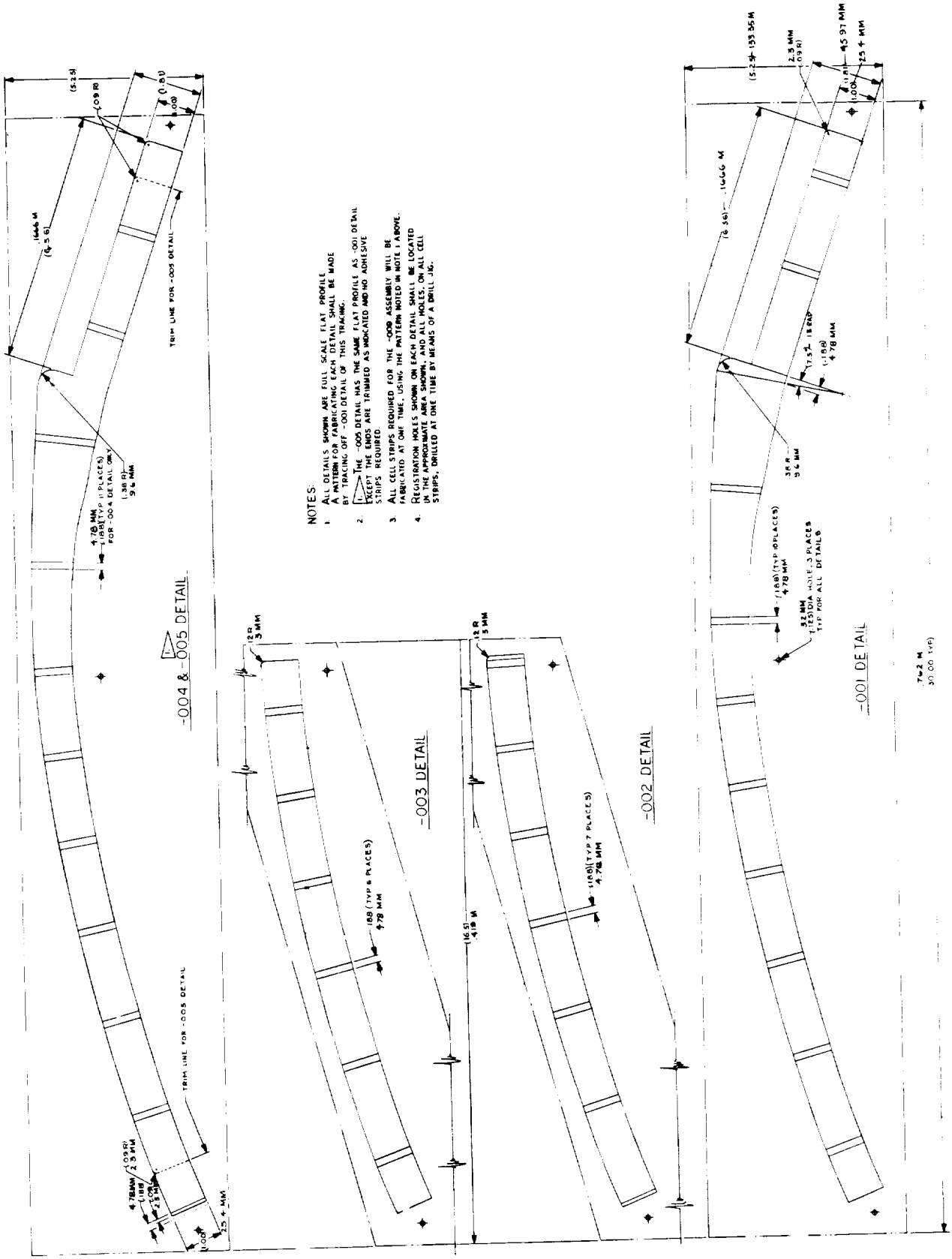

Figure 18. - (Concl)

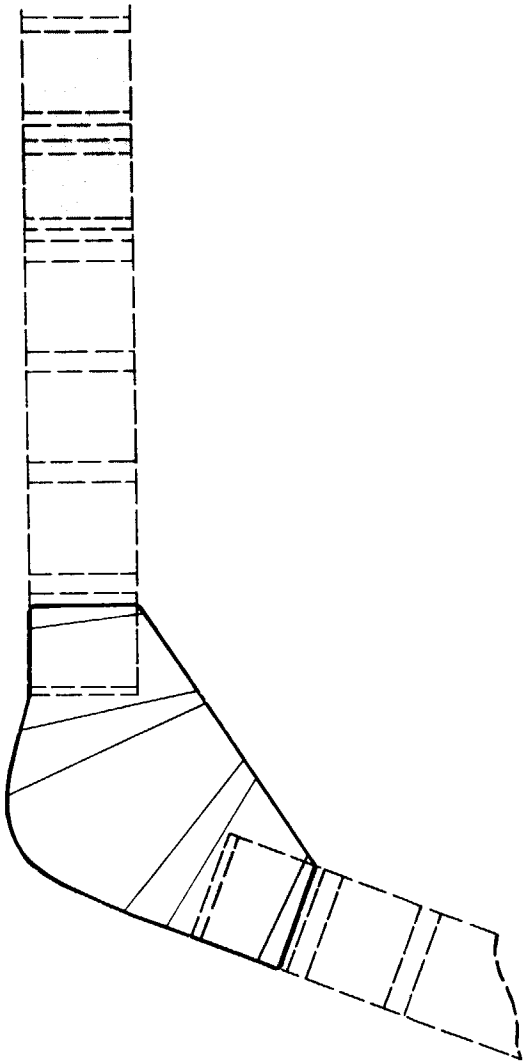

Figure 19. - Modified Design for C Panel
(Lower Barrel-to-Dome Transition)

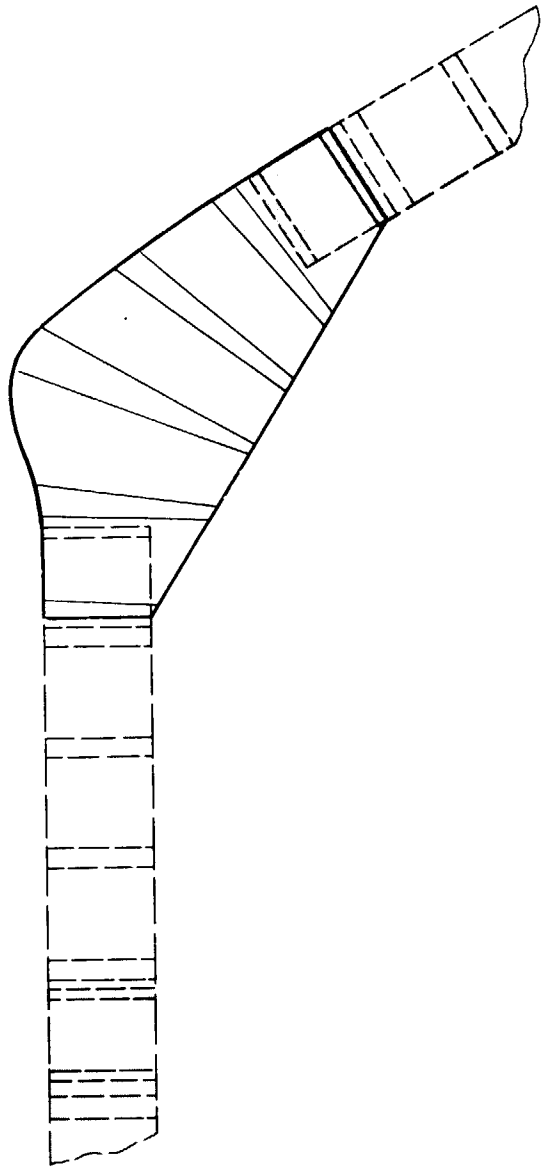

Figure 20. - Modified Design for E Panel
(Upper Barrel-to-Dome Transition)

QUANTITY/DASH NO	PART NO.	ZONE	SER SYM	DESCRIPTION	STOCK SIZE	MATERIAL OR VENDOR	MFR CODE	MATERIAL SPECIFICATION	FINISH OR MFR CODE	CHG
	SEALS			ADHESIVE		SILICONE		RTV-560		
16				SCREW, RD.HD.MACH	8-32 X .38 LG					
1				G PANEL						
8				F PANEL						
1	-002			EXPANSION RING		SILICONE		RTV-560 CAST		
1	-001			ANGLE RING		FIBERGLASS-EPOXY				

ODD DASH NO SHOWN — EVEN DASH NO OPP — LIST OF MATERIAL

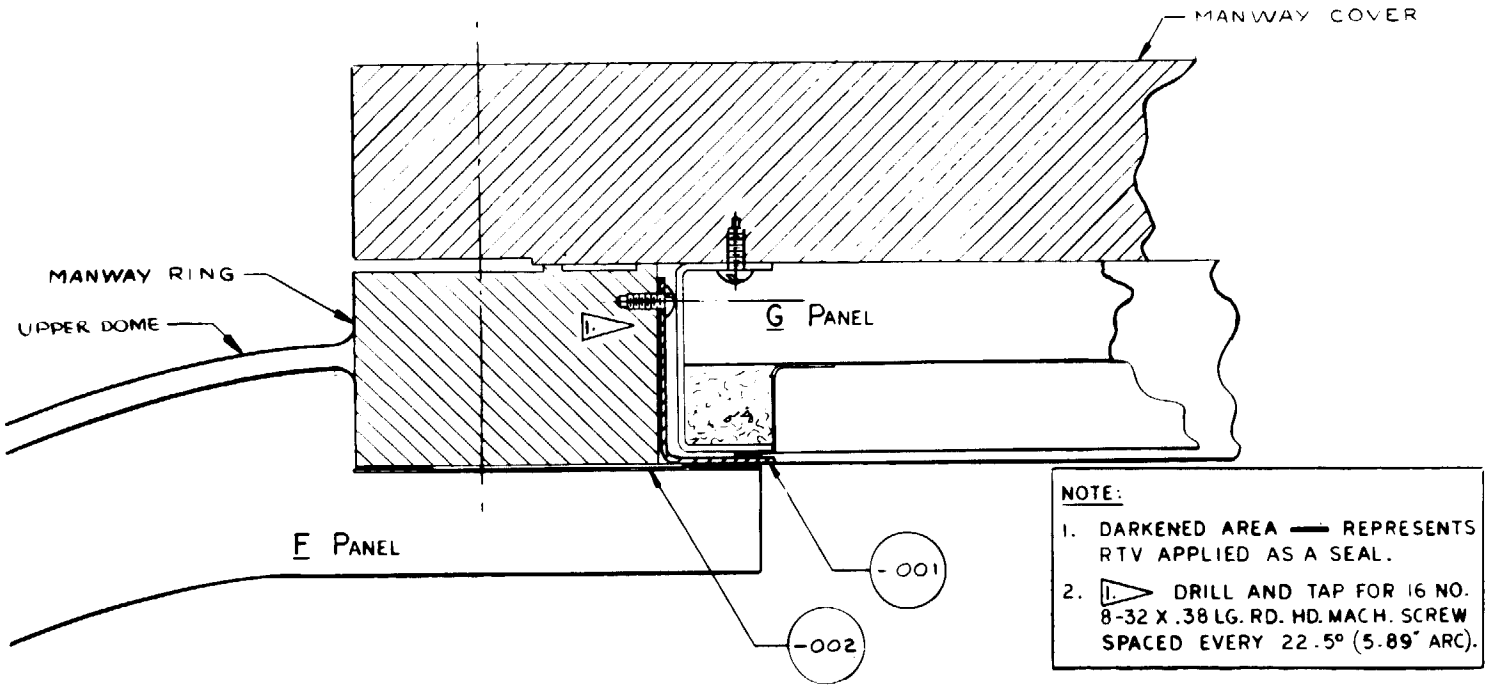

Figure 21. - Manway Closure Design

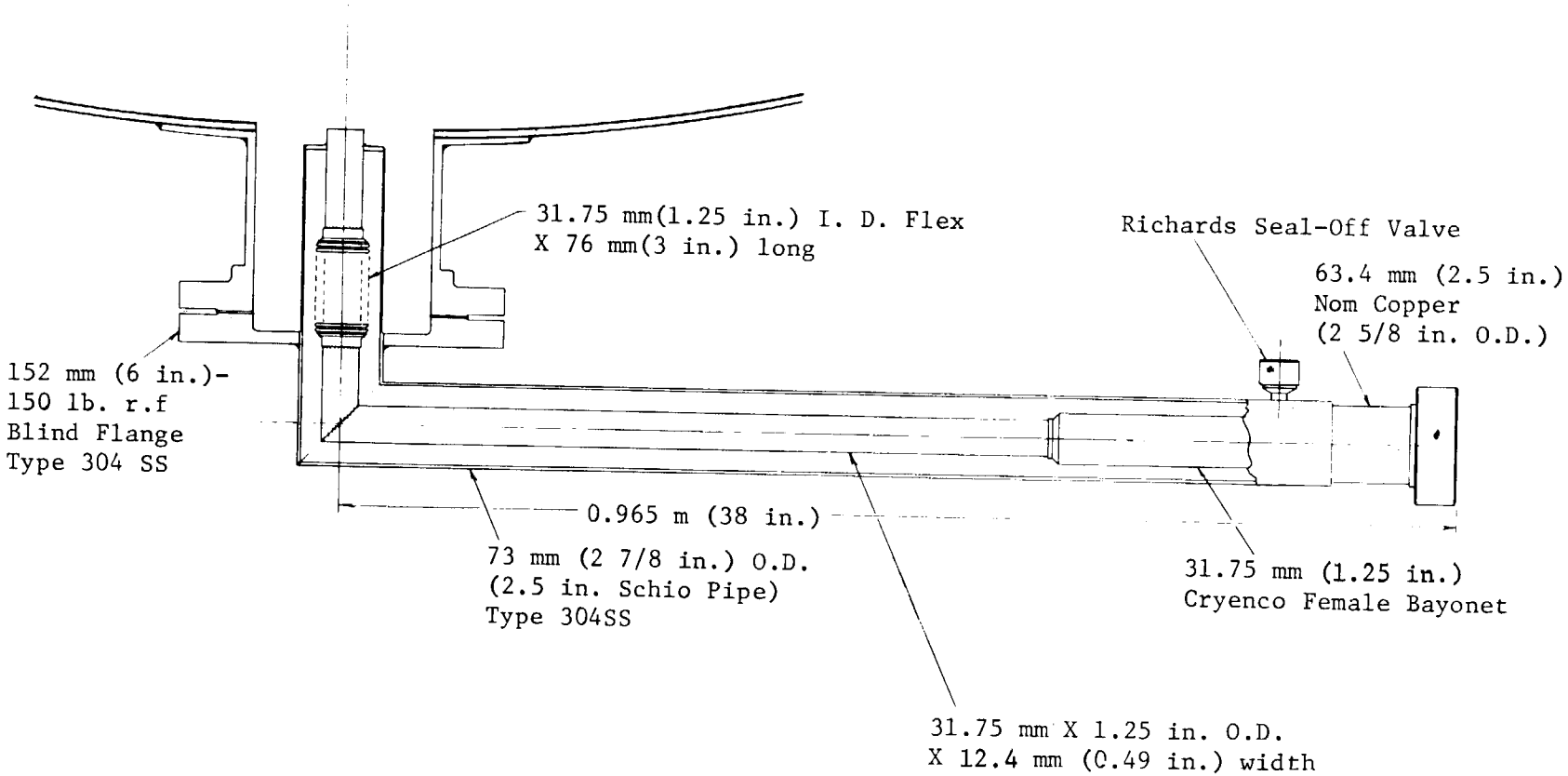

Figure 22. - Vacuum-Jacketed Fill Adapter

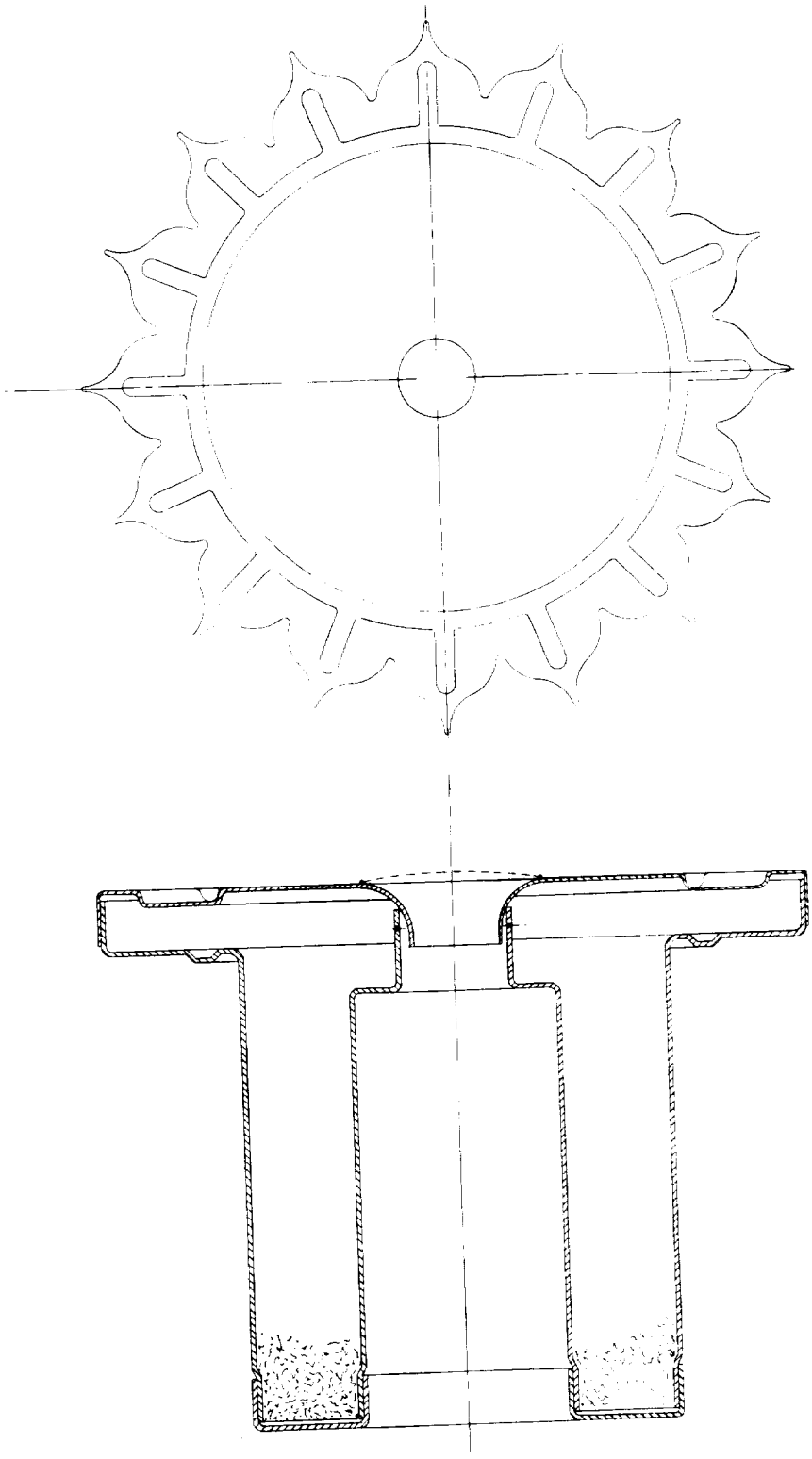

Figure 23. - Insulation Plug, Fill and Drain Port

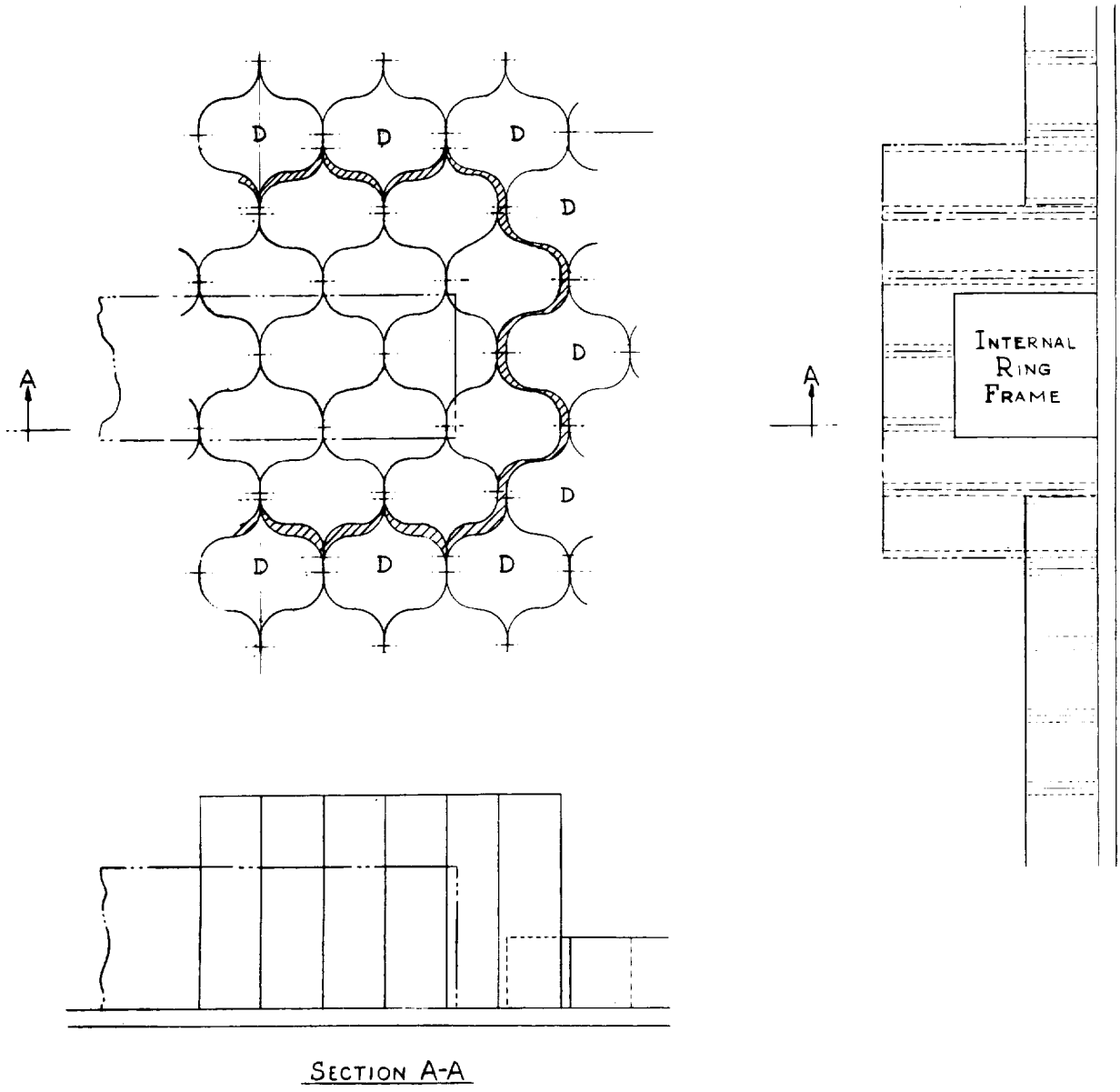

Figure 24. - Approach for Insulating Over Wall Mounted Hardware Items

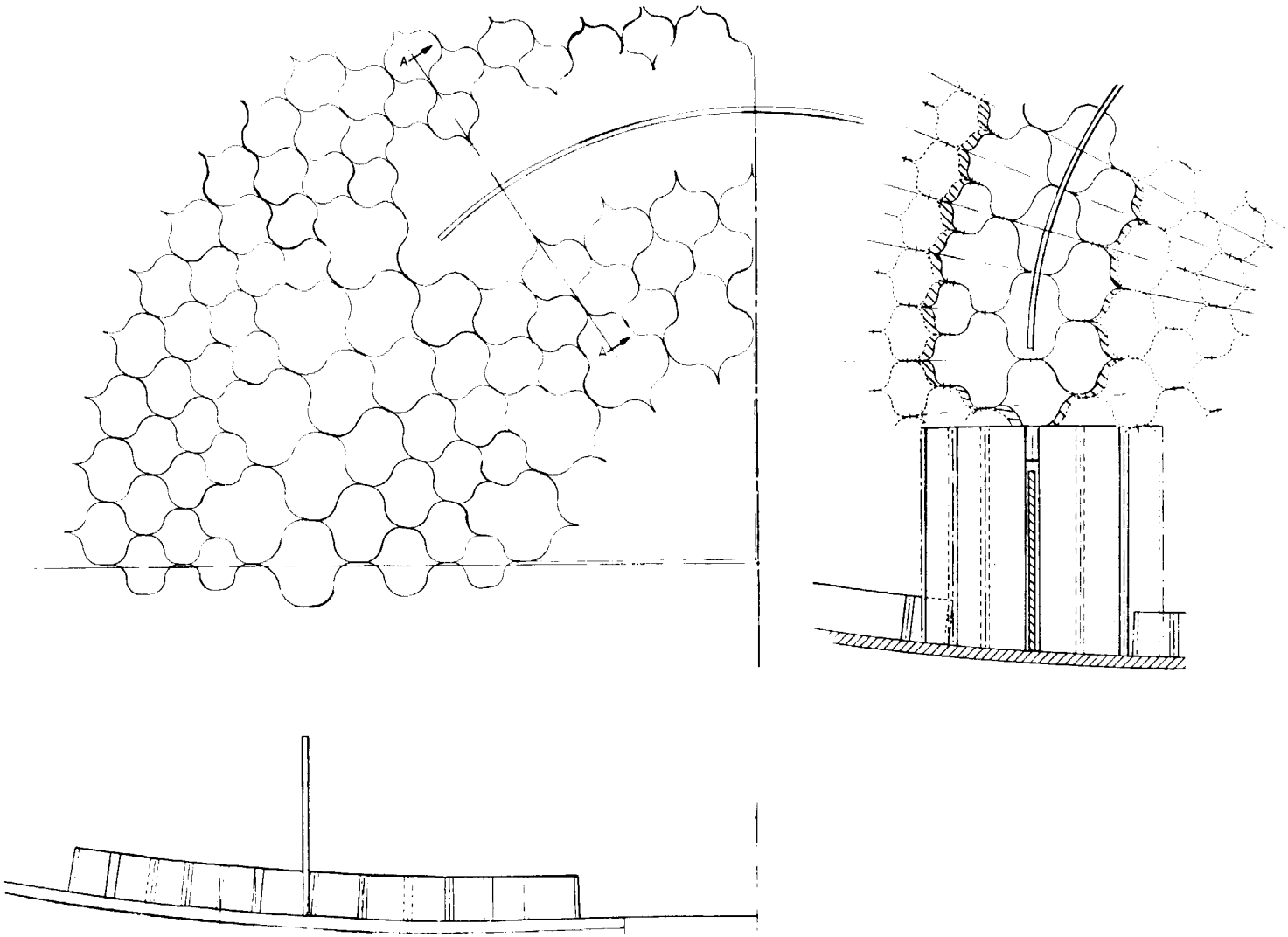

Figure 25. - Method of Insulating Around
Semi-Cylindrical Baffle

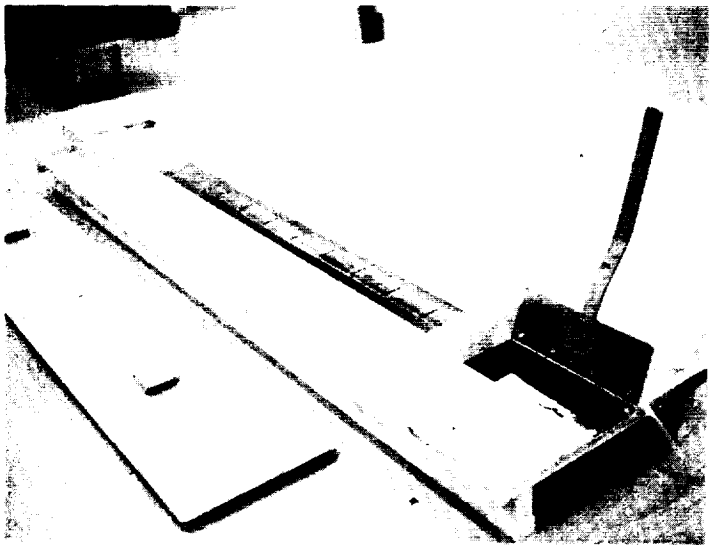

Figure 26 Core Printing Fixture

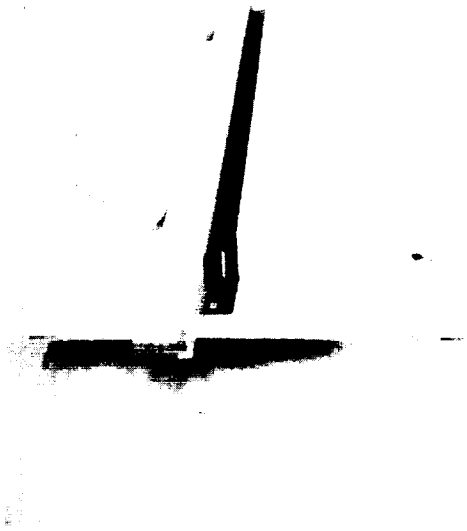

Figure 27 Core Stacking Fixture for Flat-Pattern Bonding

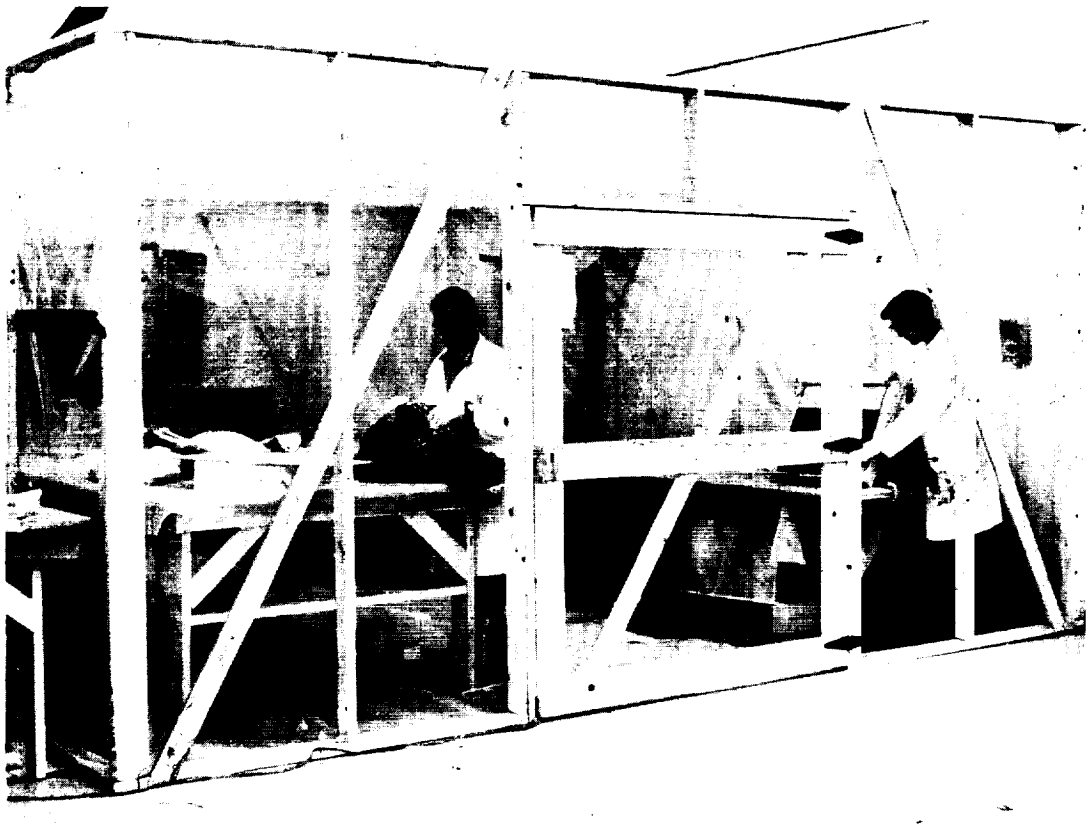

Figure 28 Controlled Humidity Room

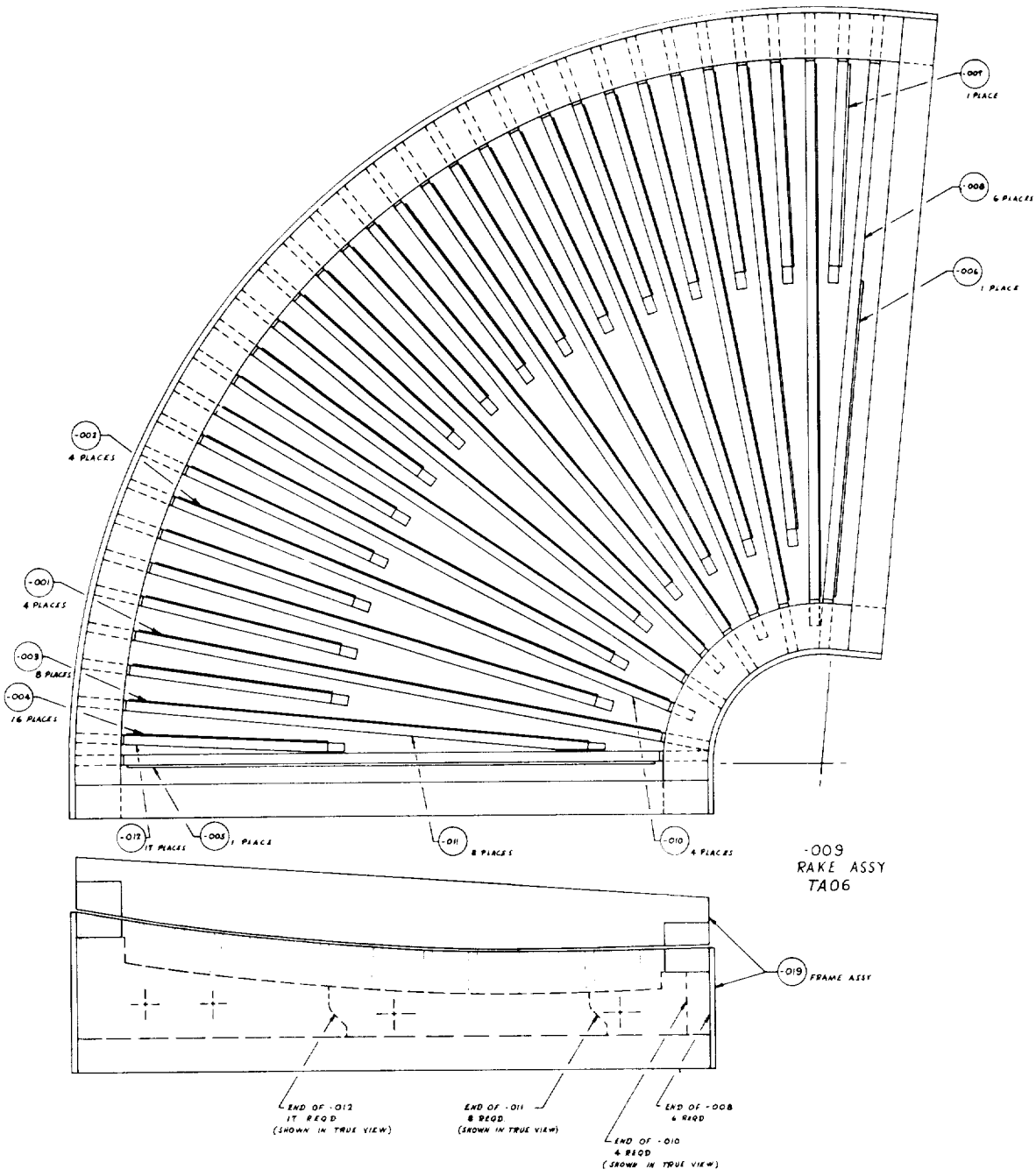

Figure 29. - Assembly Tool Design for A Panel

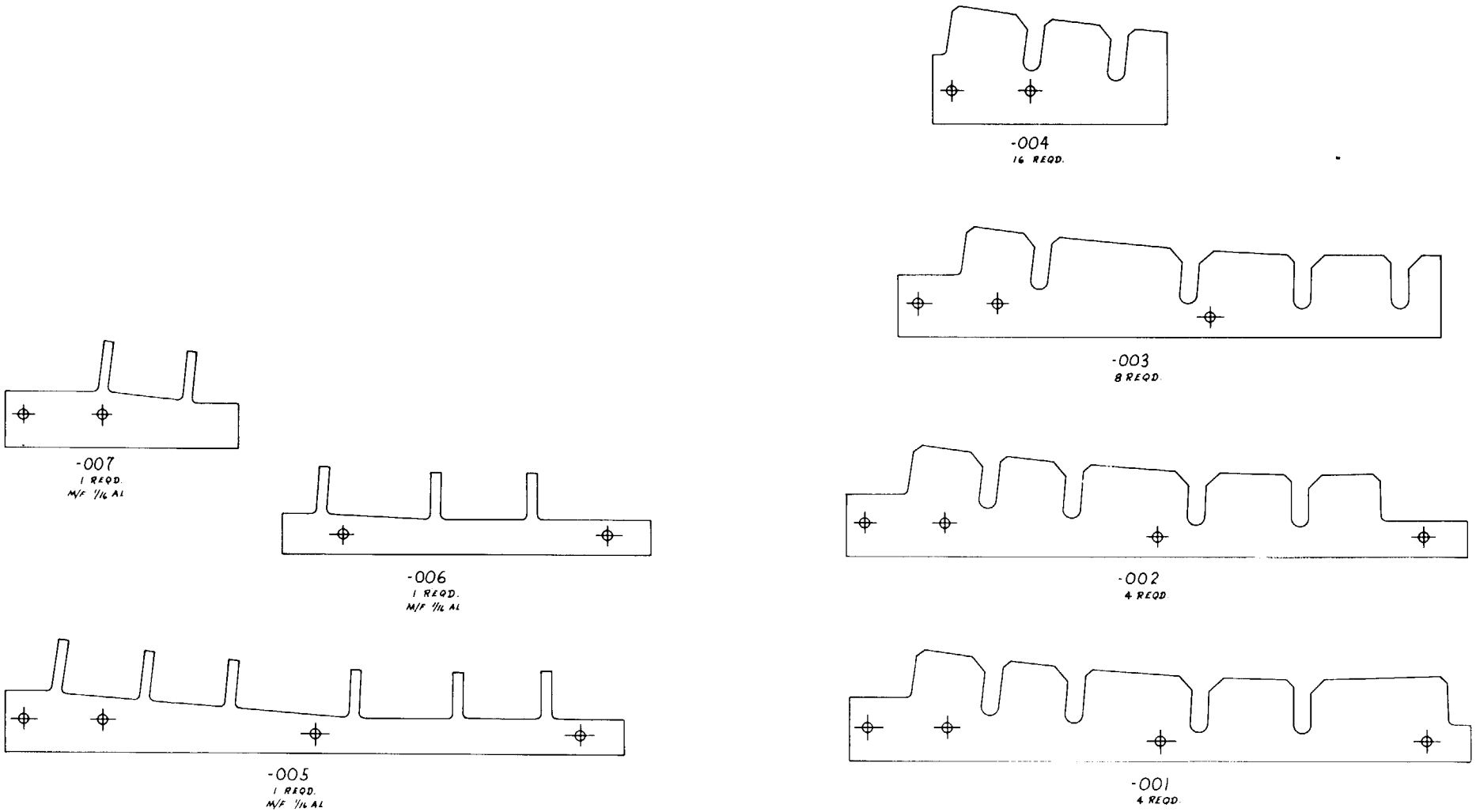

Figure 29. - (concl)

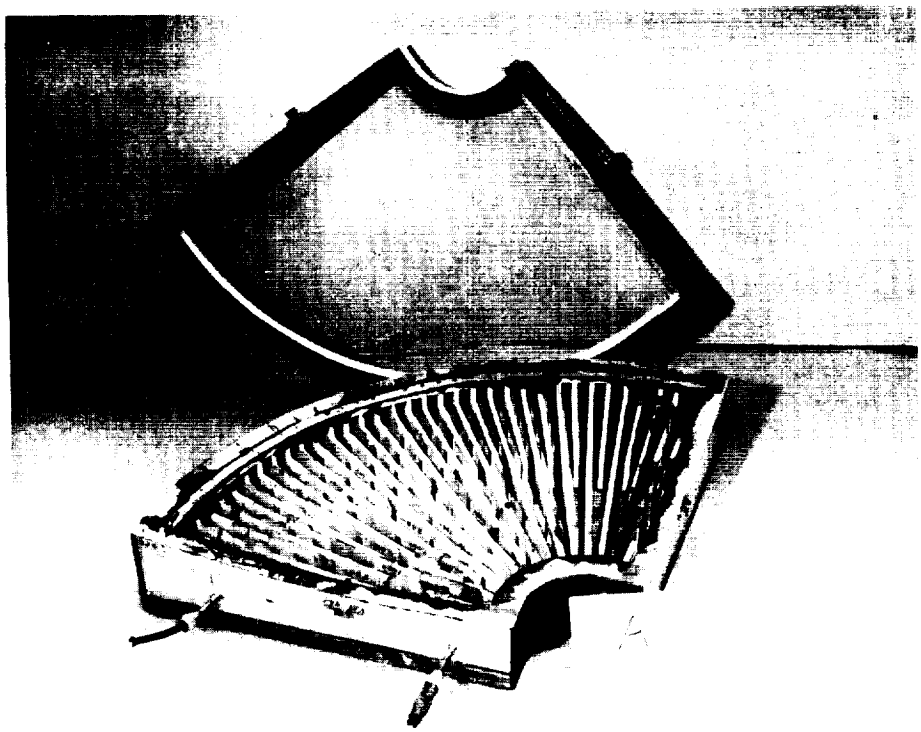

Figure 30 A Panel Assembly Rake/Vacuum Box

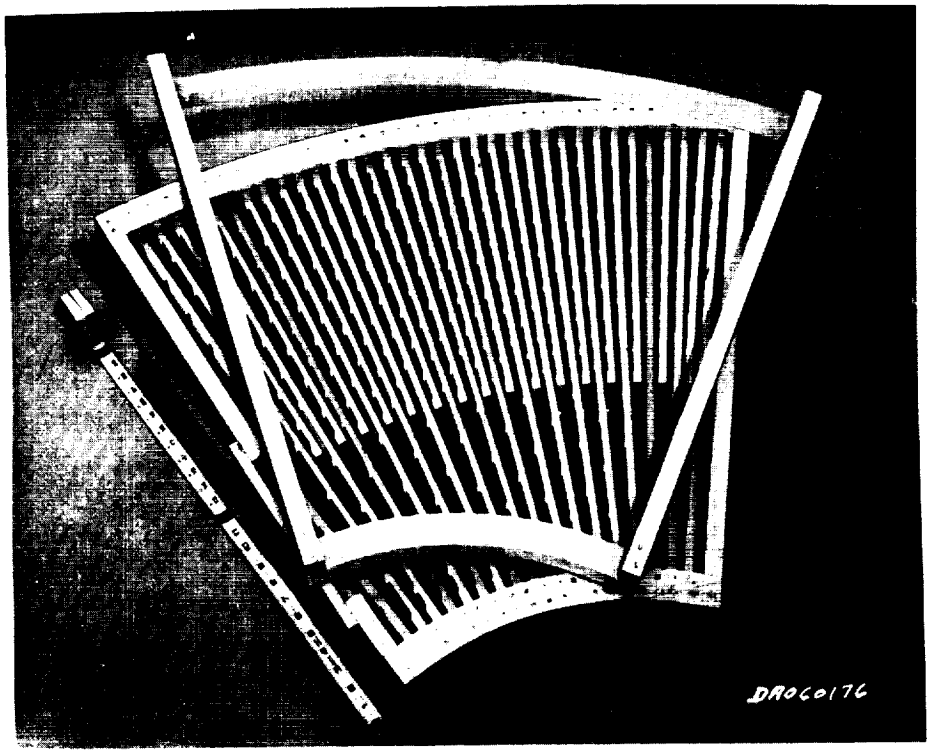

Figure 31 B Panel Assembly Rake/Vacuum Box

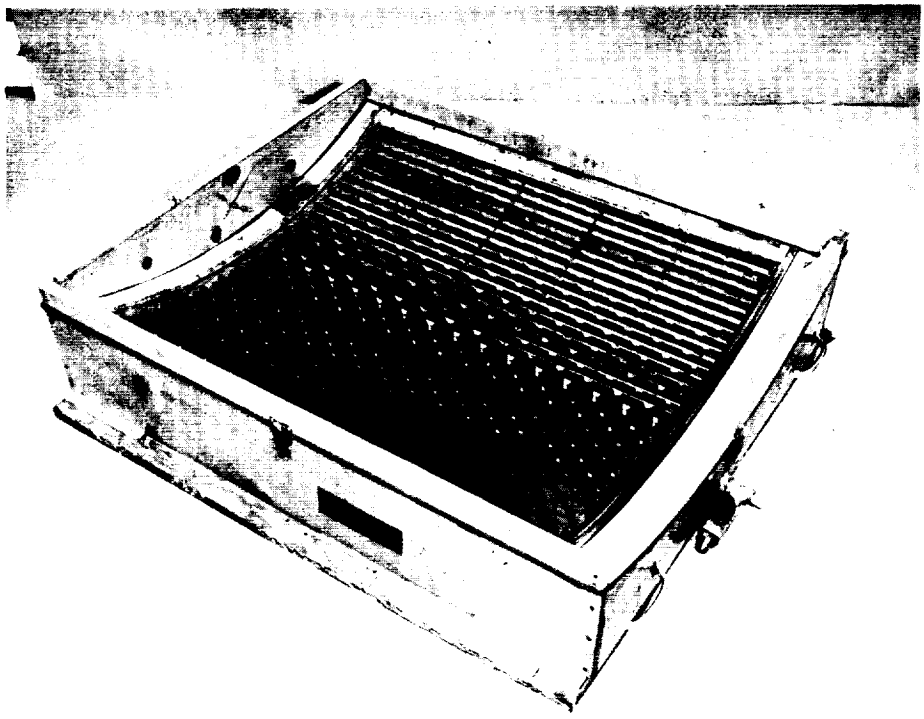

Figure 32 D Panel Assembly Rake/Vacuum Box

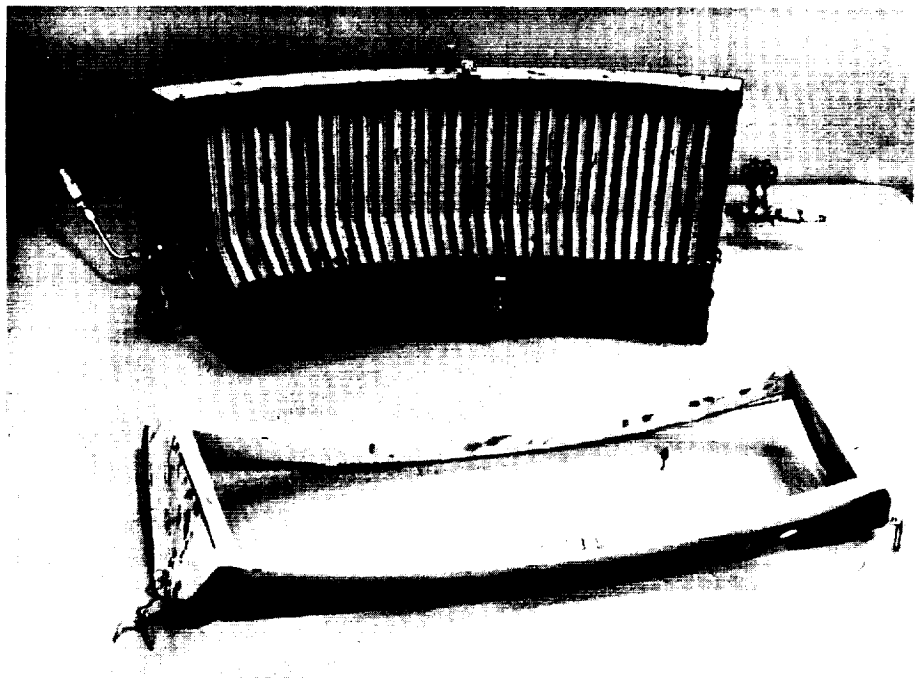

Figure 33 E Panel Assembly Rake/Vacuum Box

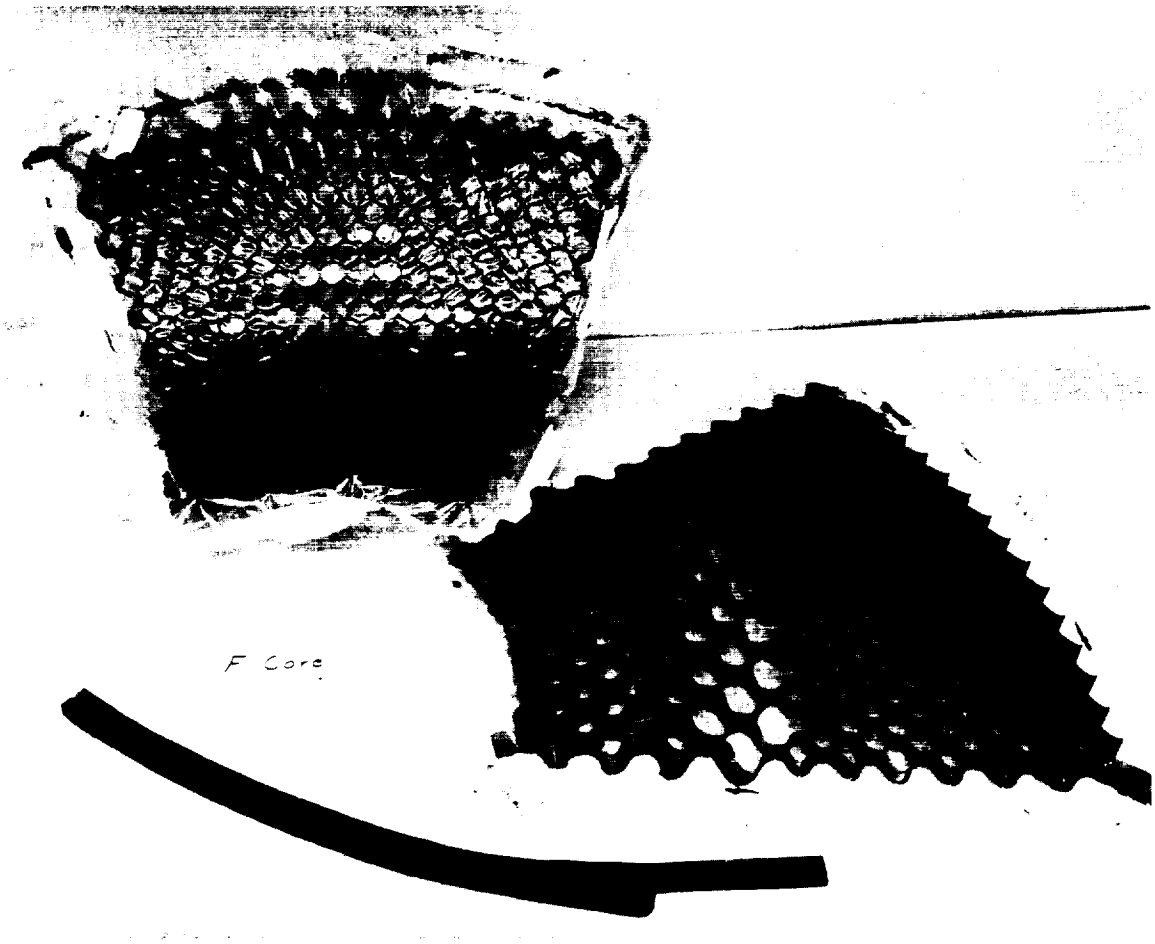

Figure 34 F Panel Core Assembly and Panels after Facesheet Assembly

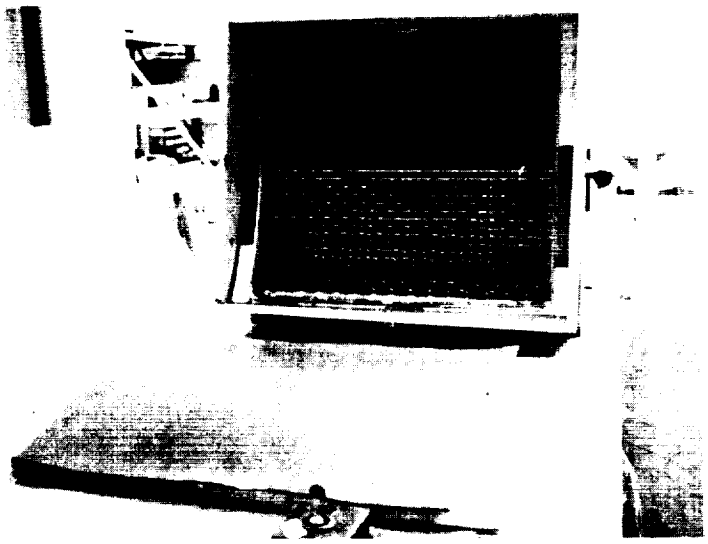

Figure 35 Dimpling Heater Blanket

Figure 36 Insulation Panel in Dimpling Fixture

Figure 37 Dimpling Fixture

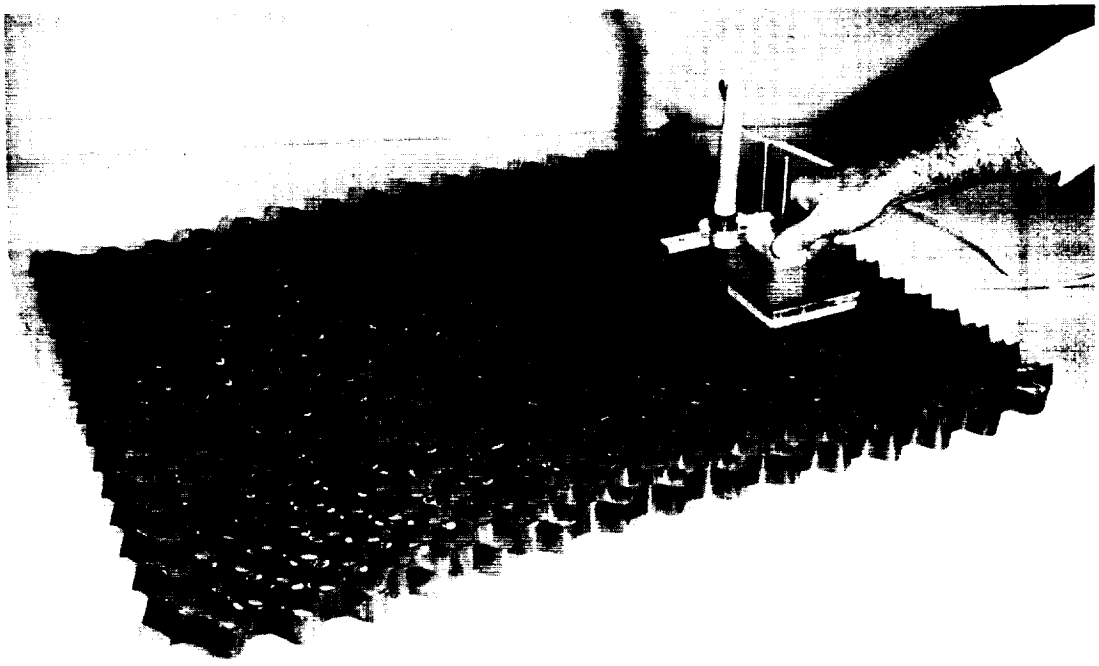

Figure 38 Trimmed Panel during Perforation (Contract NAS3-14384)

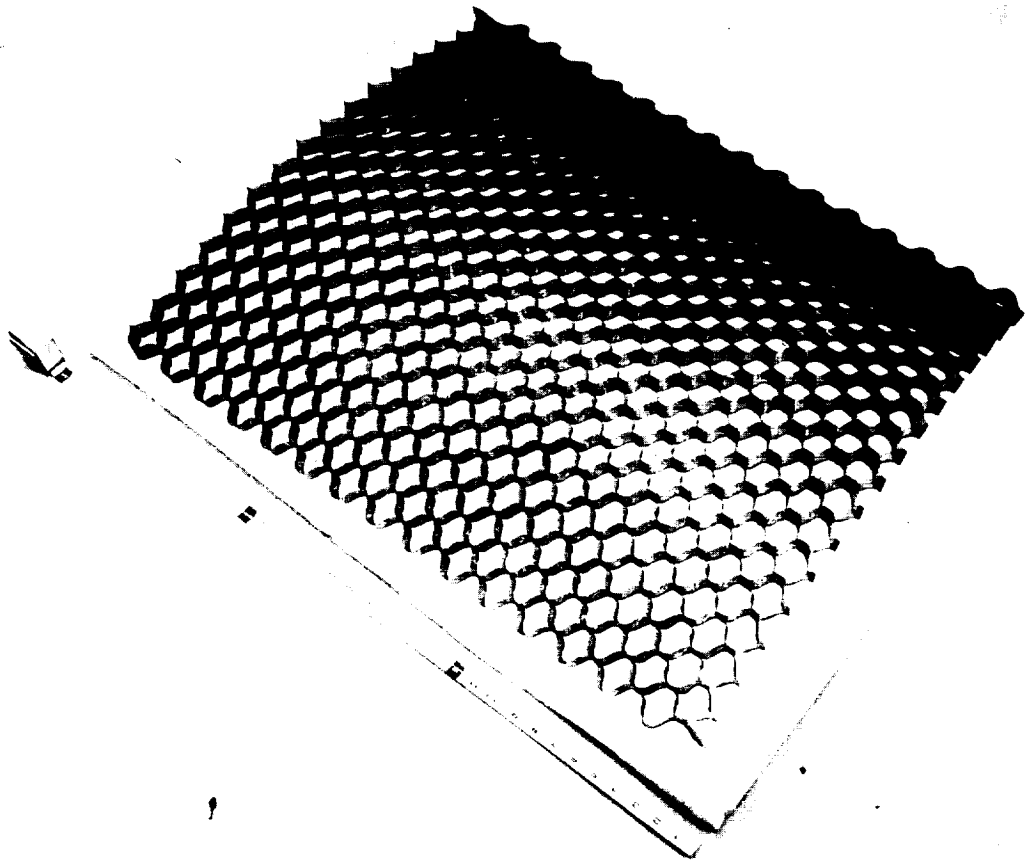

Figure 39 D Panel after Facesheet Trim

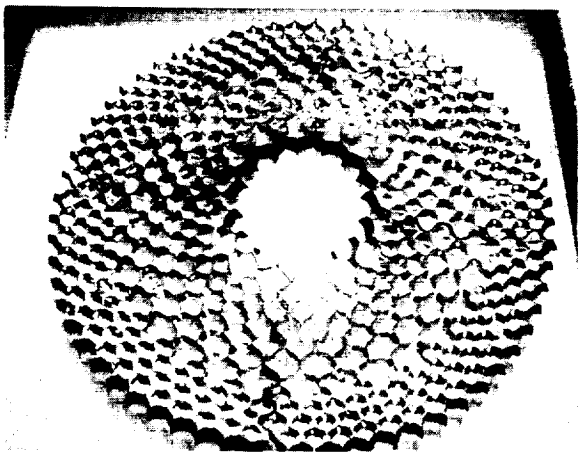

Figure 40 Four A Panels Nested to Form Complete Ring

Figure 41 Fiberglass Plug Fabrication with Pneumatic Punch

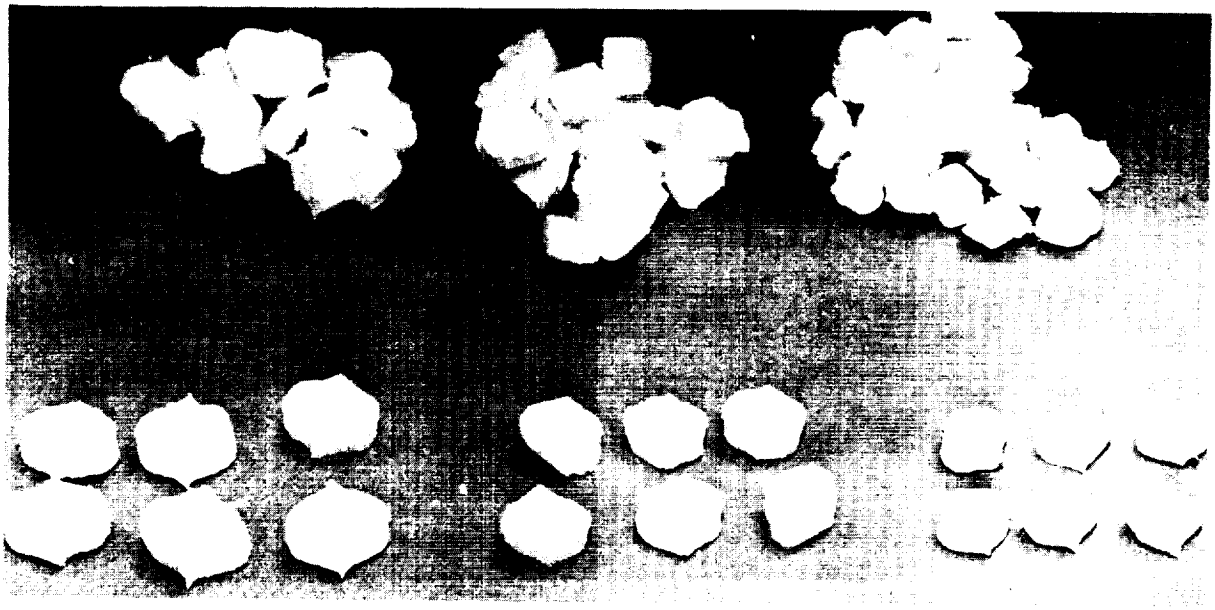

Figure 42 Fiberglass Plugs

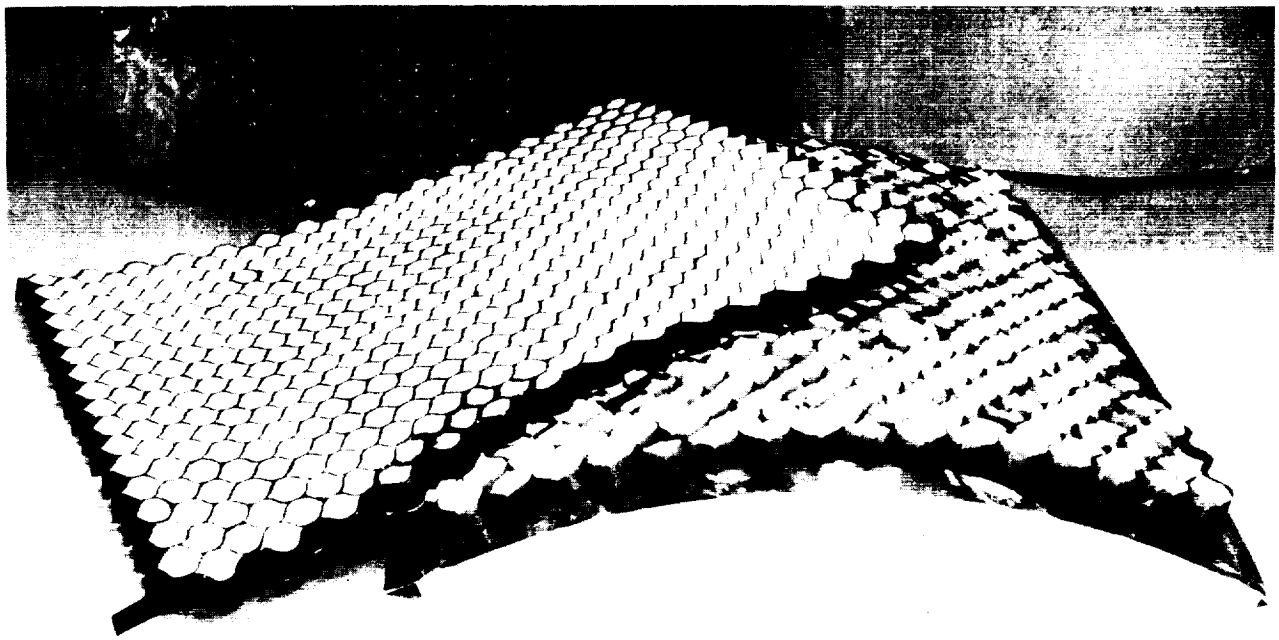

Figure 43 D Panels after Installation of Fiberglass Plugs

Figure 44 Leak Checking

Figure 45 Distorted Cell on Facesheet Side before Being Repaired

Figure 46 Distorted Cell on Facesheet Side after Being Repaired

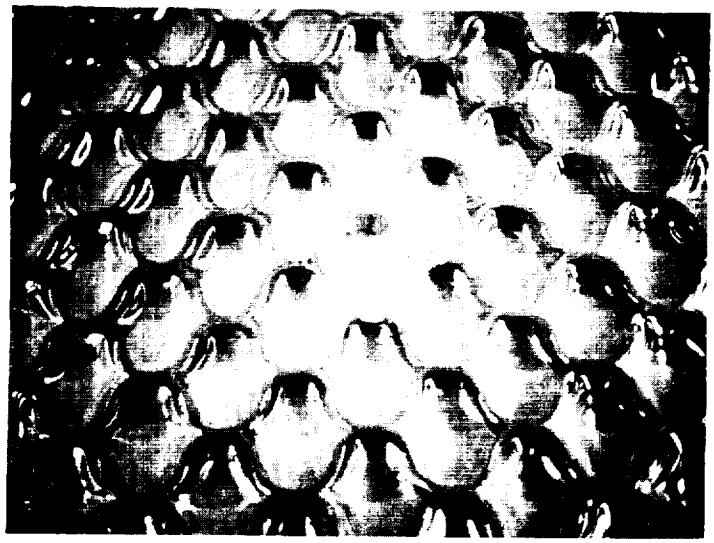

Figure 47 Specimen with Facesheet Patch

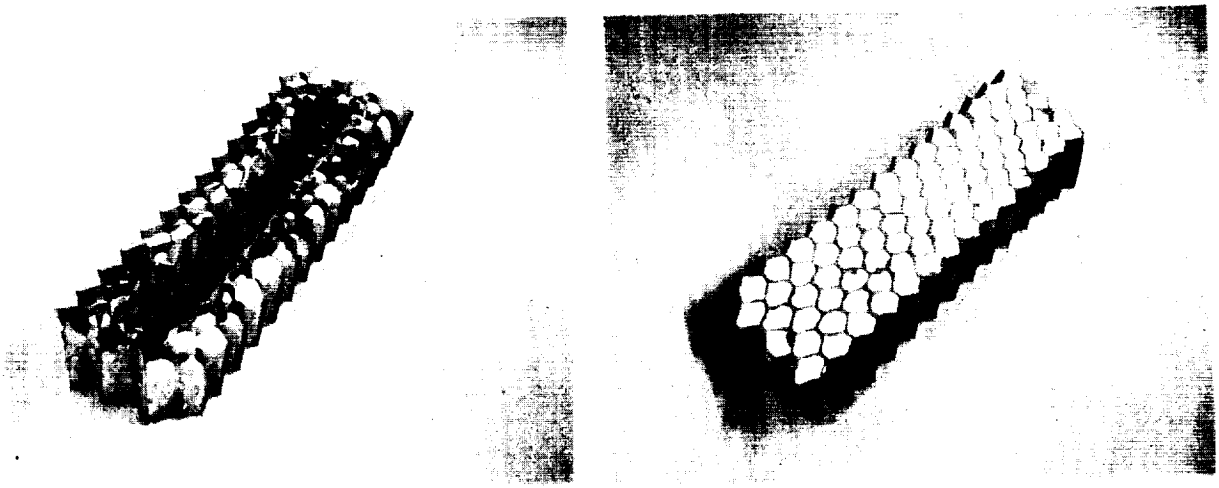

Figure 48 Special Panel to Cover Ring Frame Segment

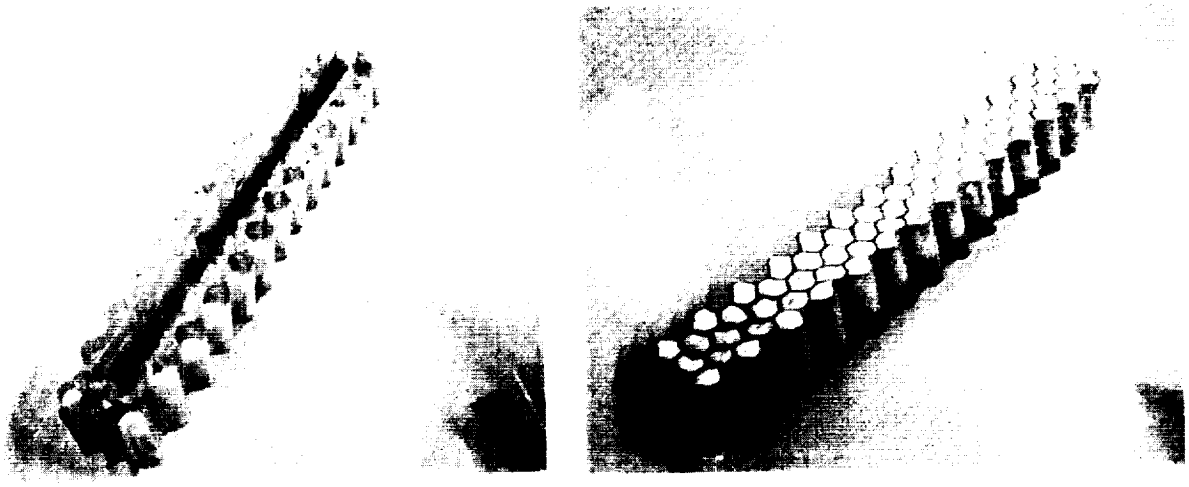

Figure 49 Special Panel to Cover Vertical Stringer Segment

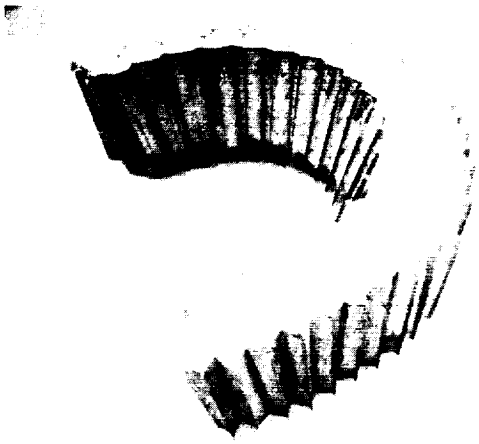

Figure 50 Special Panel to Cover Simulated Outlet

Figure 51 Special Panel for Attach Bracket

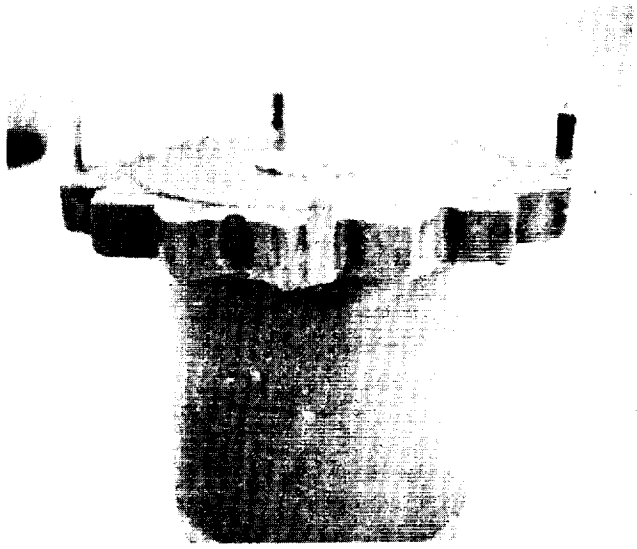

Figure 52 Fill and Drain Adapter Plug

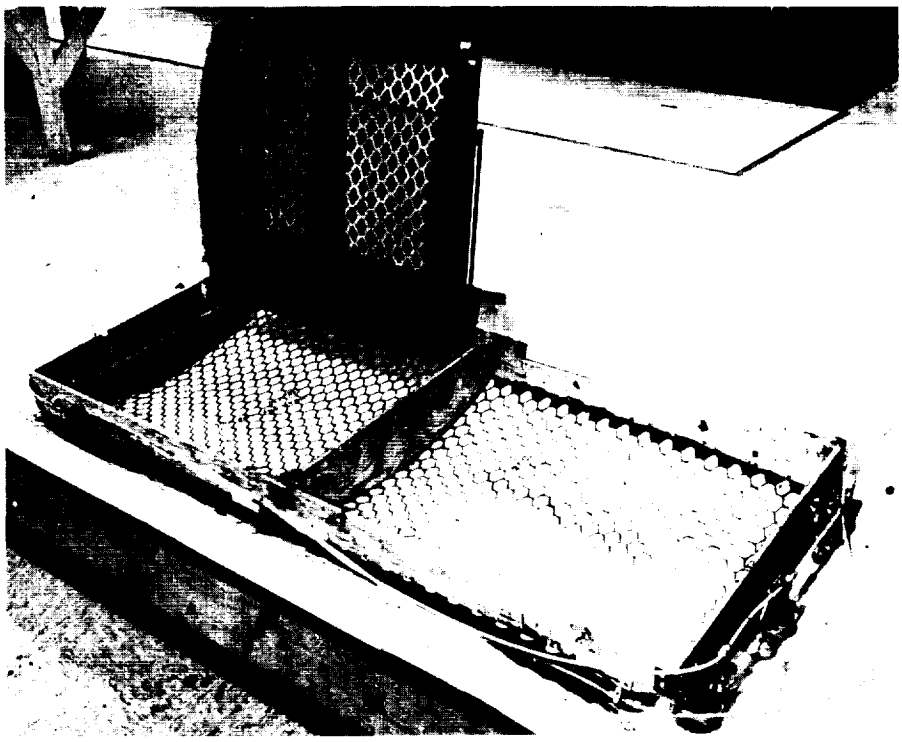

Figure 53 Installation Tool Shown With Stencil in Place on the Upper Panel Section Following Completion of Test

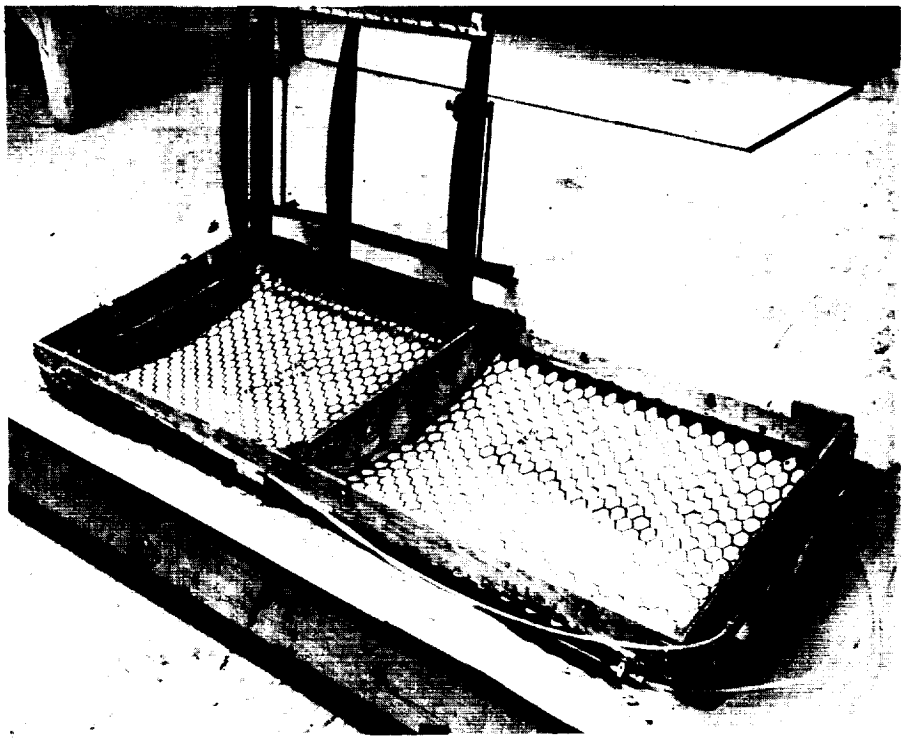

Figure 54 Installation Tool with Stencil Removed

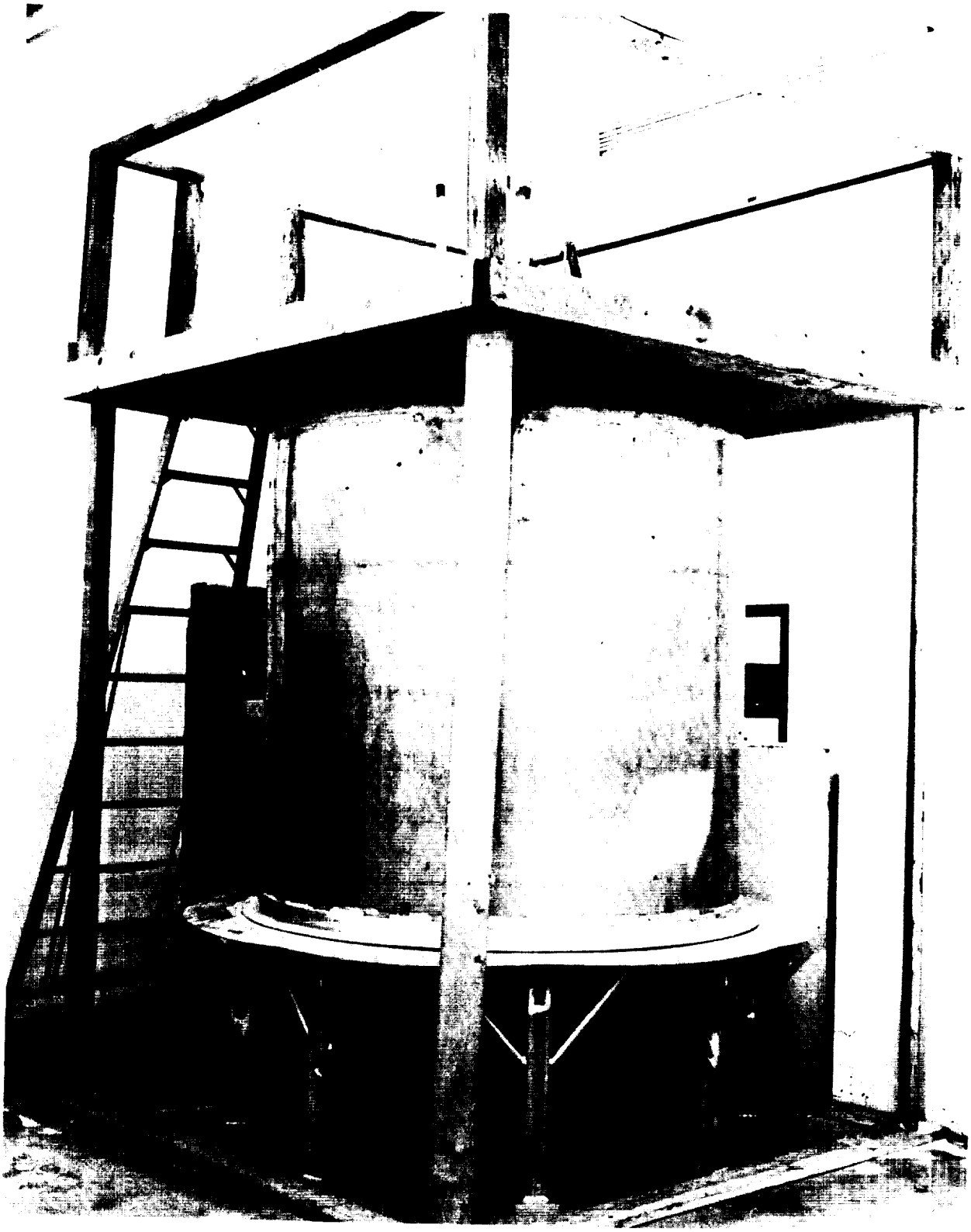

Figure 55 Tank in Upright Position Showing Access Scaffold

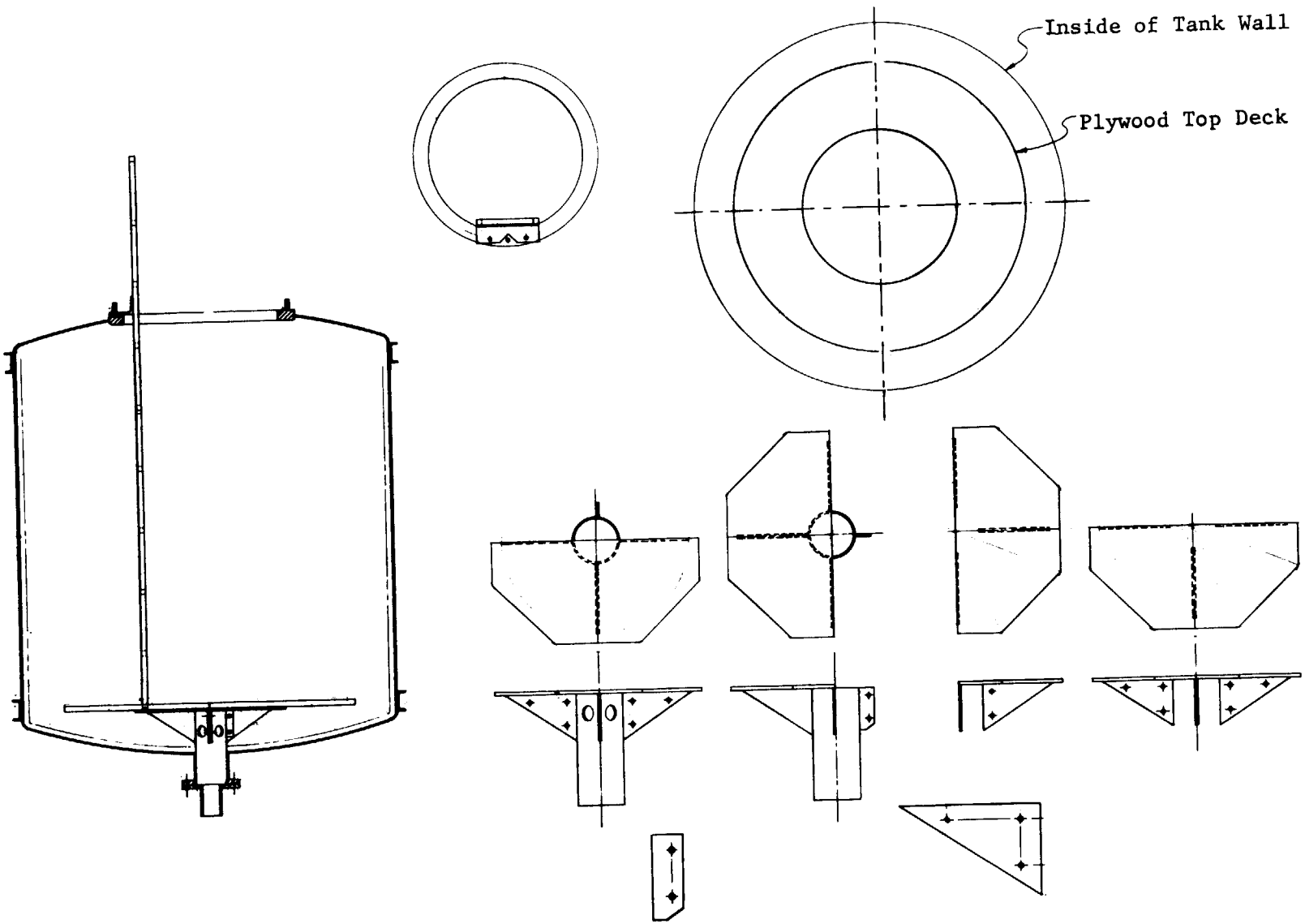

Figure 56 Work Platform Design

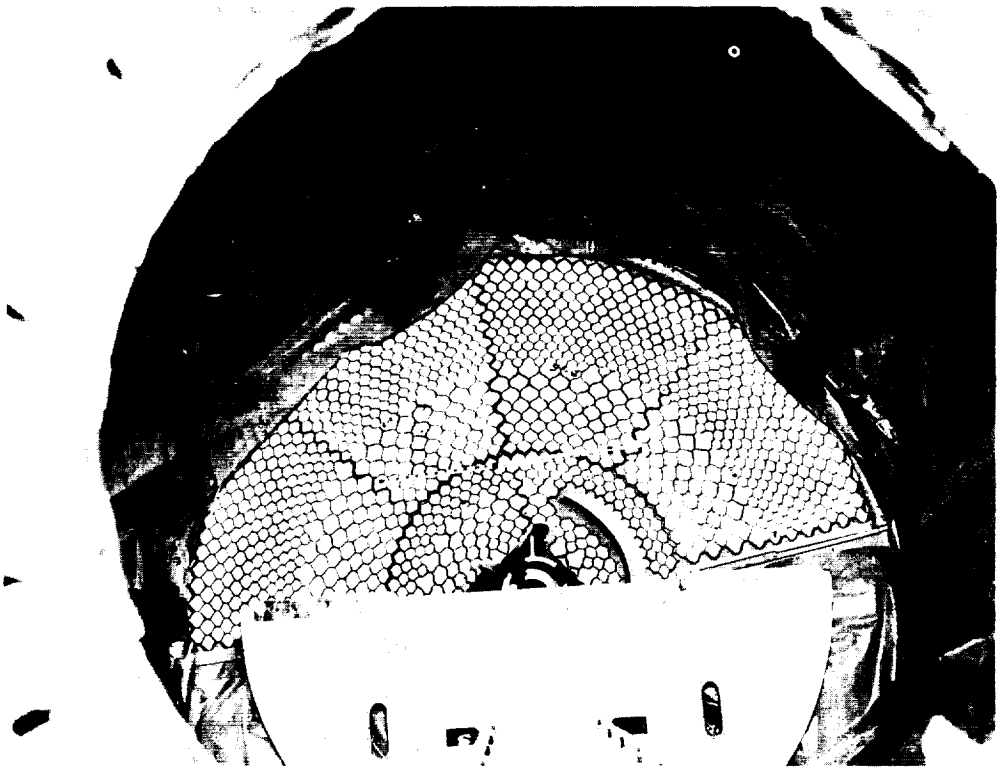

Figure 57 Insulation Panels as Installed in Tank Bottom

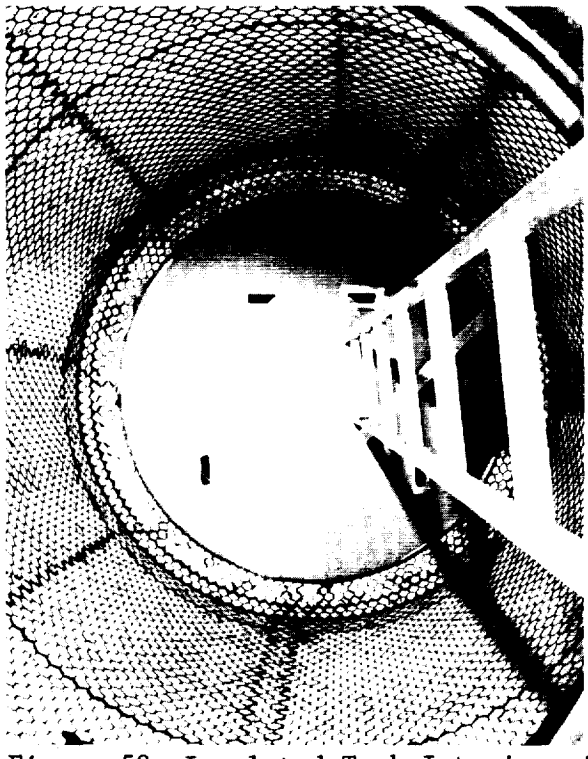

Figure 58 Insulated Tank Interior with Ladder and Work Platform in Place

Figure 59 Simulated Internal Hardware before Insulation

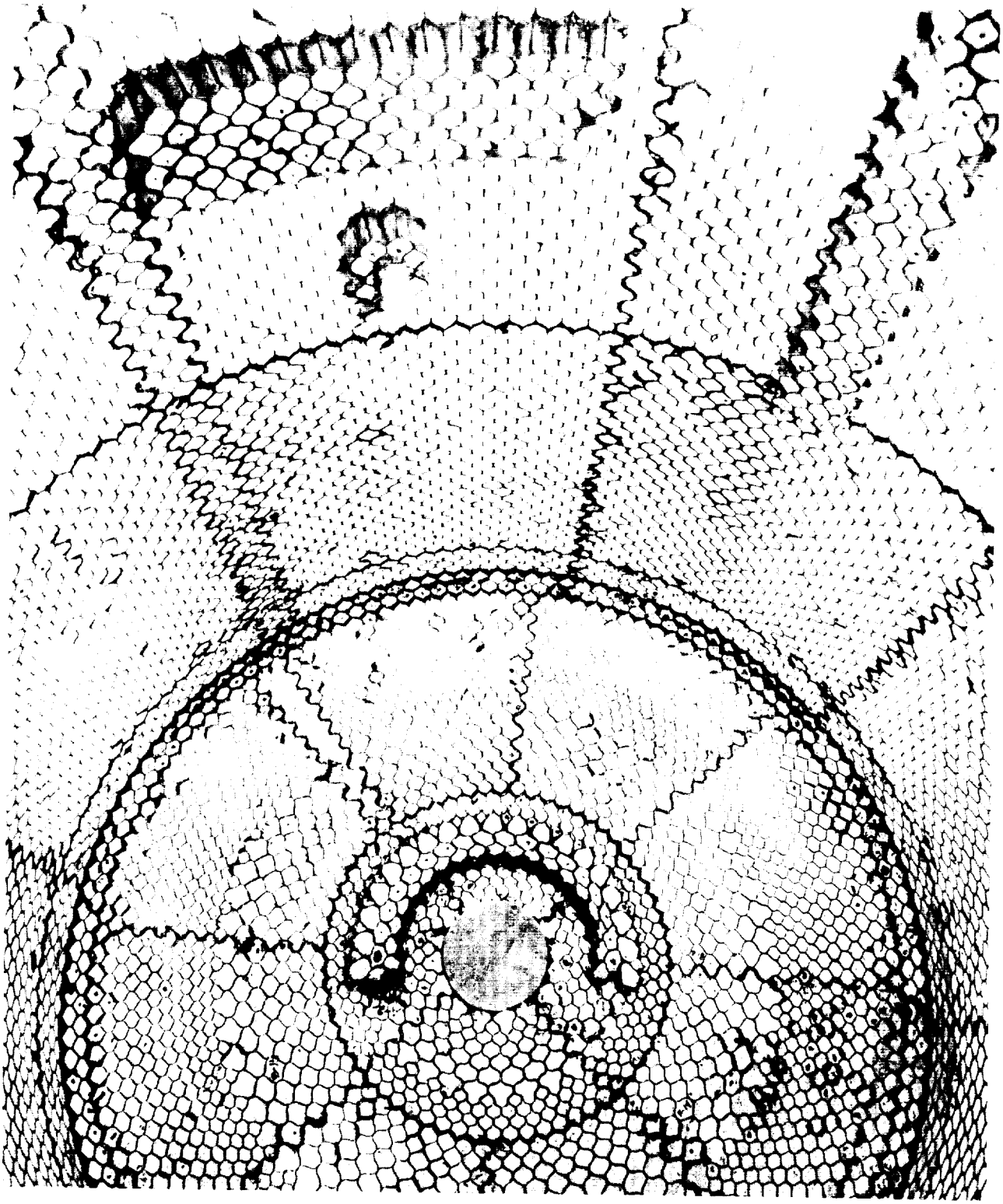

Figure 60 Tank Interior after Installation of Special Panels

Figure 61 Upper Portion of Insulated Tank Interior

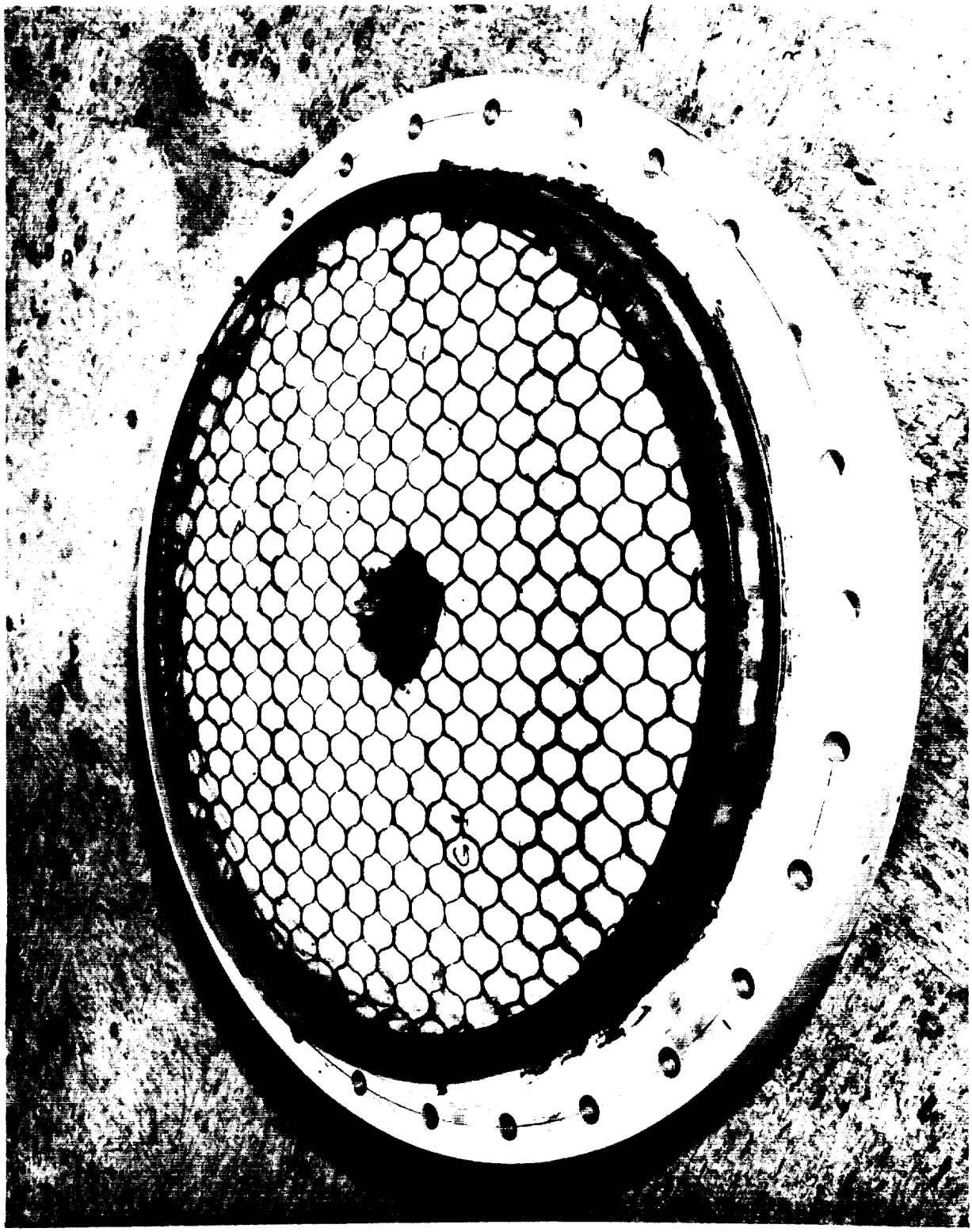

Figure 62 Insulated Manway Cover

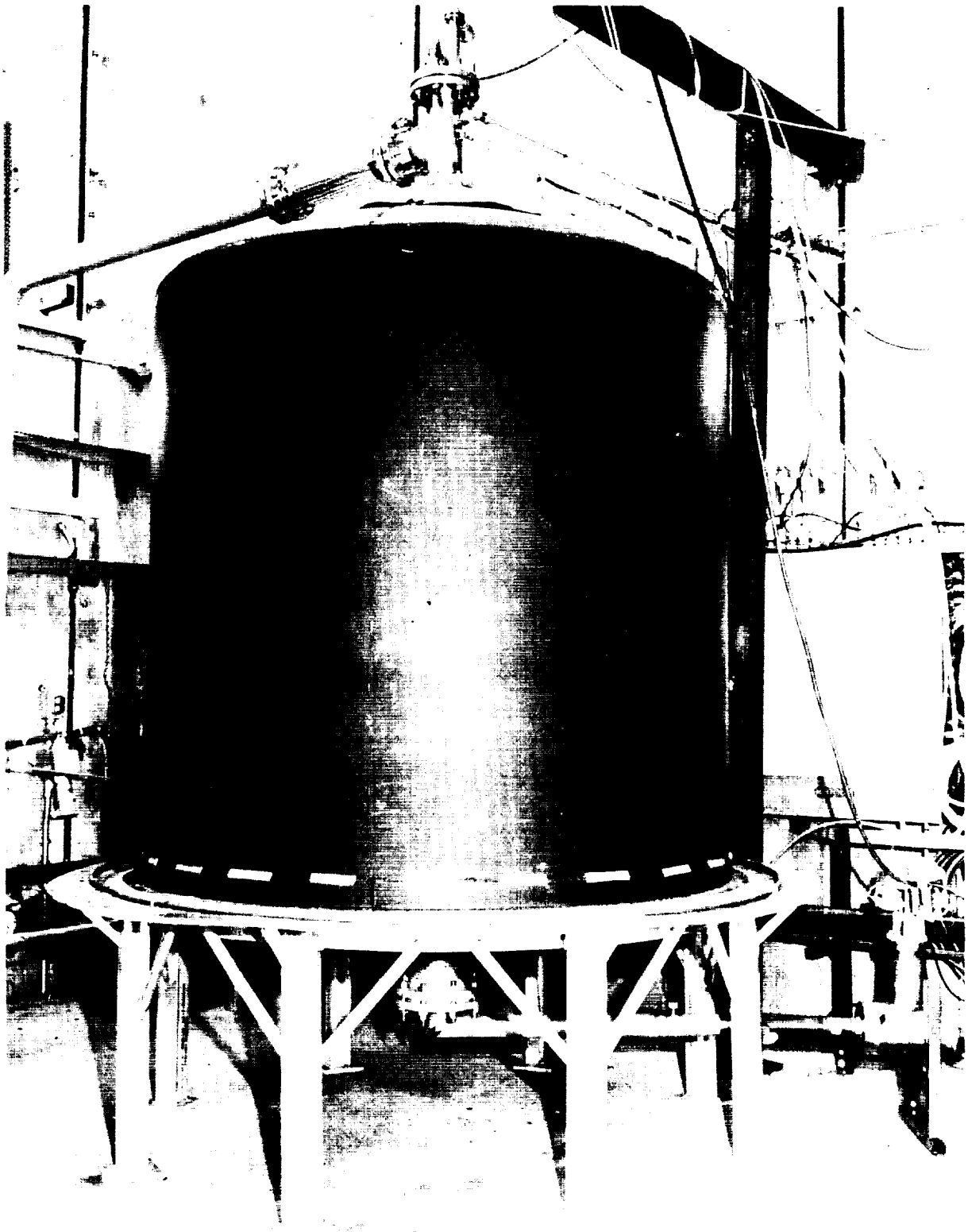

Figure 63. - Tank Installed in Test Cell

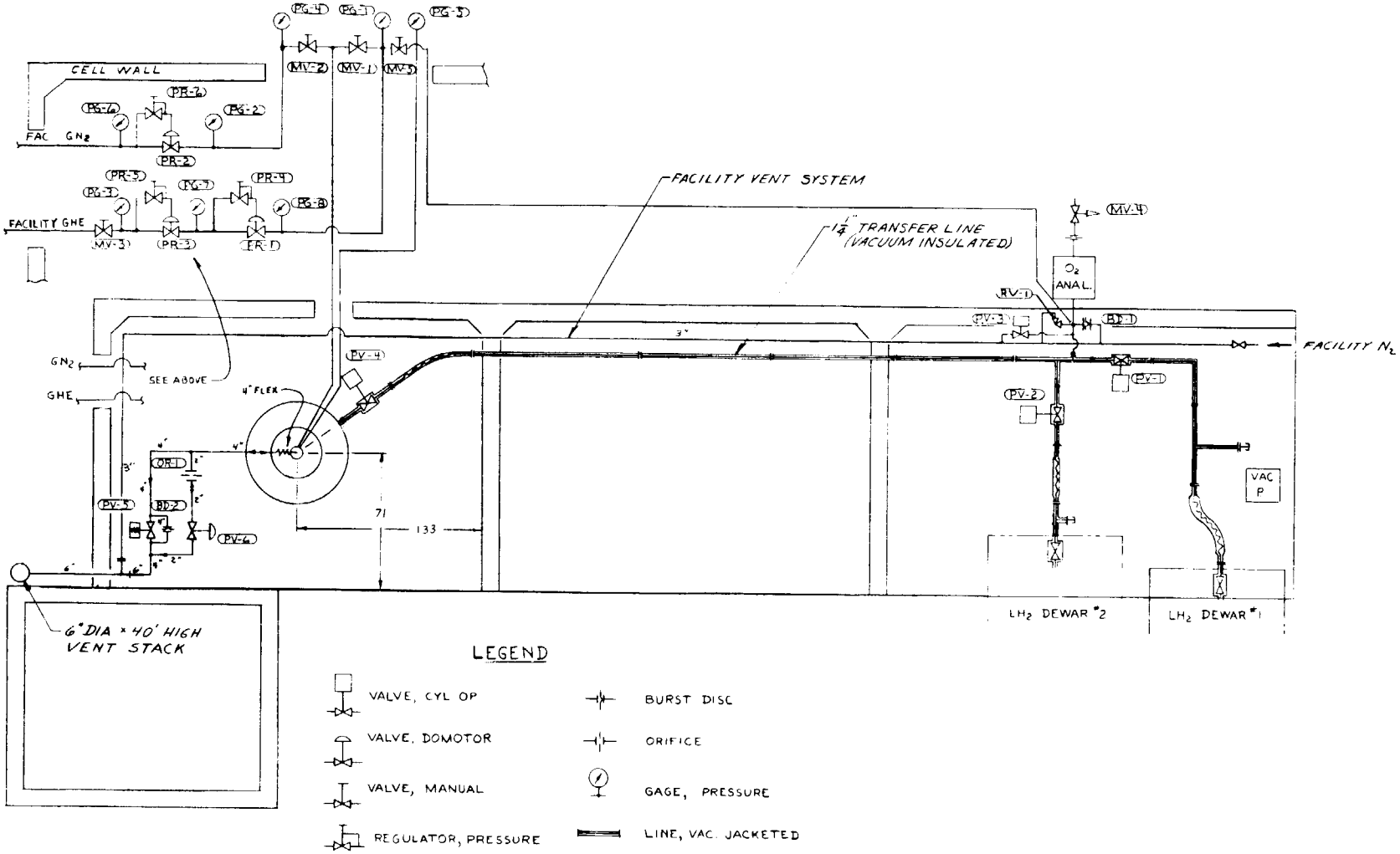

Figure 64. - Test Installation and Plumbing

Figure 65. - Fill Adapter Assembly

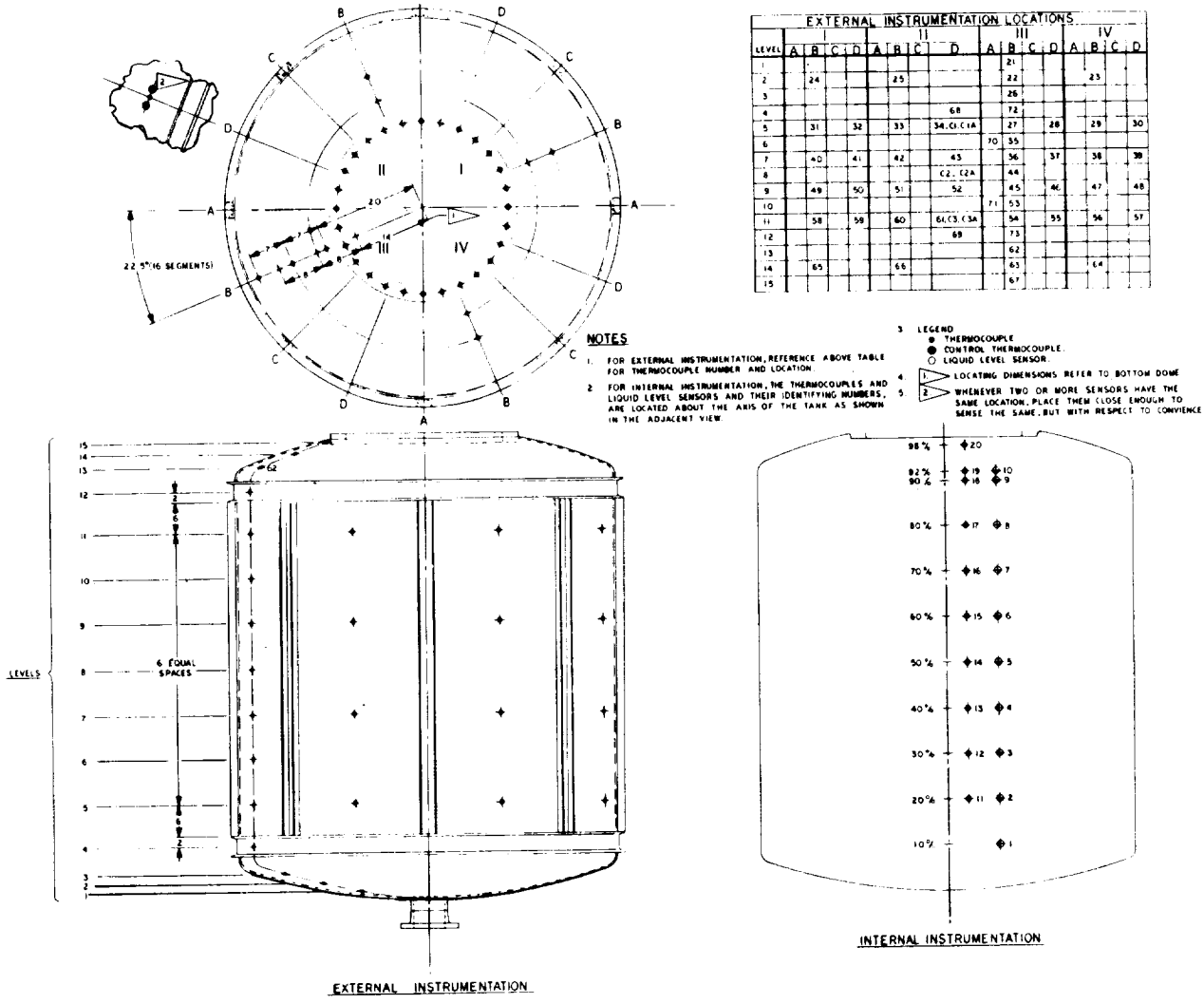

Figure 66. - Tank Instrumentation

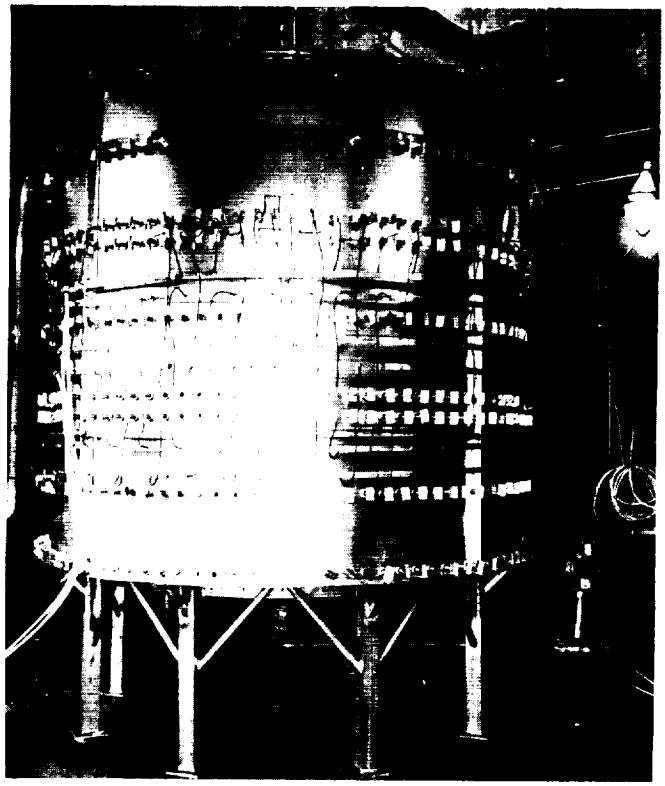

Figure 67. - Test Setup with Heat Chamber in Place

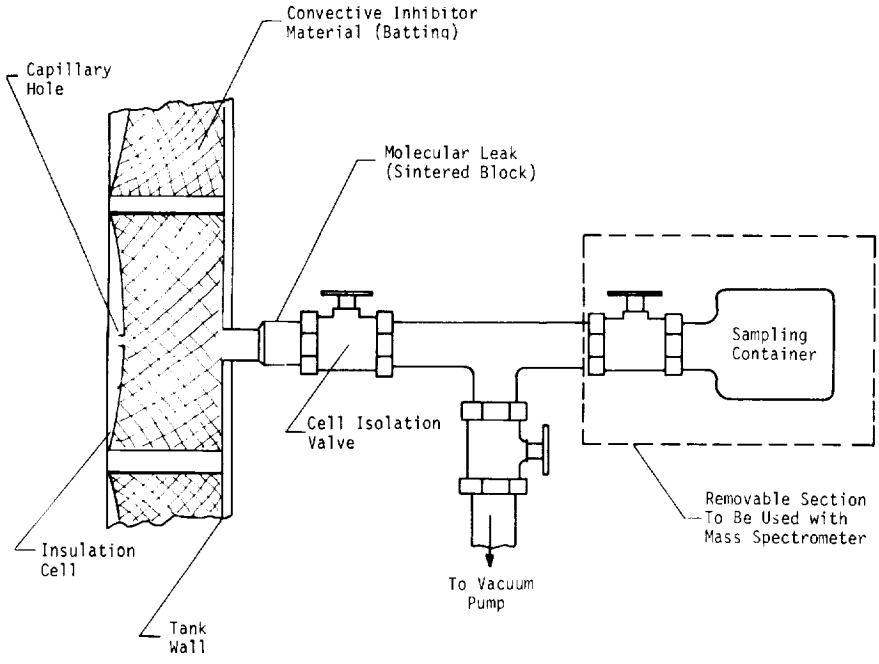

Figure 68. - Cell Sampling System

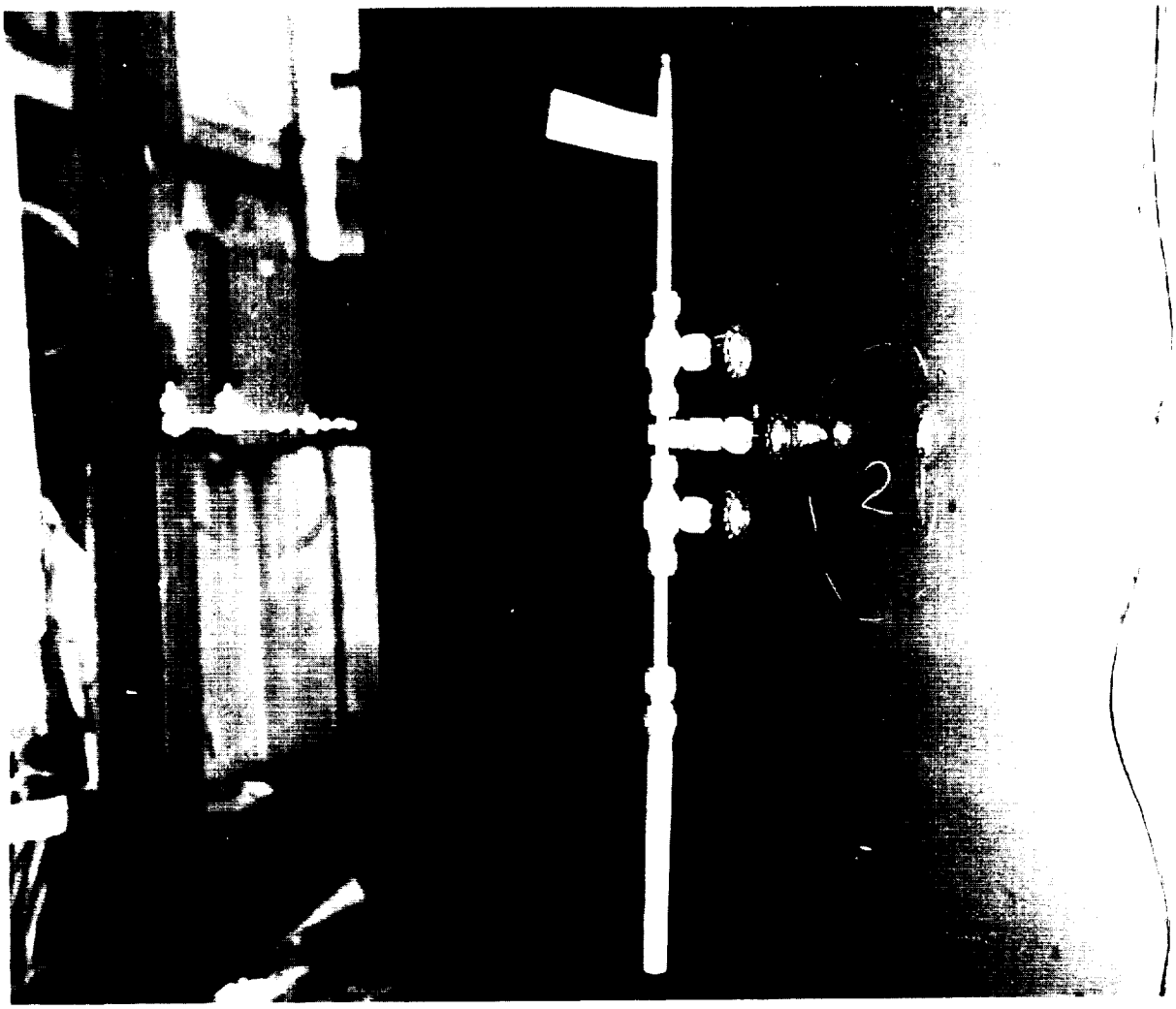

Figure 69. - Purge Sampling Assembly Installed on Tank

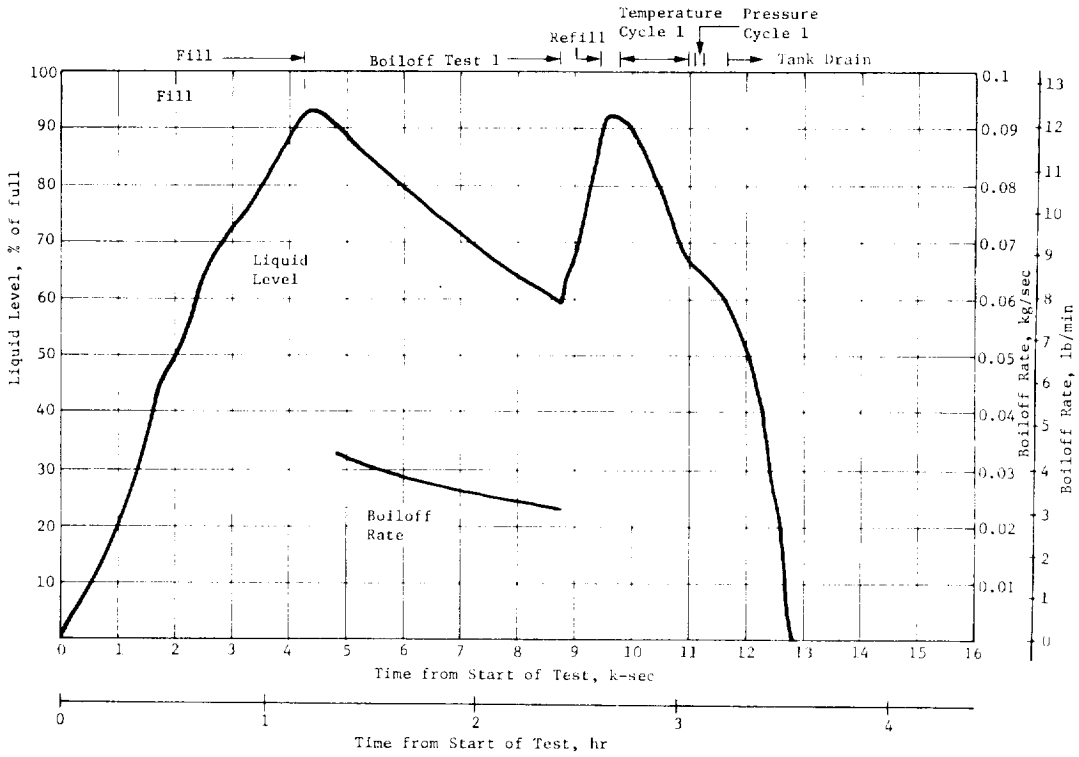

Figure 70. - Liquid Level and Boiloff Rate vs Time for Test No. 1

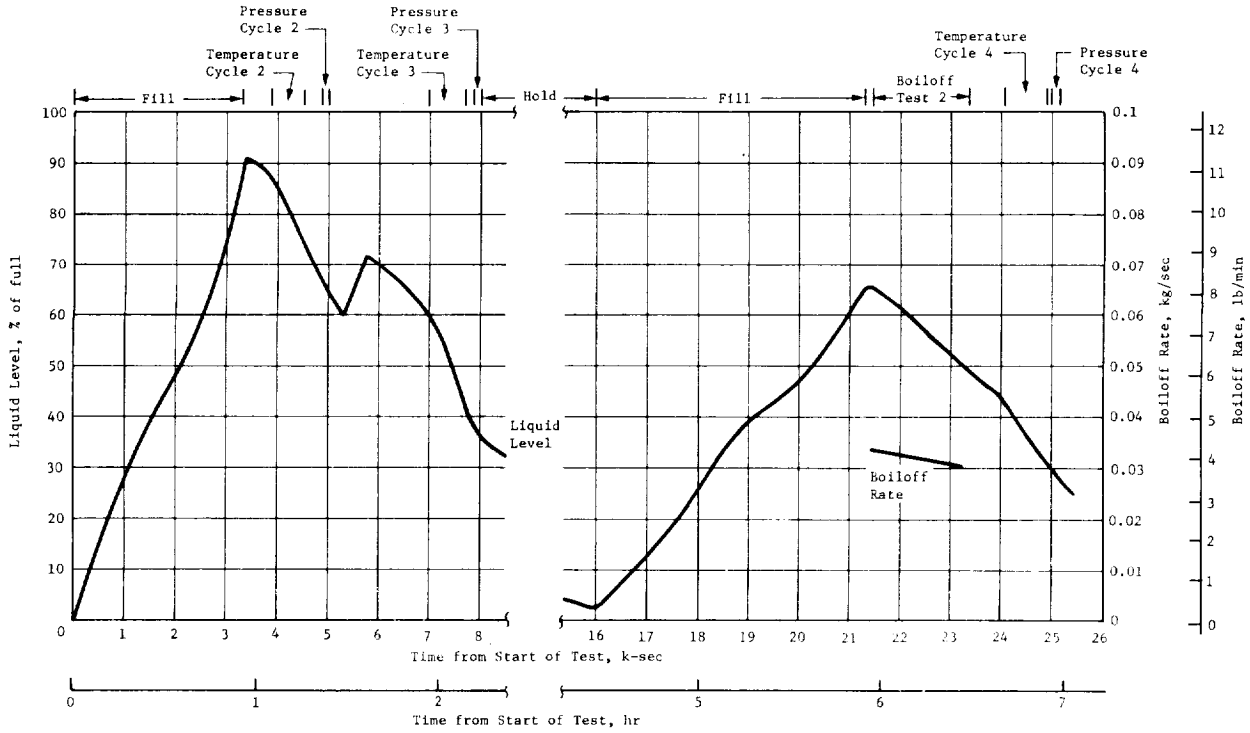

Figure 71. - Liquid Level and Boiloff Rate vs Time for Test No. 2

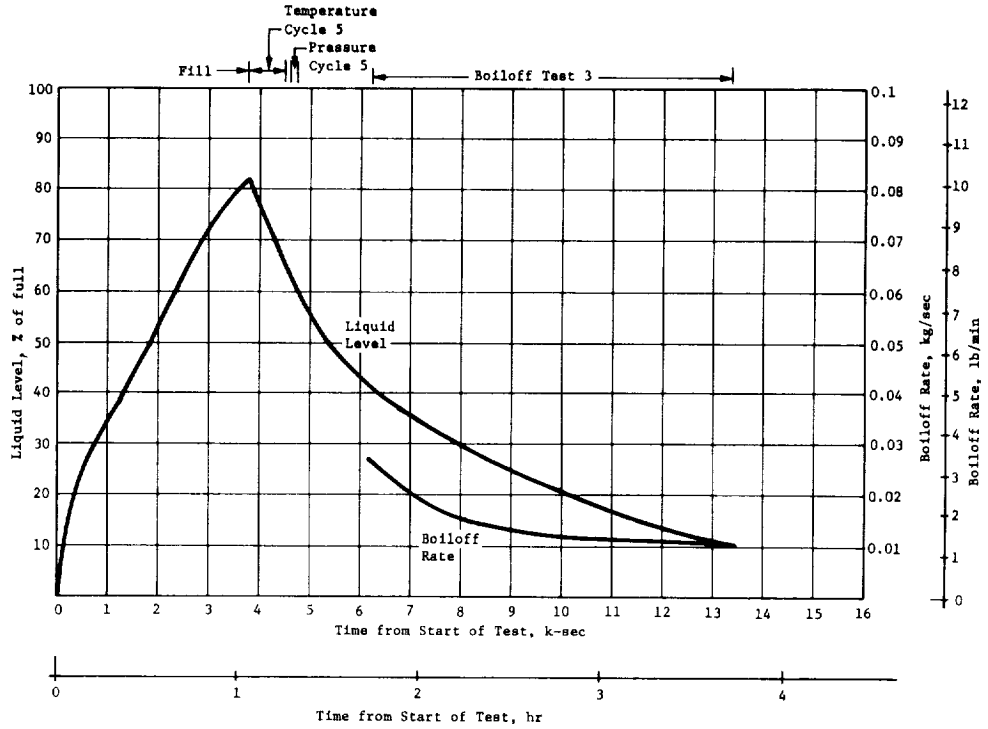

Figure 72. - Liquid Level and Boiloff Rate vs Time for Test No. 3

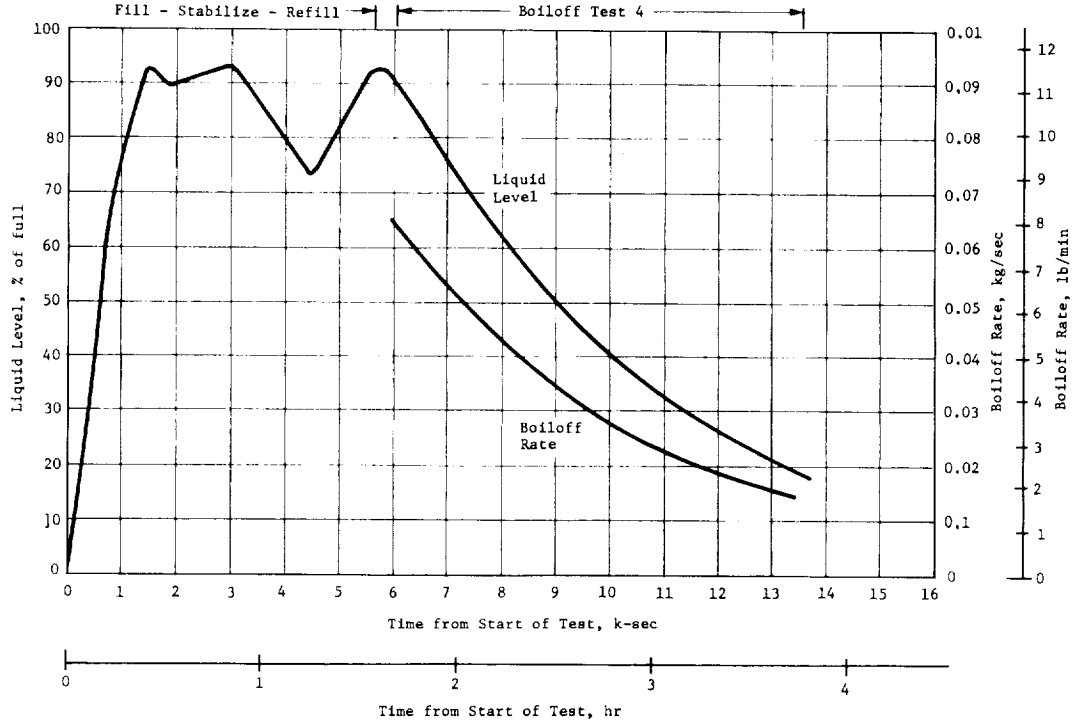

Figure 73. - Liquid Level and Boiloff Rate vs Time for Test No. 4

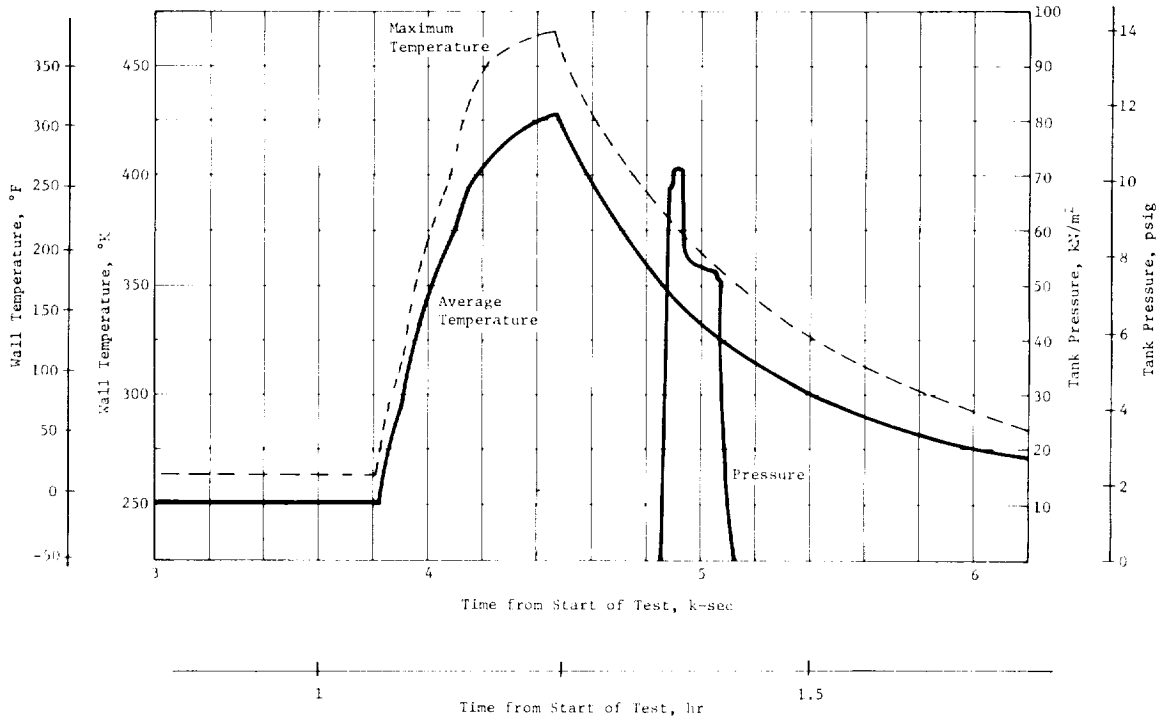

Figure 74. - Temperature and Pressure vs Time for Temperature/Pressure Cycle 2

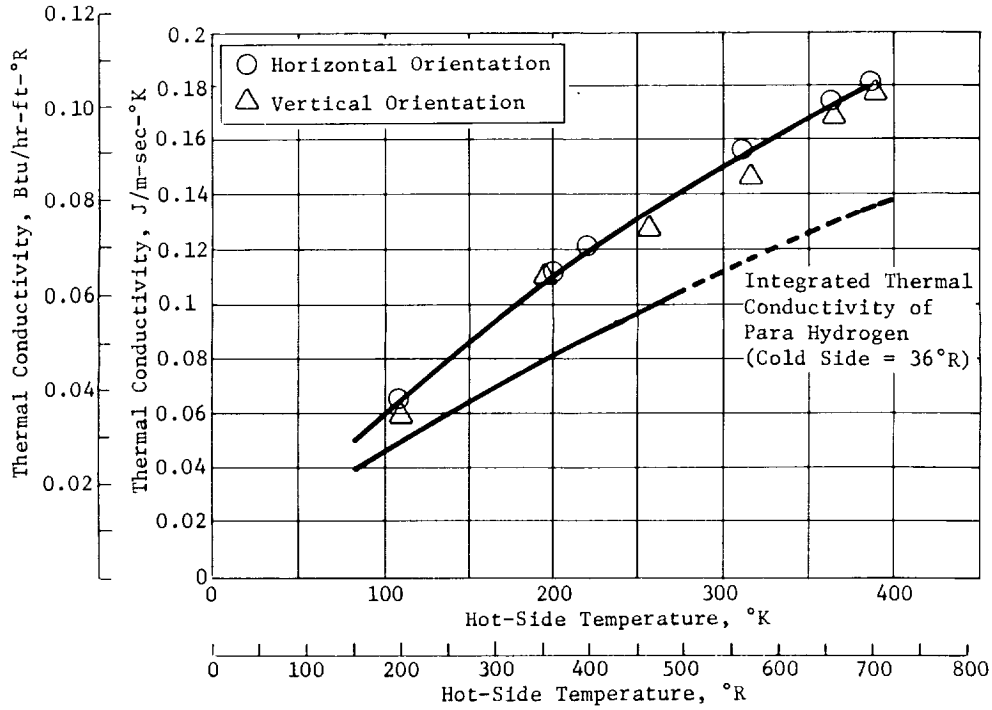

Figure 75. - Thermal Conductivity Test Results (Contract NAS8-25974)

APPENDIX A

MANUFACTURING DATA

Panel Prefabrication Procedure

The following process plan describes the steps required to fabricate insulation panels for tanks with simple and compound curvature. Type A panels are rectilinear-core panels for insulating sections with simple curvature (cylindrical or barrel sections of a tank). Type B panels are ring-segment panels with a radiating-core-ribbon pattern for insulating sections with compound curvature (domes or a transition between a dome and cylinder).

The special tools required for fabrication are listed in table VII. The "X" in the tool number refers to the designation of the specific panel for which the tool is designed. Panel and tool dimensions are specified on the detailed panel drawing.

TABLE VII. - FABRICATION TOOLING

Tool No.	Description
TX01	Drill template
TX02*	Short strip trim template
TX03	Print stencil
TX04	Stacking press
TX05	Outline trim template
TX06	Assembly tool (assembly rake/vacuum box)
TX10	Dimpling vacuum box
TX12	Contour form
TX14	Vacuum box lid (carrier frame)
TX15	Transfer sheet (rubber or polyethylene)
TX16	Expansion tool
TY17†	Filler plug die sets
TY18	Filler plug insertion tool
T001	Dimple depth tool

*This tool is used only for panels that have both short and long core ribbons.

†The "Y" corresponds to the filler plug designation, which may not correspond to the designation of the panel(s) in which it is used.

INTERNAL INSULATION SYSTEM PROCESS PLAN

DATE (REV.) 5-9-72

S/A IDENT. _____ STEP 5 SHEET 1 of 2

SUBSTEP	OPERATION
	This step is for assembling the core for Type A or Type B panels. Tools needed for this step are a paper cutter, water basin, drill and No. 30 drill bit, bandsaw and special no-set fine-toothed blade, print frame, scissors, scraper blade, marker pen, drill template (TX01), short strip trim template (TX02) for B panels, print stencil (TX03), stacking press (TX04), trim template (TX05), expansion tool (TX16), oven, and humidity room. Materials needed for this step are rolls of 5-mil-thick Kapton film in the required widths, cheesecloth, gaseous nitrogen, RTV-156 adhesive, and core assembly storage boxes.
a.	Using the paper cutter, cut the required number of Kapton strips in accordance with the panel drawing.
b.	For B panels, align the Kapton strips between the halves of the drill template (TX01). Clamp the halves together. Drill the positioning holes as indicated by the template. Remove the strips from the template. For A panels, proceed to Substep d.
c.	For B panels,* position the short strips between the halves of the short strip trim template (TX02) and clamp the halves together. Using the bandsaw and special blade, trim the end of the strips marked "TRIM." Remove the strips from the template halves.
d.	Clean the Kapton strips with trichlorethylene.
e.	Place the strips in the water basin and soak them for a minimum of 12 hr.
f.	Insert the print stencil (TX03) in the printing frame.
g.	Remove the Kapton strips from the water trough and dry them with cheesecloth. Place the dry strips side by side on cheesecloth spread on top of the workbench.
h.	Start the nitrogen purge in the print frame and add enough RTV-156 to one end of the stencil to finish stenciling the required number of strips for one panel.
i.	Place a strip in position on the alignment pins in the print frame. For A panels, align the strip end with the "START" line and perforate the strip with the punch. For B panels, refer to the appropriate panel drawing to find the sequence for perforating the short and long strips.
j.	Apply the RTV-156 to the strip through the specified openings of the stencil (in accordance with the applicable panel drawing), using the scraper blade to apply and remove excess adhesive.
	*This step trims the ends of short ribbons, which are inaccesible after assembly.

INTERNAL INSULATION SYSTEM PROCESS PLAN

DATE (REV.) 5-9-72

S/A IDENT. _____ STEP 5 SHEET 2 of 2

SUBSTEP	OPERATION
k.	Remove the printed strip from the print frame and place it, adhesive-side up, on the alignment pins of the stacking press (TX04). For A panels, the first strip is indexed in the "A" position (see appropriate drawing), the second in the "B" position, and each subsequent strip is alternated. For B panels, refer to the panel drawing.
ℓ.	Repeat Substeps j thru ℓ until all but the last strip has been printed.
m.	Place the unprinted strip in the stacking press on the alignment pins. For A panels, punch the last strip (Substep j) and place it in the stacking press in the "A" position.
n.	Place the top half (pressure bar) of the stacking press on the alignment pins and clamp the halves together at the preset stop. (Note that more than one core assembly can be pressed at one time if the correct preset stop is used to account for the thickness of the additional assemblies.)
o.	Place the stacking press in the humidity room and leave the assembly in position for a minimum of 12 hr to cure the adhesive.
p.	Remove the core assembly from the stacking press and leave it in the humidity room for a minimum of 72 hr.
q.	Expand the core on the expansion tool (TX16) and visually inspect the assembly for bondline quality. If any bondline is defective or questionable, the discrepancy shall be noted on a tag and attached to the core. The assembly will be reviewed by the program manager for final disposition. Remove the core from the expansion tool.
r.	Place the core assembly in the outline trim template (TX05) and clamp the template halves together. For A panels, place the strip assembly between the guide pins of the template, with the "TRIM" end of the template at the center of one of the strip-end bondlines and with the template windows centered over the adjacent bondline. Trim the outline of the core using the bandsaw equipped with the special blade. For A panels, only the ends of the core are trimmed. Inspect the trimmed edges.
s.	Heat the oven to 450°F, place the unexpanded core assembly in the oven, and postcure the adhesive at 450°F for a minimum of 4 hr.
t.	Turn off the oven, remove the core, and allow the core to cool to room temperature.
u.	Apply the ID number to the core with the marker pen.
v.	Store the core in poly bags until primed. Then deliver the core to the QC station for approval.

INTERNAL INSULATION SYSTEM PROCESS PLAN

DATE (REV.) 5-9-72

S/A IDENT. _____ STEP 10 SHEET 1 of 1

SUBSTEP	OPERATION
	This step is for making the facesheet for A and B panels. Tools and special equipment required for this step are scissors and a humidity room. Materials required for this step are double-etched, 2-mil-thick Teflon film, 1-mil-thick Kapton film, cheesecloth, DC-1200 primer, and core assembly storage boxes.
a.	Cut the facesheet material (Kapton or Teflon) with scissors to the dimensions specified on the drawing.
b.	Place the facesheet on a clean sheet of polyethylene. Wipe the facesheet on both sides with toluene and allow to dry. Wipe the DC-1200 primer on both sides of the facesheet in two directions. Visually check for complete coverage as the primer is being applied.
c.	Allow the primer to air-dry for a minimum of 30 minutes at ambient conditions.
d.	Place the facesheet in the humidity room (minimum 40% RH) on a drying rack for a minimum of 3 hr.
e.	Visually inspect the sheet to verify that all areas of the sheet were covered.

INTERNAL INSULATION SYSTEM PROCESS PLAN

DATE(REV.) 5-9-72

S/A IDENT. _____ STEP 15 SHEET 1 of 1

SUBSTEP	OPERATION
	This step is for applying the DC-1200 primer to the core assembly. Tools and special equipment required for this step are the expansion tool (TX16), spray gun, storage box, and humidity room. Material required for this step is the DC-1200 primer. The core assembly (Step 5) is also required for this step.
a.	Remove a core assembly from the humidity room. Clean the core assembly by sloshing it in a tray filled with trichlorethylene. Shake off the excess liquid and assemble the panel immediately on the expansion tool (TX16). Allow the solvent to completely evaporate before proceeding to the next step.
b.	Spray the DC-1200 primer on the top surface of the core in four directions.
c.	Visually inspect the core to verify that all areas on the top surface are covered.
d.	Discard any unused primer and clean the spray gun with naphtha if no further priming is to be done within 1 hr. Store the gun with a small amount of naphtha in the can.
e.	Allow the core to air dry for 30 minutes at ambient conditions.
f.	Place the core in the humidity room and allow the primer to cure for a minimum of 6 hr.
g.	Store the core in a storage box in the humidity room or proceed to Step 25.

INTERNAL INSULATION SYSTEM PROCESS PLAN

DATE(REV.) 5-9-72

S/A IDENT. _____ STEP 20 SHEET 1 of 1

SUBSTEP	OPERATION
	This step is for mixing the RTV-560 adhesive for bonding the core and facesheet. Equipment needed for this step are a paper mixing cup and spatula. Materials needed for this step are RTV-560 adhesive and standard catalyst (dibutyl tin dilaurate or Thermalite 12).
a.	Weigh the required quantity of RTV-560 in a paper mixing container.
b.	Add 0.25 percent by weight of standard catalyst to the RTV-560.
c.	Mix thoroughly by hand with a spatula for a minimum 5 minutes. (Note: This mixing time is appropriate for quantities of from 1 to 3 lb adhesive.) The adhesive should be used immediately.

INTERNAL INSULATION SYSTEM PROCESS PLAN

DATE(REV.) 5-9-72

S/A IDENT. _____ STEP 25 SHEET 1 of 1

SUBSTEP	OPERATION
	This step is for bonding the facesheet to the core assembly of the A or B panels. Tools and special equipment needed for this step are the assembly tool (TX06), vacuum box lid (TX14), notched trowel, transfer sheet (TX15), vacuum pump system, and humidity room. Materials needed for this step are the mixed RTV-560 adhesive (Step 20) and a core assembly storage box. Completed subassemblies needed for this step are a core assembly (Step 5) and facesheet (Step 10). This entire step is performed in the humidity room.
a.	Remove a core assembly from the storage box in the humidity room and expand it on the assembly tool (TX06). Check to verify that all cells are properly fitted on the rake.
b.	Carefully place the transfer sheet (TX15) on the surface of the vacuum box lid (TX14).
c.	Spread a uniform thickness of 1/16 in. of RTV-560 on the transfer sheet with a notched trowel.
d.	Invert the assembly tool. Attach the assembly tool to the lid of the vacuum box.
e.	Open the vacuum valve to the vacuum box and evacuate the box to a vacuum of approximately 0.11 psi (3 in. of water column). This forces the adhesive up against the core. After 3 minutes, break the vacuum box back to ambient pressure.
f.	Remove the lid of the vacuum box and the transfer sheet from the base. Do not return the base to the upright orientation until substep i. Allow the core to drip for 10 minutes.
g.	Place a facesheet (from Step 10) on the vacuum box lid and reassemble the vacuum box.
h.	Evacuate the vacuum box to 0.50 psi (14 in. of water column) and maintain this vacuum for a minimum of 12 hr.
i.	Break the system back to ambient pressure and remove the lid of the vacuum box.
j.	Remove the panel from the assembly tool by loosening the edges of the facesheet and then lifting the panel with air pressure.
k.	Visually inspect the facesheet core bond for bonding integrity. If any part of the bondline is defective or questionable, the discrepancy shall be noted on a tag attached to the panel. The panel will be reviewed by the program manager for final disposition.
ℓ.	Place the panel in a storage box in the humidity room.

INTERNAL INSULATION SYSTEM PROCESS PLAN

DATE(REV.) 5-9-72

S/A IDENT. _____ STEP 30 SHEET 1 of 1

SUBSTEP	OPERATION
	This step is for dimpling the facesheet of the A or B panels. Tools and special equipment required for this step are the dimpling heater,* thermocouple readout device, variable power transformer, vacuum pump system, and dimple depth tool (T001). Material needed for this step is a core assembly storage box. The completed subassembly needed for this step is a completed core and facesheet panel for Step 25. The panels should have been cured for 48 hr in the humidity room before dimpling.
a.	Remove a panel from the humidity room and install it in the dimpling/vacuum box (TX10) under the dimpling heater frame.
b.	Turn on both heaters to full power. Attach the vacuum line and vacuum metering gage. Evacuate the vacuum box to between 1.0 and 1.1 psi (28 to 30 in. water column). When the temperature of the heated air, as measured at the thermocouple mounted approximately 1 in. in front of the heater, reaches (510°F), adjust the heater power to maintain a temperature of 510 to 530°F.
c.	Move the heater back and forth slowly over the facesheet (approximately 2 in./sec, to be determined from experience) until well formed dimples are achieved. This requires approximately one minute.
d.	Lock the heater assembly in the hold position. Inspect a representative number of cells with the depth tool (T001) to verify that a dimple depth of 0.090 times the greater of the cell height or width (3/16-in. for barrel panels) has been achieved. This completes the first stage of the dimpling operation.
e.	Increase the heater power to maximum and adjust the vacuum valve to reduce the vacuum level to 0.32 to 0.36 psi (9 to 10 in. water column). When the temperature of the heated air reaches 590°F, adjust the power level to hold a temperature of 590 to 620°F.
f.	Repeat the dimpling procedure of substep c, using approximately the same traverse rate and total time.
g.†	Again inspect a sufficient number of cells to assure that the dimples are uniform and that the dimple depth is at least 0.075 times the greater of the cell height or width, or 5/32-in. for the barrel panels. A small amount of decrease in dimple depth will result from the second dimpling stage as the Teflon is brought the near its melting temperature.
h.	Turn off power to the heater and remove the vacuum from vacuum box.
i.	Remove panel from vacuum box and store in storage box or proceed to Step 35.
	*A hand-held heater may be used for panels with unusual curvature.
	†The minimum dimple depth will vary, depending on cell size.

INTERNAL INSULATION SYSTEM PROCESS PLAN

DATE(REV.) 5-9-72

S/A IDENT. _____ STEP 35 SHEET 1 of 1

SUBSTEP	OPERATION
	This step is for perforating the facesheet of the A or B panels. Tools and special equipment required for this step are a soldering iron equipped with an 0.035-in. needle and a variable power supply. The completed subassembly required for this step is a dimpled panel from Step 30.
a.	Turn on the soldering iron to the preset power and allow the needle to heat. If the panel is stored, remove it from the storage box and place it on a suitable work surface.
b.	Perforate the facesheet of each cell near its center. Before each perforating process, the operator shall practice perforating on a practice panel until consistently good results are achieved.
c.	Visually inspect the facesheet to verify that each cell has been perforated and that the hole is not enlarged. Repeat Substep b for any unperforated cells. If the perforation in any cell appears to be enlarged, note the cell(s) on a tag attached to the panel. The panel will be reviewed by the program manager for final disposition.
d.	Store the panel in the storage box or proceed to Step 40.

INTERNAL INSULATION SYSTEM PROCESS PLAN

DATE(REV.) 5-9-72

S/A IDENT. _____ STEP 40 SHEET 1 of 1

SUBSTEP	OPERATION
	This step is for trimming the facesheet of the A or B panels. Tools and special equipment required for this step are a No. 11 X-Acto knife. The completed subassembly required for this step is a perforated panel from Step 35.
a.	If the panel is stored, remove it from the storage box and place it on an appropriate work surface.
b.	Using a No. 11 X-Acto knife, trim the excess facesheet material close to the perimeter of the core, removing approximately half of the outside bondline.
c.	Visually inspect the core assembly to verify that the facesheet was trimmed properly. Any discrepancies shall be noted in a tag attached to the panel. The panel will be reviewed by the program manager for final disposition.
d.	Store the panel in a storage box or proceed with Step 45.

INTERNAL INSULATION SYSTEM PROCESS PLAN

DATE(REV.) 5-9-72

S/A IDENT. _____ STEP 45 SHEET 1 of 1

SUBSTEP	OPERATION
	This step is for making and installing the fiberglass filler plugs for the A or B panels. Tools and special equipment needed for this step are the filler plug die sets (TY17), punch press, contour form (TX12), spray gun, and filler plug insertion tool (TY18). Materials needed for this step are rolls of 1/2-in. thick fiberglass, DC-1200 primer, and a core assembly storage bag. The completed subassembly required for this step is a trimmed panel (from Step 40).
a.	Place the halves of the filler plug die set (TY17) in the punch press and punch the required number of filler plugs according to the filler plug usage table.
b.	Clean the open side of the core by sloshing it in a tray filled with trichlorethylene. Shake off the excess liquid and allow the core to dry.
c.	Position a panel on the contour form (TX12) with the facesheet against the form.
d.	Install the filler plugs using the insertion tool (TY18). Two 1/2-in.-thick plugs are inserted into each cell.
e.	Inspect each cell to verify that the outermost surface of the filler plug in each cell is depressed between 1/32 and 1/16 in. below the outside edge of the core. Adjust any plugs as required.
g.	Using the spray gun, apply the DC-1200 primer to the exposed area of the core and to the outside perimeter of the panel.
h.	Allow the primer to air dry for a minimum of 30 minutes at ambient conditions.
i.	Place the panel in the humidity room (minimum 40% RH) and allow the primer to cure for a minimum of 3 hr.
j.	Place the completed assembly in a storge bag or box. The completed panel is now ready for insulation on the test tank.

Quality Control Checklist

QC CRITERIA FOR INTERNAL INSULATION

A. CORE FABRICATION

1. The Panel ID number on the core must be clearly legible, and be marked on the side of core at one corner.

2. The width of node bond lines must be in accordance with the fabrication drawing, to within 1.6 mm (±1/16 in.).

3. Node bonds must be complete to within 0.005 in. of the ribbon edge on both sides.

4. Node bonds must be free of voids that traverse more than 1/4 the width of the bond line.

5. The thickness of the bond line must be measured at a minimum of four places on both sides of core assembly. Record the minimum and maximum bond thickness (obtained by subtracting the thickness of two ribbons).

6. Ribbon tears - Core ribbons must be free of tears on both sides.

7. The ribbon pattern (order of assembly) must be in accordance with the fabrication drawing.

8. The trim outline (for contoured panels) must be in accordance with the master drawing within ±0.8 mm (±1/32 in.) at all places.

9. Trimmed core surfaces must be smooth and free of discontinuities in excess of 0.13 mm (0.005 in.).

10. End node bonds must be trimmed in accordance with the panel drawing to within ±0.8 mm (±1/32 in.).

11. Edges of adjacent core ribbons must not mismatch in alignment by more than 0.13 mm (0.005 in.) on both sides.

B. PRIMING

1. Core Priming

   a. Verify that the proper cure cycle has been completed.
   b. Verify by visual inspection that primer has been applied to all of the core surface to within 6 mm (1/4 in.) of the edge of the facesheet.

2. Facesheet Priming

   a. Verify by visual Inspection that primer has been applied to both sides of the Teflon facesheet.
   b. Verify that the proper cure cycle has been completed.

3. ID - If not present already, apply a panel identification number to the corner of the facesheet using a black felt-tip marker.

C. FACESHEET ASSEMBLY

1. Verify the integrity of the primer and adhesive bond by failing a short portion of the bond [approximately 6 mm (1/4 in.)] at each of the untrimmed corner tabs.

2. Inspect the width of the bond lines at the facesheet. If the width is less than 0.5 mm (0.020 in.), leakcheck the affected cells to ensure that the bond is complete. If the width exceeds 5 mm (0.200 in.), inspect further to determine whether a satisfactory dimple will be obtained.

3. Discontinuities or skips in bond lines on either side of the core ribbon are unacceptable.

4. Inspect the core node bonds for voids in the bond lines.

5. Perimeter cells shall not be distorted beyond limits as indicated by gages. Internal cells shall not be distorted so as to cause straight cell walls.

6. Wrinkling of the facesheet shall not cause leakage between cells.

7. The core ribbons shall not be torn.

D. DIMPLING

1. Verify that the dimpling temperature and pressure parameters recorded on the process record sheet are in accordance with current procedure and properly signed off by the operator.

2. Measure the depth of the dimple for at least 20 cells, including cells adjacent to all edges. 90% of the cells so measured must have a minimum dimple depth of 0.075 the maximum of the height or width of the cell. No cell shall have a dimple depth factor of less than 0.065.

3. Verify by visual inspection that the dimple extends well into the corners of each cell.

4. Inspect the entire facesheet to verify that there are no holes.

E. PERFORATING AND TRIMMING

1. Measure the size of at least 20 holes in the facesheet. Each hole must be between 0.635 and 1.14 mm (0.025 and 0.045 in.) in diameter.

2. Visually inspect the entire facesheet to verify--

   a. that the holes are round, to the extent that the maximum and minimum dimensions are within the tolerances specified in (1) above.
   b. that the holes and facesheet are free of tears.
   c. that all cells have been perforated.

3. Inspect the entire perimeter to verify that--

   a. the facesheet-to-core bond is intact.
   b. adhesive is not completely removed, at any point, from the outside of the core ribbons.
   c. the maximum amount of facesheet and adhesive remaining beyond the core ribbon does not exceed 0.8 mm (1/32 in.).

F. FINAL INSPECTION

1. Inspect the panel on both sides to verify that all filler plugs are installed properly, and that--

   a. no gaps or cocked plugs are visible.
   b. all filler plugs are depressed between 0.8 and 3 mm (1/32 and 1/8 in.) below the back of the core, and that no filler material extends across any cell wall.

2. Verify that the primer has been applied uniformly to the back side of the panel.

3. Perform an overall inspection to detect any defects that may be visible and to verify that the panel has an acceptable appearance.

PANEL INSPECTION RECORD

PANEL ID_____

A. CORE FABRICATION

1. Verify ID marked on Core _____
2. Node Bonds in Tolerance _____
3. Short Node Bonds _____
4. Skips in Node Bonds _____
5. Bond Line Thickness _____
6. Ribbons Tears _____
7. Ribbon Pattern _____
8. Trim Outline in Tolerance _____
9. Trim Finish _____
10. End Trim in Tolerance _____
11. Ribbon Alignment _____

OK FOR STEPS 10 & 15

By_____Date_____

B. PRIMING

1. Core Priming _____
2. Facesheet Priming _____
3. Facesheet Identified _____

OK FOR STEP 25

By_____Date_____

C. FACE SHEET ASSEMBLY

1. Bond/Primer Integrity _____
2. Bond Line Width _____
3. Bond Line Skips _____
4. Voids at Core Node _____
5. Cell Distortion _____
6. Wrinkles _____
7. Ribbon Tears _____

OK FOR STEP 30

By_____Date_____

D. DIMPLING

1. Verify Dimpling Parameters _____
2. Dimple Depth _____
3. Dimple Into Corners _____
4. Holes in Facesheet _____

OK FOR STEPS 35 & 40

By_____Date_____

E. PERFORATING & TRIMMING

1. Hole Size _____
2. Hole Uniformity _____
   a. Hole Shape _____
   b. Tearing _____
   c. All Cells Perforated _____
3. Trim _____
   a. Damage to Perimeter Bond _____
   b. Overtrim _____
   c. Undertrim _____

OK FOR STEP 45

By_____Date_____

F. FINAL INSPECTION

1. Filler Plug Installation _____
2. Back Side Priming _____
3. Overall Appearance _____

PANEL READY FOR INSTALLATION

By_____Date_____

REPORT DISTRIBUTION

National Aeronautics & Space Administration
Lewis Research Center
21000 Brookpark Road
Cleveland, Ohio 44135

1 Attn: Contracting Officer, MS 500-313
5 E. A. Bourke, MS 500-205
1 Technical Report Control Office, MS 5-5
1 Technology Utilization Office, MS 3-16
2 AFSC Liaison Office, 501-3
2 Library
1 Office of Reliability & Quality Assurance, MS 500-111
1 J. W. Gregory, Chief, MS 500-
1 J. J. Notardonato, Project Manager, MS 500-
1 N. T. Musial, MS 500-113
1 D. A. Petrash, MS 500-204
1 A. V. Zimmerman, MS 500-318
1 J. R. Barber, MS 500-
3 J. B. Esgar, MS 60-4

1 Director, Physics & Astronomy Programs, SG
Office of Space Science
NASA Headquarters
Washington, D.C. 20546

1 Director, Planetary Programs, SL
Office of Space Science
NASA Headquarters
Washington, D.C. 20546

1 Director, Manned Space Technology Office, RS
Office of Aeronautics & Space Technology
NASA Headquarters
Washington, D.C. 20546

2 Director Space Prop. and Power, RP
Office of Aeronautics & Space Technology
NASA Headquarters
Washington, D.C. 20546

1 Director, Launch Vehicles & Propulsion, SV
Office of Space Science
NASA Headquarters
Washington, D.C. 20546

1 Director, Materials & Structures Div, RW
Office of Aeronautics & Space Technology
NASA Headquarters
Washington, D.C. 20546

1 Director, Advanced Manned Missions, MT
Office of Manned Space Flight
NASA Headquarters
Washington, D.C. 20546

1 National Aeronautics & Space Administration
Ames Research Center
Moffett Field, California 94035
Attn.: Library

1 National Aeronautics & Space Administration
Flight Research Center
P.O. Box 273
Edwards, California 93523
Attn: Library

1 Director, Technology Utilization Division
Office of Technology Utilization
NASA Headquarters
Washington, D.C. 20546

1 Office of the Director of Defense
Research & Engineering
Washington, D.C. 20301
Attn: Office of Asst. Dir. (Chem Technology)

1 Office of Aeronautics & Space Technology, R
NASA Headquarters
Washington, D.C. 20546

10 NASA Scientific and Technical Information Facility
P.O. Box 33
College Park, Maryland 20740
Attn: NASA Representative

1 National Aeronautics & Space Administration
Goddard Space Flight Center
Greenbelt, Maryland 20771
Attn: Library

1 National Aeronautcis & Space Administration
John F. Kennedy Space Center
Cocoa Beach, Florida 32931
Attn: Library

1 National Aeronautics & Space Administration
Langley Research Center
Langley Station
Hampton, Virginia 23365
Attn: Library

1 National Aeronautics & Space Administration
Manned Spacecraft Center
Houston, Texas 77001
Attn: Library
1 W. Chandler
1 W. Dusenberry
1 C. Yodzis

1 National Aeronautics & Space Administration
George C. Marshall Space Flight Center
Huntsville, Alabama 35912
Attn: Library
1 J. M. Stukey
1 I. G. Yates
1 E. H. Hyde

1 Jet Propulsion Laboratory
4800 Oak Grove Drive
Pasadena, California 91103
Attn: Library
1 L. Stimson
1 J. Kelly
1 R. Breshears

1 Defense Documentation Center
Cameron Station
Building 5
5010 Duke Street
Alexandria, Virginia 22314
Attn: TISIA

1 RTD (RTNP)
Bolling Air Force Base
Washington, D.C. 20332

1 Arnold Engineering Development Center
Air Force Systems Command
Tullahoma, Tennessee 37389
Attn: Library

1 Advanced Research Projects Agency
Washington, D.C. 20525
Attn: Library

1 Aeronautical Systems Division
Air Force Systems Command
Wright-Patterson Air Force Base
Dayton, Ohio
Attn: Library
1 AFML (MAAE)
1 AFML (MAAM)

1 Air Force Rocket Propulsion Laboratory (RPM)
Edwards, California 93523
Attn: Library

1 Air Force FTC (FTAT-2)
Edwards Air Force Base, California 93523
Attn: Library

1 Air Force Office of Scientific Research
Washington, D.C. 20333
Attn: Library

1 Space & Missile Systems Organization
Air Force Unit Post Office
Los Angeles, California 90045
Attn: Technical Data Center

1 Office of Research Analyses (OAR)
Holloman Air Force Base, New Mexico 88330
Attn: Library
RRRD

1 U.S. Air Force
Washington, D.C.
Attn: Library

1 Commanding Officer
U.S. Army Research Office (Durham)
Box CM, Duke Station
Durham, North Carolina 27706
Attn: Library

1 Bureau of Naval Weapons
Department of the Navy
Washington, D.C.
Attn: Library

1 Director (Code 6180)
U.S. Naval Research Laboratory
Washington, D.C. 20390
Attn: Library

1 Picatinny Arsenal
Dover, New Jersey 07801
Attn: Library

1 Air Force Aero Propulsion Laboratory
Research & Technology Division
Air Force Systems Command
United States Air Force
Wright-Patterson AFB, Ohio 45433
Attn: APRP (Library)

1 Electronics Division
Aerojet-General Corporation
P.O. Box 296
Azusa, California 91703
Attn: Library

1 Space Division
Aerojet-General Corporation
9200 East Flair Drive
El Monte, California 91734
Attn: Library

1 Aerojet Ordnance and Manufacturing
Aerojet-General Corporation
11711 South Woodruff Avenue
Fullterton, California 90241
Attn: Library

1 Aerojet Liquid Rocket Company
P.O. Box 15847
Sacramento, California 95813
Attn: Technical Library 2484-2015A

1 Aeronutronic Division of Philco Ford Corp.
Ford Road
Newport Beach, California 92663
Attn: Technical Information Department

1 Aerospace Corporation
2400 E. El Segundo Blvd.
Los Angeles, California 90045
Attn: Library-Documents

1 Arthur D. Little, Inc.
20 Acorn Park
Cambridge, Massachusetts 02140
Attn: Library
1 R. B. Hinckley

1 Astropower Laboratory
McDonnell-Douglas Aircraft Company
2121 Paularino
Newport Beach, California 92163
Attn: Library

1 ARO, Incorporated
Arnold Engineering Development Center
Arnold AF Station, Tennessee 37389
Attn: Library

1 Susquehanna Corporation
Atlantic Research Division
Shirley Highway & Edsall Road
Alexandria, Virginia 22314
Attn: Library

1 Beech Aircraft Corporation
Boulder Facility
Box 631
Boulder, Colorado
Attn: Library

1 Bell Aerosystems, Inc.
Box 1
Buffalo, New York 14240
Attn: Library

1 Instruments & Life Support Division
Bendix Corporation
P.O. Box 4508
Davenport, Iowa 52808
Attention: Library

1 Boeing Company
Space Division
P.O. Box 868
Seattle, Washington 98124
Attn: Library
1 D. H. Zimmerman

1 Boeing Company
1625 K Street, N.W.
Washington, D.C. 20006

1 Chemical Propulsion Information Agency
Applied Physics Laboratory
8621 Georgia Avenue
Silver Spring, Maryland 20910

1 Chrysler Corporation
Missile Division
P.O. Box 2628
Detroit, Michigan
Attn: Library

1 Chrysler Corporation
Space Division
P.O. Box 29200
New Orleans, Louisiana 70129
Attn: Librarian

1 Curtiss-Wright Corporation
Wright Aeronautical Division
Woodridge, New Jersey
Attn: Library

1 University of Denver
Denver Research Institute
P.O. Box 10127
Denver, Colorado 80210
Attn: Security Office

1 Fairchild Stratos Corporation
Aircraft Missiles Division
Hagerstown, Maryland
Attention: Library

1 Research Center
Fairchild Hiller Corporation
Germantown, Maryland
Attn: Library

1 Republic Aviation
Fairchild Hiller Corporation
Farmington, Long Island
New York

1 General Dynamics/Convair
P.O. Box 1128
San Diego, California 92112
Attn: Library
1 R. Tatro

1 Missiles and Space Systems Center
General Electric Company
Valley Forge Space Technology Center
P.O. Box 8555
Philadelphia, Pa. 19101
Attn: Library

1 General Electric Company
Flight Propulsion Lab. Department
Cincinnati, Ohio
Attn: Library

1 Grumman Aircraft Engineering Corporation
Bethpage, Long Island, New York
Attn: Library

1 Honeywell Inc.
Aerospace Division
2600 Ridgeway Road
Minneapolis, Minnesota
Attn: Library

1 IIT Research Institute
Technology Center
Chicago, Illinois 60616
Attn: Library

1 Ling-Temco-Vought Corporation
P.O. Box 5907
Dallas, Texas 75222
Attn: Library

1 Lockheed Missiles and Space Company
P.O. Box 504
Sunnyvale, California 94087
Attn: Library

1 Linde--Division of Union Carbide
P.O. Box 44
Tonawanda, N.Y. 11450
Attn: G. Nies

1 Marquardt Corporation
16555 Saticoy Street
Box 2013 - South Annex
Van Nuys, California 91409

1 Denver Division
Martin Marietta Corporation
P.O. Box 179
Denver, Colorado 80201
Attn: Library
1 G. C. Skartvedt

1 Western Division
McDonnell Douglas Astronautics
5301 Bolsa Ave
Huntington Beach, California 92647
Attention: Library
1 P. Klevatt

1 McDonnell Douglas Aircraft Corporation
P.O. Box 516
Lambert Field, Missouri 63166
Attn: Library
1 L. F. Kohrs

1 Rocketdyne Division
North American Rockwell Inc.
6633 Canoga Avenue
Canoga Park, California 91304
Attn: Library, Department 596-306

1 Space & Information Systems Division
North American Rockwell
12214 Lakewood Blvd.
Downey, California
Attn: Library
1 E. Hawkinson

1 Northrop Space Laboratories
3401 West Broadway
Hawthorne, California
Attn: Library

1 Purdue University
Lafayette, Indiana 47907
Attn: Library (Technical)

1 Goodyear Aerospace Corporation
1210 Massilon Road
Akron, Ohio 44306
Atten: C. Shriver

1 Hamilton Standard Corporation
Windsor Locks, Connecticut 06096
Attn: Library

1 Stanford Research Institute
333 Ravenswood Avenue
Menlo Park, California 94025
Attn: Library

1 TRW Systems Inc.
1 Space Park
Redondo Beach, California 90278
Attn: Tech. Lib. Doc. Acquisitions

1 United Aircraft Corporation
Pratt & Whitney Division
Florida Research & Development Center
P.O. Box 2691
West Palm Beach, Florida 33402
Attn: Library

1 United Aircraft Corporation
United Technology Center
P.O. Box 358
Sunnyvale, California 94038
Attn: Library

1 Vickers Incorporated
Box 302
Troy, Michigan

1 Airesearch Mfg. Div.
Garrett Corporation
3951 Sepulveda Blvd
Los Angeles, Cal 90009

1 Airesearch Mfg. Div.
Garrett Corp.
402 South 36th Street
Phoenix, Arizona 85034
Attn: Library

1 Commanding Officer
U.S. Naval Underwater Ordnance Station
Newport, Rhode Island 02844
Attention: Library

1 National Science Foundation, Engineering Division
1800 G. Street N.W.
Washington, D.C. 20540
Attn: Library

1 G. T. Schjeldahl Company
Northfield, Minn. 55057
Attention: Library

1 General Dynamics
P.O. Box 748
Fort Worth, Texas 76101

1 Cryonetics Corporation
Northwest Industrial Park
Burlington, Massachusetts

1 Institute of Aerospace Studies
University of Toronto
Toronto 5, Ontario
Attn: Library

1 FMC Corporation
Chemical Research & Development Center
P.O. Box 8
Princeton, New Jersey 08540

1 Westinghouse Research Laboratories
Beulah Road, Churchill Boro
Pittsburgh, Pennsylvania 15235

1 Cornell University
Department of Materials Science & Eng.
Ithaca, New York 14850
Attn: Library

1 Marco Research & Development Co.
Whittaker Corporation
131 N. Ludlow Street
Dayton, Ohio 45402

1 General Electric Company
Apollo Support Dept. P.O. Box 2500
Daytona Beach, Florida 32015
Attn: C. Bay

1 E. I. DuPont, DeNemours and Company
Eastern Laboratory
Gibbstown, New Jersey 08027
Attention: Library

1 Esso Research and Engineering Company
Special Projects Unit
P.O. Box 8
Linden, New Jersey 07036
Attention: Library

1 Minnesota Mining and Manufacturing Company
900 Bush Avenue
St. Paul, Minnesota 55106
Attention: Library